WP 4 Intermediate + Final Reports: Sustainability assessment. Unveiling Structure–Performance Relationships in HER Catalysts for Sustainable and Scalable Hydrogen Production

Table of contents:

1. Introduction 3
1.1. HER fundamentals and performance metrics **3**
1.2. From structure to catalytic performance in HER **6**
1.3. Scope and objectives of the review **12**
2. Experimental approaches to study HER catalysts **13**
2.1. Synthesis and structural characterization **13**
2.2. Electrochemical evaluation **17**
2.3. Spectroscopic and microscopic insights **18**
3. Theoretical and computational approaches **19**
3.1. Density functional theory modeling **19**
3.2. Machine learning and high-throughput screening **21**
3.3. Multiscale modeling **25**
4. Key structure-property relationships in HER catalysts **29**
4.1. HER catalysts in acidic media **29**
4.1.1. Noble metal-based catalysts (Pt, Pd, etc.) 30
4.2. HER catalysts in alkaline media **32**
4.2.1. Transition metal compounds (sulfides, phosphides, carbides, nitrides) ..33
4.2.2. Hybrid and interface-engineered catalysts 36
4.3. HER catalysts in acidic/alkaline media **39**
4.3.1. Carbon-based and non-metallic catalysts 41
4.3.2. MXenes as Emerging HER Electrocatalysts 45
5. Challenges and future perspectives **47**
5.1 Remaining knowledge gaps **47**

5.2. Design strategies for next-generation HER catalysts **48**
5.3. Integration with full water-splitting systems **48**
5.4 Sustainability considerations in HER catalysts **50**
5.5 Stability Testing and Benchmarking **51**
6. Conclusions **53**
References **53**
7. Comparative HER performance and derived sustainability indicators for all investigated catalyst samples developed in DEMADES..... **75**

1. Introduction

1.1. HER fundamentals and performance metrics

Green hydrogen, produced through water electrolysis driven by renewable energy sources, is widely regarded as the most environmentally sustainable option, as it eliminates the carbon emissions typically associated with conventional, fossil fuel-based hydrogen production ("gray hydrogen") [1-3]. Fig. 1 illustrates the principle of the hydrogen evolution reaction (HER) within a water electrolysis system and a fuel cell, both of which rely on catalytic processes.

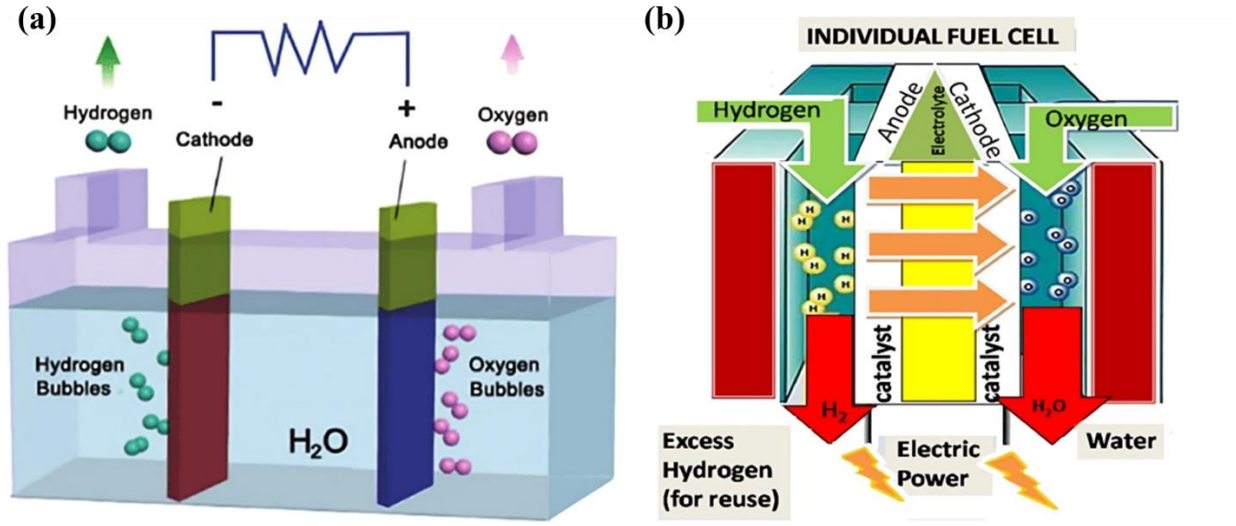


Fig. 1. (a) Schematic of HER mechanism in a water electrolysis system; **(b)** fuel cell operation involving catalysts. Reproduced with permission from [4, 5].

Hydrogen is increasingly recognized as a vital clean energy carrier due to its high gravimetric energy density (146 $kJ \cdot g^{-1}$), renewability, and zero carbon emissions when produced from sustainable sources [2, 6, 7]. As the global energy landscape shifts toward carbon neutrality, hydrogen emerges as a promising alternative to fossil fuels, enabling large-scale energy storage, grid stabilization, and the decarbonization of transportation and industrial sectors [1, 2, 7]. However, the environmental sustainability of hydrogen depends critically on its method of production. In water electrolysis, the HER serves as the cathodic half-reaction, wherein protons (in acidic media) or water molecules (in alkaline media) are reduced to generate molecular hydrogen. The HER mechanism typically involves a sequence of elementary steps, which proceed in both acidic and alkaline environments [8-10]:

(I) ***Volmer step (electrochemical adsorption)***:

Acidic media: $H_3O^+ + e^- + M \rightarrow M–H + H_2O$

Alkaline media: $H_2O + e^- + M \rightarrow M–H + OH^-$

(II) ***Heyrovsky step (electrochemical desorption):***

Acidic media: $M–H + H_3O^+ + e^- \rightarrow M + H_2 + H_2O$

Alkaline media: $M–H + H_2O + e^- \rightarrow M + H_2 + OH^-$

(III) ***Tafel step (chemical desorption):***

$2M–H \rightarrow 2M + H_2$

Here, M denotes a catalytic surface site, and M–H represents the adsorbed hydrogen intermediate. The overall HER may proceed via either the Volmer-Heyrovsky or Volmer-Tafel pathway, depending on the nature of the catalyst and the reaction conditions [8-10]. Table 1 provides an overview of key catalyst classes along with their structural characteristics relevant to HER performance.

Table 1: Summary of catalyst classes and key structural features.

Catalyst class	Structural characteristics
Carbides and nitrides (Mo_2C, VN)	High conductivity, robust lattice
MXenes	2D transition metal carbides/nitrides with tunable terminations
Noble metals (Pt, Pd)	High density of active sites, metallic bonding
Single-atom catalysts (M-N-C, M-S-C)	Isolated metal atoms on doped carbon supports
Transition metal phosphides (Ni_2P, CoP)	Metallic conductivity, tunable electronic structure
Transition metal sulfides (MoS_2, WS_2)	Layered structures, active edge sites, basal plane inert

The evaluation of HER catalysts is based on several key performance metrics that collectively determine their efficiency and practical applicability [11, 12]. The first parameter for consideration is ***overpotential (η)***. It represents the additional potential required beyond the thermodynamic equilibrium to drive the HER at a specific rate. Catalysts with lower overpotentials are generally more efficient, as they require less energy input to initiate the reaction.

The second parameter is a ***Tafel slope (b)*** derived from the Tafel equation ***($\eta = b \log j + a$)***. This parameter provides insight into the reaction kinetics and rate-determining step. Characteristic Tafel slopes, approximately 120, 40, or 30 $mV \cdot dec^{-1}$, are indicative of Volmer, Heyrovsky, or Tafel step limitations, respectively [11-14]. In practice, many noble metal catalysts (e.g. Pt in acid) display slopes close to 30 $mV\ dec^{-1}$, consistent with a rapid Volmer/Heyrovsky equilibrium followed by a slower Tafel step under acidic conditions. Meanwhile, some transition metal sulfides or phosphides exhibit slopes near 40 $mV\ dec^{-1}$, hinting that the Heyrovsky step may be limiting. In contrast, certain non-noble catalysts (e.g. metal carbides) may display slopes approaching ~ 120 $mV\ dec^{-1}$, suggesting that the initial Volmer (or proton/electron transfer) step is sluggish, possibly due to slow water dissociation or surface adsorption kinetics. However, this assignment should be viewed cautiously: actual Tafel slopes can depend on surface hydrogen coverage, potential range, pH, catalyst structure, and non-ideal effects (mass transport, bubble formation, double layer effects). Thus, the observed "cardinal" values 120, 40, 30 $mV\ dec^{-1}$ should be taken as idealized benchmarks rather than absolute mechanistic proofs.

The third parameter is the exchange current density ***(j_0)***. It refers to the current density at zero overpotential and serves as a measure of the intrinsic catalytic activity. A higher j_0 value reflects superior catalytic performance [11]. And the final important parameter for consideration is stability. The long-term durability of a catalyst under operational conditions is critical for practical applications. Stability is typically assessed through accelerated durability tests or prolonged electrolysis experiments, with consistent performance indicating robust catalyst longevity [2].

The key HER parameters, such as overpotential, Tafel slope, exchange current density, and long-term stability, serve as essential indicators for characterizing catalytic performance. These metrics not only quantify the efficiency and kinetics of the HER process but also provide valuable insights into underlying reaction mechanisms. Their systematic analysis enables the rational assessment of catalyst activity, paving the way for establishing meaningful structure-property relationships that guide the development of next-generation HER electrocatalysts.

It should be noted that HER catalysis fundamentally differs in acidic and alkaline media due to distinct reaction mechanisms, proton sources, and kinetic barriers, which strongly influence catalyst design strategies. In acidic media, HER proceeds primarily via the reduction of hydronium ions (H_3O^+) to adsorbed hydrogen intermediates on catalyst surfaces, which subsequently combine to form molecular hydrogen. This process generally exhibits faster kinetics because protons are readily available and do not require water dissociation. The elementary steps typically involve the Volmer step (proton adsorption) followed by either the Heyrovsky or the Tafel step for hydrogen desorption. Noble metals such as platinum often perform exceptionally in acid, thanks to their near-optimal hydrogen binding energy, resulting in low overpotentials, high exchange currents, and efficient proton–electron transfer. The simplicity of proton availability in acidic environments enables catalysts to effectively mediate proton-electron transfer without additional energy barriers from water splitting [9, 15-17].

In contrast, HER in alkaline electrolytes depends on water molecules as the proton source, involving an additional energy-consuming step related to water dissociation. In this environment, the Volmer step includes not only proton–electron transfer but also the adsorption and breaking of H_2O, producing adsorbed hydrogen (H*) and hydroxide (OH^-) species. This extra requirement generally slows down the overall process, resulting in higher overpotentials compared to acidic media. Therefore, designing effective alkaline HER catalysts requires simultaneously promoting efficient water dissociation and optimizing hydrogen adsorption–desorption energetics. Transition-metal compounds (such as oxides, hydroxides, nitrides, phosphides, and sulfides), heterostructures, and doped materials have shown promise because they can offer bifunctional active sites that aid both water activation and H_2 evolution [18-21]. Recent advancements highlight that strategies like defect engineering, interface construction, and electronic structure modulation

can significantly lower the energy barrier for water splitting, helping to overcome the inherent kinetic limitations of alkaline HER.

Furthermore, the identity and nature of active catalytic sites can differ substantially between acidic and alkaline environments, not only in terms of their electronic structure but also with respect to morphology, surface termination, and exposure. For example, in transition-metal dichalcogenides, edge sites are often recognized as the dominant active centers for HER in acidic media. In contrast, in alkaline electrolytes, terrace sites, interfacial boundaries, or defect-rich regions may play a more significant catalytic role due to the added requirement of water dissociation [22]. These environment-dependent variations in active site relevance underscore the need for medium-specific catalyst design, supported by tailored synthesis strategies and advanced characterization techniques, to maximize performance under the targeted operating conditions.

Recognizing the distinct pathways and reaction environments of HER, this review provides an in-depth analysis of catalyst structure–property relationships through a bifurcated discussion. Catalysts optimized for acidic HER are examined, with emphasis on metallic platinum-group materials, their atomic-scale features, and recent advances in single-atom systems. Catalysts tailored for alkaline HER are also discussed, highlighting transition metal phosphides, sulfides, carbides, and hybrid interfaces that facilitate both water dissociation and hydrogen evolution. This structured approach contextualizes catalytic performance within the fundamental chemistry of HER at different pH conditions, demonstrating how targeted structural and electronic modifications address environment-specific challenges and guide the rational design of catalysts for acid or alkaline electrolyzers.

1.2. From structure to catalytic performance in HER

The performance of HER catalysts is intricately governed by structure-property relationships. Understanding how catalyst composition, morphology, electronic structure, and surface characteristics influence activity is essential for the rational design and optimization of efficient HER electrocatalysts. The elemental composition and atomic configuration of a catalyst determine the nature, distribution, and density of active sites. For instance, single-atom doping in transition metal chalcogenides such as Co-doped $CoSe_2$ nanobelts can precisely tailor local atomic coordination, effectively tuning the ratio of metal-nitrogen to metal-chalcogen bonds. This atomic-level compositional control directly modulates hydrogen adsorption energies and reaction kinetics, thereby enhancing HER performance [23].

In addition to composition, catalyst morphology significantly impacts HER efficiency. Parameters such as surface area, active site exposure, and mass transport are closely linked to the shape, size, and dimensionality of the catalyst. Low-dimensional nanostructures, including nanotubes, nanosheets, and nanobelts, offer high surface-to-volume ratios and open architectures that can dynamically evolve under

operating conditions. Phenomena such as gas bubble formation and shear forces within the electrolyte can induce morphological transformations that improve mass transport and expose new active sites, ultimately boosting catalytic activity [24].

Furthermore, constructing nanoscale heterostructures by integrating two or more materials offers a powerful strategy to design catalytically active interfaces with enhanced performance and selectivity. For example, Zhang et al. [25] engineered a MoS_2/Ni_3S_2 heterostructure and employed high-angle annular dark-field scanning transmission electron microscopy (HAADF-STEM) along with charge density difference mapping to elucidate interfacial electronic properties, as shown in Fig. 2. Their analysis revealed significant charge transfer across the interface, leading to the generation of new active sites and markedly improved HER activity. Such interface engineering enables the synergistic integration of complementary material properties, facilitating the development of high-performance HER catalysts.

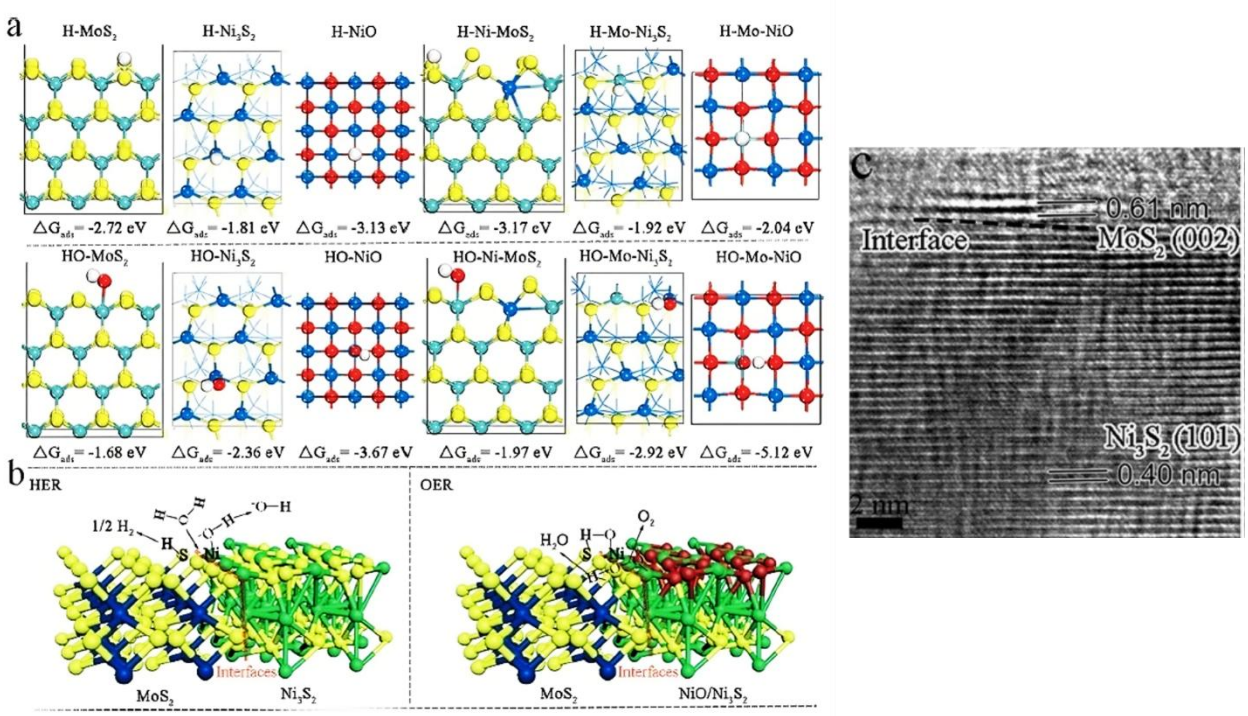


Fig. 2. MoS_2/Ni_3S_2 heterostructure, illustrating electron transfer at the interface and the creation of new active sites, resulting in enhanced HER activity: **(a)** chemisorption models of H and OH intermediates on the surfaces of MoS_2, Ni_3S_2, NiO, and the heterostructures MoS_2/Ni_3S_2 (Ni-MoS_2 and Mo-Ni_3S_2 models) and MoS_2/NiO (Ni-MoS_2 and Mo-NiO models), respectively, and **(b)** the suggested mechanisms for the dissociation of H_2O, OH, and OOH intermediates on the MoS_2/Ni_3S_2 heterostructures. Red=O, white=H, blue=Mo, green=Ni, and yellow=S; **(c)** high-resolution transmission electron microscopy of MoS_2/Ni_3S_2 heterostructures; reproduced with permission from [25].

The adsorption and desorption steps central to the HER are strongly influenced by surface defects, atomic coordination, and the local chemical environment. Structural features such as vacancies, edges, and heteroatom dopants can create highly active catalytic sites by modulating local electronic density and enhancing proton-electron transfer kinetics [26-28].

Fig. 3a illustrates the atomic structure and dispersion of single-atom catalysts (SACs), emphasizing how isolated metal atoms, such as Pt anchored onto supports like graphene or defective carbon matrices serve as discrete catalytic centers. This atomic dispersion maximizes surface exposure and catalytic efficiency while preventing the formation of less active metal clusters through aggregation [29, 30]. The enlarged section of Fig. 3a further provides structural characterization via techniques such as extended X-ray absorption fine structure analysis, which confirms the local coordination environment around single metal atoms. Typically, these atoms are coordinated with light elements: carbon, nitrogen, or oxygen from the support material, verifying true atomic dispersion. Such configurations are essential for optimizing hydrogen adsorption/desorption dynamics, which directly affect HER efficiency.

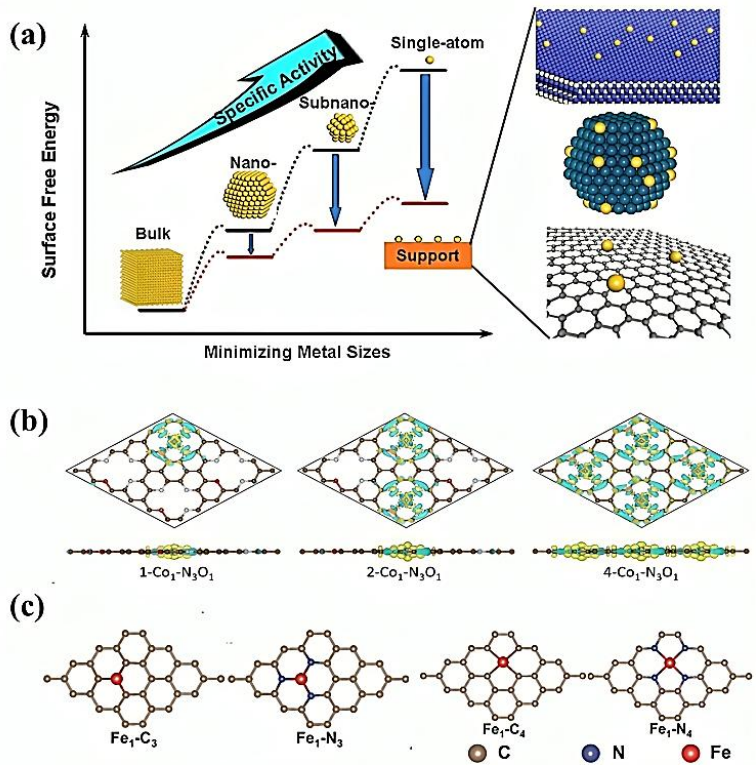


Fig. 3. (a) Visualization of isolated metal atoms anchored on the support, where each atom is a single catalytic site for hydrogen evolution and structural characterization confirming atomic dispersion from the absence of metal–metal coordination peaks and prevalence of metal–support interactions, indicating the enhanced catalytic accessibility and activity of atomic site catalysts for HER, reproduced from [29, 30], **(b)** charge density variation in cobalt single-atom sites (Co_1-N_3O_1) as their density increases from one to four per unit, showing enhanced electronic connectivity and a shift of the Co d-band center toward the Fermi level, which promotes improved hydrogen

evolution activity, reproduced from [31], and **(c)** comparative adsorption energies of H_2O, H, OH, and CO on four iron single-atom configurations (Fe_1-C_3, Fe_1-C_4, Fe_1-N_3, Fe_1-N_4), revealing how the coordination environment influences catalytic performance and resistance to CO poisoning, reproduced with permission from [32].

Additionally, Fig. 3b shows how increasing the density of cobalt single-atom sites (Co_1–N_3O_1) on a support material changes the electronic structure and charge distribution. As the number of active Co sites rises (from one to four per unit), there is a significant boost in charge delocalization within the support, confirmed by Bader charge analysis. Interestingly, the average charge transfer from each Co atom drops as site density increases, indicating a shift in the local electronic environment. This change causes the Co d-band center to move closer to the Fermi level, which improves hydrogen adsorption and overall HER kinetics [31].

Fig. 3c compares four different configurations of iron-based single-atom catalysts: Fe_1–C_3, Fe_1–C_4, Fe_1–N_3, and Fe_1–N_4, along with their varying adsorption affinities for key species such as H_2O, H, OH, and CO. The results highlight how local coordination environments affect catalytic behavior. For instance, Fe_1–N_4 shows weaker CO adsorption compared to its carbon-coordinated counterparts, making it more resistant to CO poisoning, which is crucial for maintaining catalytic performance under practical conditions. These findings emphasize the importance of atom-specific coordination design in improving both the activity and durability of HER catalysts [32, 33].

Introducing vacancies or defect sites into catalyst structures can generate unsaturated coordination environments that serve as highly active centers for hydrogen adsorption and evolution. Defect engineering, particularly in two-dimensional (2D) materials and nanoparticles, has proven to be an effective strategy for enhancing HER kinetics by fine-tuning the balance between hydrogen binding strength and release efficiency [24, 27, 34]. By deliberately introducing structural imperfections, the electronic structure and surface reactivity of catalysts can be modulated to improve their catalytic performance.

One prominent example is the work by Voiry et al. [35], who investigated the effect of sulfur vacancies on the HER activity of MoS_2 nanosheets, as illustrated in Fig. 4. Using aberration-corrected scanning transmission electron microscopy (STEM), they directly imaged and quantified sulfur vacancy concentrations and established a positive correlation between vacancy density and HER activity. These vacancies create localized unsaturated coordination environments that optimize hydrogen adsorption energies and facilitate electron transfer at the active sites. Complementary density of states (DOS) calculations revealed the emergence of mid-gap states induced by sulfur vacancies, further supporting their critical role in enhancing charge transport and accelerating HER kinetics.

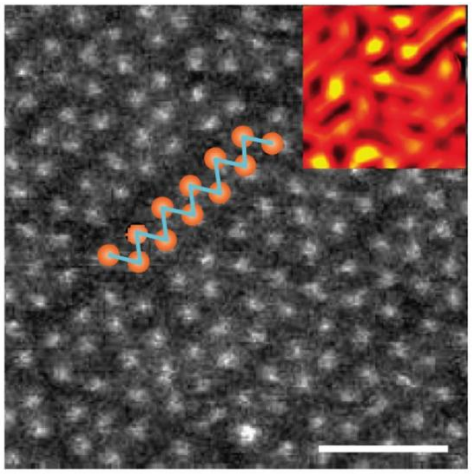


Fig. 4. Aberration-corrected STEM images showing sulfur vacancies in MoS_2 nanosheets. Defect sites are highlighted, and their role in increasing HER activity is discussed, supported by corresponding density of states calculations; reproduced with permission from [35]: scale bar, 1 nm.

Incorporation of heteroatoms or single metal atoms into catalyst lattices effectively modulates the electronic structure and local coordination environment, thereby tuning catalytic performance. Single-atom doping strategies have revealed volcano-shaped correlations between atomic configuration and HER activity, as illustrated in Fig. 5, emphasizing the pivotal role of dopant identity and bonding environment in optimizing catalytic efficiency [23, 26]. Specifically, Fig. 5a and 5b demonstrate that osmium single-atom catalysts (SACs) in acidic media and platinum SACs in alkaline media both exhibit volcano-type relationships, highlighting the profound influence of electronic structure on HER activity.

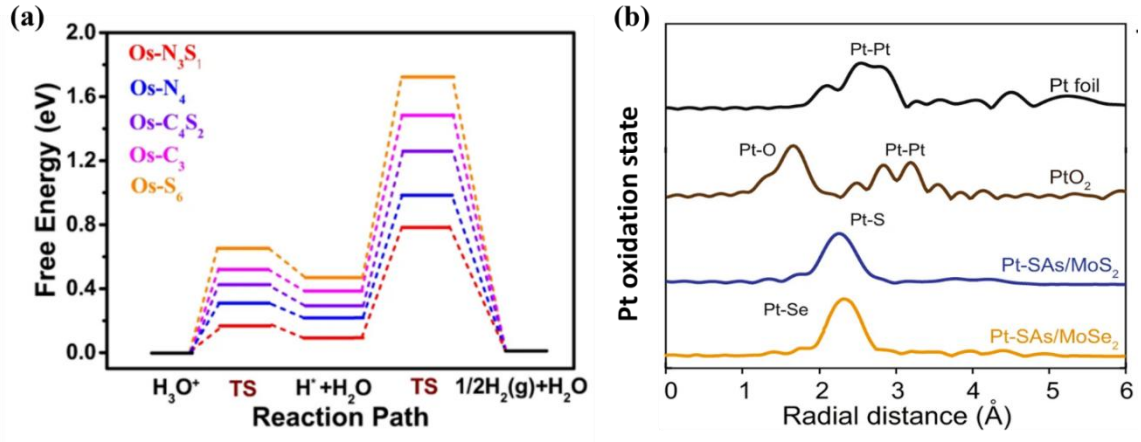


Fig. 5. Volcano-shaped correlations in HER systems; **(a)** correlation between Os oxidation state and overpotential at 10 mA/cm^2 for HER in acidic media. The optimal catalyst Os-N_3S_1 (+1.3 oxidation state) exhibits the lowest overpotential of 22 mV, reproduced with permission from [39]; **(b)** relationship between Pt oxidation state and HER catalytic activity in alkaline electrolyte. The catalyst with a Pt oxidation state of ~+2 achieves the highest activity, reproduced with permission from [40].

Fig. 5b details the HER activity of platinum SACs under alkaline conditions, showing that an intermediate platinum oxidation state of approximately +2 achieves an optimal balance between hydrogen and hydroxide adsorption energies. This balance promotes efficient water dissociation and hydrogen desorption, thus enhancing overall catalytic performance. Similarly, Fig. 5a presents the volcano relationship between the oxidation state of Os single atoms and acidic HER activity. The minimum overpotential is observed at a moderate oxidation state (~+1.3) in Os-N_3S_1 SACs, where the hydrogen adsorption energy is finely tuned via modulation of antibonding states in the Os-H bond. These findings underscore a fundamental principle in single-atom catalyst design for HER: neither excessively strong nor weak adsorption is desirable, but rather an optimized electronic structure that maximizes catalytic activity across different metals and reaction environments.

Beyond doping, mechanical strain, whether biaxial or uniaxial, can adjust interatomic distances and electronic band structures, further tuning the adsorption energies of reaction intermediates. Techniques such as core-shell architecture strain engineering, and the design of low-dimensional, flexible catalysts have been employed to enhance intrinsic activity and stability during HER [24]. Moreover, heterogeneous interfaces formed between distinct materials or phases facilitate charge redistribution, generate synergistic active sites, and provide efficient electron transfer pathways. A notable example is molecular catalysts immobilized on solid supports, where interface engineering stabilizes active centers and significantly improves turnover frequencies [36-38].

Recent studies have progressively underscored the significance of strain engineering in enhancing the catalytic performance of HER electrocatalysts. The modulation of electronic structures via tensile or compressive strain can finely tune the adsorption energies of key reaction intermediates, thus optimizing activity and stability. For instance, Ru-Au bimetallic aerogels exhibiting strain effects demonstrate remarkable HER activity by shifting the d-band center to balance water dissociation and hydrogen adsorption processes [41]. In addition to strain engineering, interface and heterostructure design have also been shown to significantly improve HER performance. By tuning electronic structures at the interfaces of multi-component catalysts, energy barriers for hydrogen evolution can be reduced and activity optimized across both acidic and alkaline media [42, 43]. Strategies such as adjusting band offsets in layered heterostructures or strengthening metal–support interactions improve charge distribution, stabilize active sites, and achieve high current densities under industrially relevant conditions [42, 43]. Furthermore, bifunctional non-noble-metal catalysts and alternative anodic reactions have been systematically explored to enhance overall water splitting efficiency and durability, providing practical guidance for the rational design of scalable and robust electrocatalysts [44].

Thus, the structure-property relationship in HER catalysts is a multidimensional interplay of composition, morphology, electronic structure, and surface chemistry. Defects, doping, strain, and

interfaces are potent handles for manipulating these properties for the design of catalysts with ideal activity, stability, and scalability. Additional clarification of these correlations through combined experimental and theoretical studies is needed to develop next-generation HER catalysts for green hydrogen evolution.

1.3. Scope and objectives of the review

This comprehensive review presents a critical analysis of the structure–property relationships in catalysts for HER, integrating insights from both experimental studies and theoretical modeling. It encompasses a broad range of catalyst systems, including molecular complexes such as cobaloximes and cobalt diamine–dioxime compounds, as well as transition metal-based catalysts and advanced nanostructured materials. The focus of the presented work lies in elucidating how specific structural features influence key catalytic metrics, including activity, stability, and efficiency, across varying reaction conditions (acidic, alkaline, and neutral media). Emphasis is placed on understanding how factors such as atomic dispersion, coordination environment, defect engineering, electronic structure, and interface design contribute to HER performance.

Recently, an extensive review by Chen et al. comprehensively covered hydrogen production technologies, spanning generation methods, storage, and utilization [45]. In contrast, this review focuses specifically on the fundamental atomic- and nanoscale structure–property relationships that govern HER electrocatalyst activity and durability. Recent advances in heteroatom doping, defect engineering, interface design, operando characterization, and multiscale computational modeling are synthesized to provide a detailed mechanistic understanding aimed at rational catalyst design.

This work complements broader hydrogen production reviews by addressing specific challenges and opportunities within HER catalysis, emphasizing innovations in catalytic materials that are critical for efficiently scaling green hydrogen production. Catalyst behavior under realistic operating conditions, including high current densities, is critically evaluated, linking fundamental insights with practical electrolysis system considerations. By connecting atomic-scale understanding with applied catalyst engineering, this review provides a targeted resource to advance hydrogen evolution technologies.

The presented review spans literature from the past two decades, capturing recent advancements while integrating foundational studies to provide historical context. It adopts a multidisciplinary perspective, bridging chemical synthesis, electrochemistry, materials science, and computational chemistry, to deliver a holistic understanding of HER catalysis.

By clearly defining its conceptual, methodological, and chronological scope, this review aims to serve both experimentalists and theorists. It is designed to assist researchers in identifying design principles, evaluating structure–activity relationships, and guiding the development of next-generation HER catalysts.

Maintaining a balance between breadth and depth ensures the work is both rigorous and accessible, providing a valuable reference for researchers and practitioners in HER catalysis.

2. Experimental approaches to study HER catalysts

Experimental methods for investigating HER catalysts are critical for correlating catalyst structure with performance. These methods entail multiple synthesis techniques to prepare catalysts and a range of characterization tools to examine their structural and chemical properties, before and during catalysis.

2.1. Synthesis and structural characterization

The synthesis and in situ surface reconstruction of HER catalysts are comprehensively represented in Fig. 6, which outlines the dynamic structural and electronic changes that occur under reaction conditions. A conceptual overview of surface reconstruction is provided in Fig. 6a, illustrating transformations such as crystallinity changes, morphological evolution, phase transitions, interface restructuring, defect generation, and shifts in chemical composition. These interconnected processes contribute to the formation of new active sites, leading to enhanced catalytic activity.

The SAED patterns shown in Fig. 6b for NiFe layered double hydroxide (LDH) before and after HER highlight a pronounced change in crystallinity following electrochemical treatment. Such structural evolution is typically linked to increased catalytic activity, either through the exposure of additional reactive facets or the emergence of amorphous regions. The observed loss of crystallinity in the NiFe LDH after HER corresponds to the formation of an amorphous or partially disordered phase, a common phenomenon in transition metal LDHs under electrochemical conditions. This structural evolution is generally beneficial, as it increases the density of catalytically active sites, including defects and edge sites, which enhance hydrogen evolution kinetics. Simultaneously, the amorphized phase improves ion and electron transport, contributing to overall catalytic performance and stability. Such dynamic reconstruction has been widely reported and is considered a hallmark of high-performance NiFe-based HER/OER catalysts [46].

Changes in the electronic structure of the catalyst are evident from the Ni 2p and O 1s XPS spectra presented in Fig. 6c and Fig. 6d, respectively. These spectra reveal valence state modifications that correlate with enhanced adsorption and activation of HER intermediates. The morphological evolution process, including thinning and exfoliation of layered structures to improve the electrochemically active surface area and mass transport, is schematically described in Fig. 6e. Additionally, Fig. 6f illustrates the mechanism of phase reconfiguration, showing time-resolved transitions among nickel sulfide phases (e.g., α-NiS, β-NiS, Ni_3S_4) and corresponding changes in elemental distribution. This continuous transformation supports the generation of new active centers, thereby sustaining high HER efficiency under operational conditions [47].

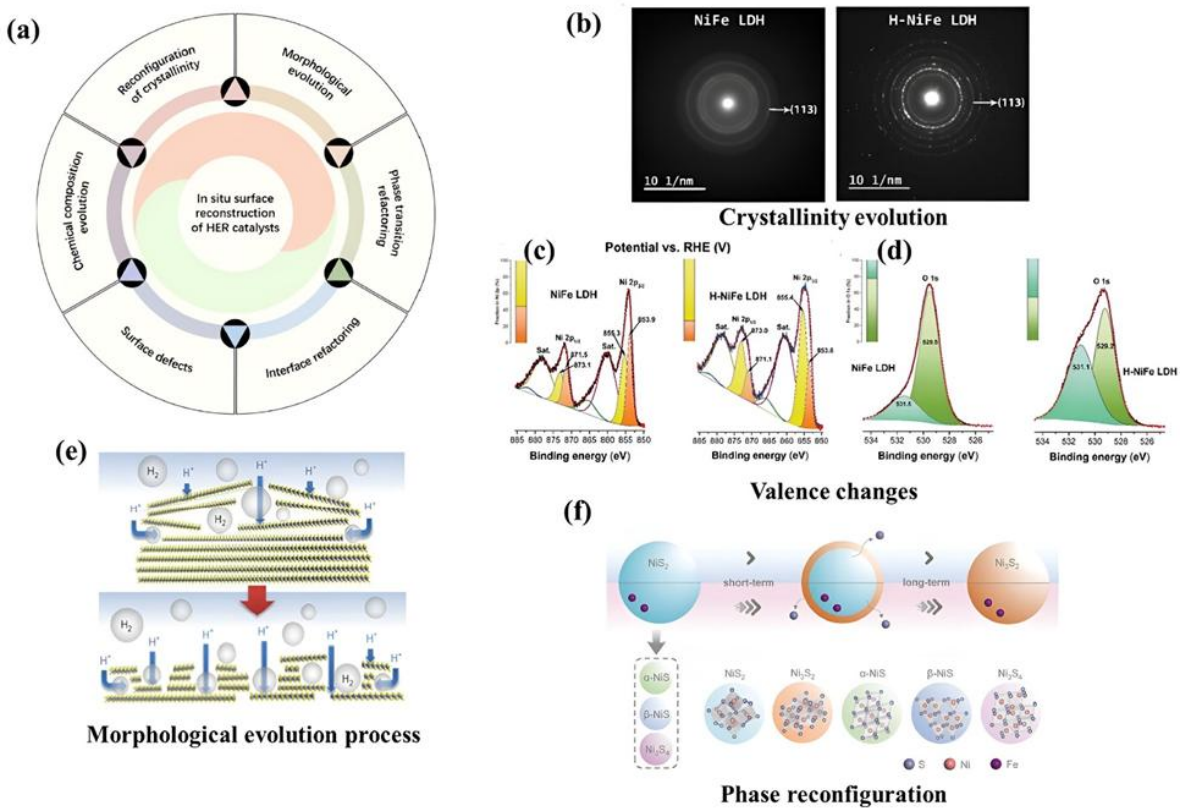


Fig. 6. Schematic representation and characterization of in situ surface reconstruction phenomena in HER catalysts: **(a)** conceptual representation delineating the primary characteristics of in situ surface reconstruction, including crystallinity reconfiguration, morphological development, phase transition/reconfiguration, interface reconfiguration, surface defects, and chemical composition evolution, **(b)** selected area electron diffraction (SAED) patterns of NiFe layered double hydroxide (LDH) before and after hydrogen evolution reaction, showing crystallinity evolution, **(c, d)** XPS spectra of Ni 2p and O 1s regions, respectively, illustrating valence state evolution during HER, **(e)** schematic illustrating morphological evolution, thinning, and exfoliation of catalyst layers during HER, and **(f)** mechanistic illustration of phase reconfiguration, illustrating the reconfiguration and redistribution of phases and elements (e.g., Ni, Fe, and S) during short- and long-term HER operation; reproduced with permission from [47].

Typical synthesis techniques of HER catalysts are as follows: (i) ***wet chemistry***: this is the conventional technique where chemical reactions in solution are used to synthesize catalysts, e.g., ***precipitation***, ***sol-gel route***, or ***hydrothermal synthesis***. It provides accurate control over morphology and composition and thus is being extensively employed for the preparation of nanoparticles, molecular complexes, and doped compounds; (ii) ***electrodeposition***: in this electrochemical technique, the catalyst materials are directly plated onto conductive substrates through the application of an electrical potential in an electrolyte solution containing metal ions. Electrodeposition is advantageous in the formation of homogeneous thin films or nanostructures with strong adhesion to electrodes, which is crucial in electrochemical HER studies; and

(iii) ***chemical vapor deposition (CVD)***: CVD involves the chemical reaction of volatile precursors in the gas phase to deposit a solid catalyst film on a substrate. It enables the synthesis of highly uniform, crystalline, and often nanostructured catalysts such as metal sulfides or alloys. For example, $Ru/RuSe_2$ nanoparticles synthesized via low-temperature CVD show excellent HER activity and scalability [48]. The selection of these techniques depends on the targeted catalyst composition, morphology, scalability, and special application requirements.

Understanding the HER catalysts at various scales is important for establishing the connection between their properties and catalytic activity. Several complementary methods are routinely used: (i) ***X-ray diffraction (XRD)***: XRD yields information on the crystalline structure, phase composition, and crystallite size of catalysts. XRD is one of the most important methods for verifying the formation of target phases and for identifying structural modifications following catalysis [49]; (ii) ***transmission electron microscopy (TEM)*** and ***scanning electron microscopy (SEM)***: TEM provides high-resolution images that allow imaging of catalyst morphology, particle size, and lattice fringes at the nanolevel, whereas SEM provides information on surface topography and morphology at lower magnifications. These imaging tools provide insight into the relationship between nanostructures and surface properties in terms of catalytic sites [50]; (iii) ***X-ray photoelectron spectroscopy (XPS)***: XPS is a surface-sensitive technique that identifies elemental composition and oxidation states on the surface of the catalyst. It helps to monitor chemical state changes during catalyst operation and is critical in establishing active site chemistry and catalyst-support interactions; and (iv) ***extended X-ray absorption fine structure (EXAFS)***: EXAFS is an atom-probe method that interrogates the local atomic environment around a specific element, providing bond lengths, coordination numbers, and disorder. This approach is highly suitable for the study of single-atom catalysts or doped materials in which local structure controls activity [51].

While ex-situ techniques provide snapshots of catalyst structure, in-situ and operando techniques (summarized in Table 2) enable observation of catalysts under actual working conditions, offering dynamic information on structural development and reaction mechanisms. They include (i) ***vibrational spectroscopies (in-situ IR and Raman)***: these methods detect adsorbed intermediates and surface species evolution during HER, allowing the determination of reaction pathways and active sites; (ii) ***operando X-ray absorption spectroscopy (XAS)***: a combination of XANES and EXAFS, operando XAS tracks oxidation state change and local structure in real time during HER, revealing how catalysts adapt upon potential application [52, 53]; and (iii) ***electrochemical mass spectrometry*** and other coupled methods: these allow simultaneous measurement of catalytic activity and product evolution, correlating structural development to performance. The use of operando techniques is ever more important since they describe the catalyst mechanism during the whole life cycle, from the initial activation through constant-rate operation to the final deactivation, giving deeper insight compared to stationary measurements.

Experimental studies of HER catalysts depend on the conjunction of special synthesis protocols and advanced characterization instrumentation. Wet chemistry, electrodeposition, and CVD all play a part in creating different catalyst structures. XRD, TEM, SEM, XPS, and EXAFS are some of the structural techniques that uncover their physical and chemical character. Most importantly, in-situ and operando methods provide real-time information about how catalysts behave during operation. This helps to connect their structure with their function and guides the smart design of better and more stable HER catalysts [54].

Table 2: Summary of in-situ/operando characterization techniques for HER catalysts.

Technique	Information provided	Spatial/Temporal resolution	Typical application
In-situ Raman spectroscopy	Surface species (intermediates, adsorbates)	~1μm, seconds	Evaluate HER-active sites, elucidating adsorbed hydrogen intermediates and active site reconstruction in MoS_x catalysts [55]
Operando XAS (XANES/EXAFS)	Electronic and geometric structures of electrocatalysts within electrode networks, particularly to elucidate the structure of active catalytic sites (electronic structures, coordination environments, and site symmetry)	Atomic, seconds-minutes	Active site evolution, tracking in-situ phase transition, identification of active sites for water dissociation, OH* adsorption, H* adsorption and H_2 evolution for NiS catalysts under HER conditions [56]
Operando ambient pressure X-ray Photoelectron spectroscopy (APXPS)	Chemical evolution of the surface	Seconds-minutes	To track the chemical evolution of the surface, enabling detection of active species by revealing of true structural evolution for Ni, Co, Fe-containing catalysts [57]
In-situ TEM	Morphology changes, nanoparticle growth	Nanometer, real-time	Structural dynamics, observing the morphology and chemical changes in layered rhenium molybdenum disulfide ($ReMoS_2$) catalysts [50], visualizing surface amorphization in Ni-doped metal phosphorus trichalcogenides ($NiPS_3$) [58], providing insights into degradation mechanisms of transition metal carbides and phosphides.

2.2. Electrochemical evaluation

The evaluation of electrochemical properties plays a crucial role in investigating HER catalysts, offering valuable insights into their performance, effectiveness, and longevity in practical applications. This evaluation typically adheres to established protocols and emphasizes key performance metrics, utilizing specific electrochemical configurations designed to produce reliable and comparable data. The typical experimental arrangement for testing the HER involves a three-electrode setup. This includes: (i) a working electrode (WE) where the catalyst is applied; (ii) a reference electrode (RE) serves to deliver a consistent potential, commonly utilizing materials such as Ag/AgCl or a saturated calomel electrode; and (iii) a counter electrode (CE), which is typically made of platinum wire or mesh, serves to complete the circuit. This arrangement facilitates accurate monitoring and assessment of the catalyst's electrochemical properties.

For enhanced mass transport and more uniform current distribution, rotating electrode techniques are often utilized. In a rotating disk electrode (RDE), the working electrode rotates at controlled speeds, improving reactant diffusion and removing gas bubbles formed during HER, which can otherwise block active sites. A rotating ring-disk electrode (RRDE) is an extension of RDE, where a ring electrode surrounds the disk, allowing simultaneous detection of reaction intermediates or products, useful for mechanistic studies and stability tests. These rotating setups are widely used to assess intrinsic catalytic activity and to perform accelerated stress tests that simulate long-term operation conditions [59-61].

Several electrochemical parameters play a crucial role in assessing the effectiveness of HER catalysts. Overpotential (η) refers to the additional voltage required beyond what is thermodynamically necessary to reach a certain current density. Lower values of overpotential suggest that the catalysts are more efficient. To accurately reflect intrinsic activity, it is most effectively reported in relation to the electrochemically active surface area (ECSA). The Tafel slope, which comes from examining the connection between current density and overpotential, offers valuable insights into the kinetics of reactions and the steps that determine the rate, helping to inform the optimization of catalysts. Turnover frequency (TOF) quantifies the production of hydrogen molecules at each active site every second, providing a clear indicator of catalytic activity that is not influenced by the amount of catalyst used. ECSA quantifies the true catalytic surface area, which can differ significantly from the geometric area due to nanostructuring, and normalizing current to ECSA helps distinguish genuine catalytic performance from surface area effects [62].

Evaluating catalyst durability is equally critical for real-world applications. Chronoamperometry, a widely used technique, involves applying a constant potential to the catalyst and monitoring the resulting current over time. A steady current response indicates that the catalyst maintains its activity, thus reflecting good operational stability. Additionally, cycling tests, often referred to as accelerated stress tests (ASTs),

subject the catalyst to repeated potential sweeps or varying reaction conditions to simulate long-term usage. Fluctuations in performance observed during these tests reveal insights into degradation mechanisms and long-term durability [60].

Complementary techniques, such as the RRDE, enable real-time tracking of intermediate species and reaction products during these durability assessments, offering a deeper mechanistic understanding. When performed under standardized conditions, typically in three-electrode configurations or using rotating electrodes, these electrochemical methods provide comprehensive data on the activity, kinetics, and longevity of HER catalysts. Such systematic evaluation is essential to guide the development of efficient, robust, and scalable technologies for sustainable hydrogen production [59].

2.3. Spectroscopic and microscopic insights

Spectroscopic and microscopic techniques are essential for understanding the intricate behavior of HER catalysts, as they offer valuable insights into surface intermediates and active sites. The process of hydrogen atoms (*H) adhering to catalyst surfaces plays a vital role in the hydrogen evolution reaction, and investigating these intermediates is essential for gaining insights into the underlying catalytic mechanisms. Methods like Fourier transform infrared spectroscopy (FTIR), Raman spectroscopy, and surface-enhanced infrared absorption spectroscopy (SHINERS) allow for the detection of these adsorbed species in real-time or during operation, effectively capturing their dynamic formation and transformation as they occur under reaction conditions. For example, sophisticated Raman techniques improved by plasmonic nanoparticles have uncovered the existence of unique hydrogen and hydroxyl intermediates on catalyst surfaces, along with their interactions with water molecules and the valence states of metals. The observations provide insight into the role of surface-bound intermediates in shaping catalytic activity and highlight how the electronic structure of the catalyst affects these interactions. This understanding is essential for guiding the development of more efficient HER catalysts [63-65].

In addition to spectroscopic data, microscopic techniques like scanning tunneling microscopy (STM) and atomic force microscopy (AFM) offer detailed images of catalyst surfaces, revealing structures at the atomic or nanometer scale. These tools enable researchers to see surface structures, imperfections, and atomic layouts directly, which are essential for pinpointing the active sites where the hydrogen evolution reaction takes place. By examining the relationship between surface topography, electronic properties, and catalytic performance, STM and AFM assist in identifying the particular structural features that contribute to enhanced activity. The integration of spectroscopic and microscopic methods provides a comprehensive understanding: spectroscopies reveal the chemical identities and behaviors of reaction intermediates, while microscopies depict the physical arrangement of active sites. Such an integrated perspective is essential for

tailoring catalyst surfaces to optimize hydrogen adsorption and evolution, ultimately enabling the development of highly efficient and durable HER catalysts under practical operating conditions [47, 66].

3. Theoretical and computational approaches

Theoretical and computational approaches have become indispensable tools in the design and optimization of HER catalysts. These methods provide atomistic-level insights into reaction mechanisms, adsorption energetics, and electronic structure, information that is often difficult to obtain experimentally. By simulating catalyst behavior under various conditions, theoretical studies help identify key descriptors of activity and guide the rational design of new materials.

Moreover, the integration of computational screening with high-throughput simulations and machine learning algorithms is significantly accelerating the discovery of efficient and cost-effective HER catalysts. When combined with experimental validation, these advanced modeling techniques form a powerful framework for uncovering structure-property-performance relationships and steering the development of next-generation catalytic systems.

3.1. Density functional theory modeling

Density functional theory (DFT) has become a crucial computational tool for understanding and predicting catalyst behavior in HER. Offering a quantum-mechanical description of electronic structure and energetics, DFT aids in uncovering fundamental catalytic mechanisms and guiding material design. A central descriptor in HER studies is the hydrogen adsorption free energy, ΔG_H^*. According to the Sabatier principle, an optimal catalyst exhibits $\Delta G_H^* \approx 0$ eV, balancing sufficient hydrogen binding without hindering desorption.

DFT enables precise calculation of ΔG_H^* by modeling hydrogen adsorption on various catalyst surfaces or active sites, revealing trends across diverse material classes, from metals to phosphides, carbides, and single-atom catalysts [67, 68]. For example, theoretically and experimentally, MoS_2 edge sites show $\Delta G_H^* \approx 0.08$ eV, correlating strongly with their high HER activity and confirming the near-thermoneutral ideal for ΔG_H^*.

Fig. 7 presents hydrogen adsorption free energies for numerous atomic-site catalysts, highlighting that those with ΔG_H^* values closest to zero, such as single-metal-atom sites or metal-doped heteroatom centers, achieve maximum catalytic performance. This comparative DFT data underscores how subtle electronic-structure modifications adjust ΔG_H^* and, by extension, activity and selectivity of single-atom catalysts.

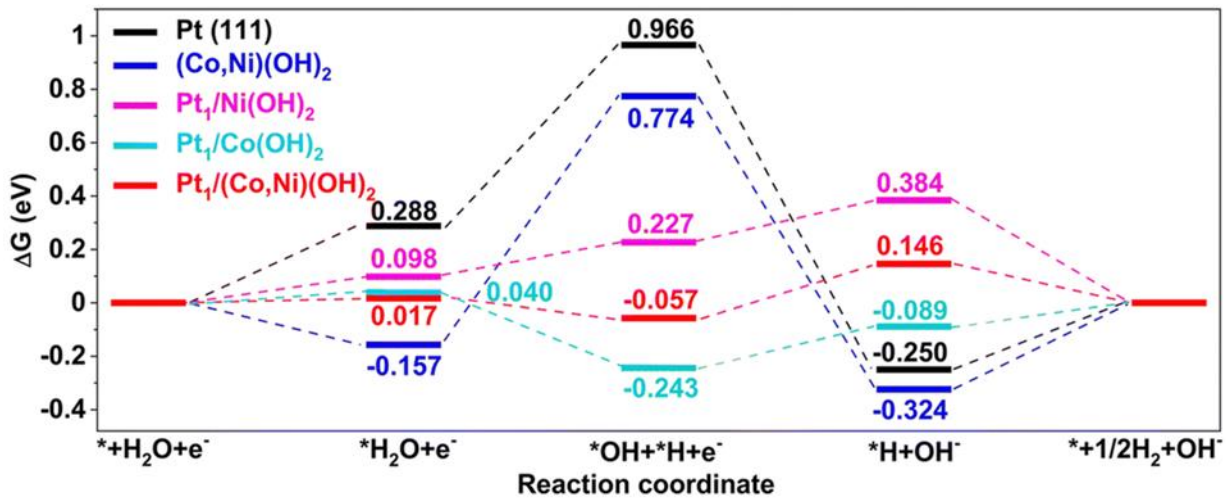


Fig. 7. The free energies of hydrogen adsorption (ΔG_H) calculated using DFT for different atomic site catalysts (ASCs) have been examined in the context of the electrochemical hydrogen evolution reaction. The plot illustrates how various atomic arrangements and dopants influence the strength of hydrogen binding, where values close to zero suggest ideal catalytic performance. This theoretical understanding supports the development of ASCs that achieve improved performance through a careful balance of hydrogen adsorption and desorption kinetics, reproduced with permission from [72].

Computational screening using ΔG_H^* as a descriptor has accelerated discovery by narrowing down candidate materials and guiding experimental validation [69]. Complementing this, analysis of the d-band center provides insight into adsorbate interactions: catalysts with a d-band center closer to the Fermi level generally exhibit stronger hydrogen adsorption, which can both enhance activity or lead to overbinding, underscoring the need for balance [70, 71].

By integrating ΔG_H^* and electronic structure descriptors like the d-band center, DFT-based approaches now offer predictive frameworks for identifying and tuning catalysts with optimal binding characteristics, streamlining the path to next-generation HER materials.

Charge transfer analysis is a critical component in understanding catalytic behavior in HER. DFT offers valuable insight into how electrons are redistributed between the catalyst surface and adsorbed hydrogen species, a factor that directly influences adsorption strength and reaction kinetics. For SACs, there is a well-established correlation between the occupancy of d-states near the Fermi level and the strength of hydrogen adsorption. A higher density of occupied d-states close to the Fermi level often results in stronger bonding with hydrogen, potentially enhancing activity. However, it is essential to recognize that this interaction is governed not solely by electronic density but also by the balance of multiple electronic factors, including charge distribution and electronegativity.

Electronic descriptors derived from DFT, such as Bader charge analysis, DOS, and the d-band center, provide a deeper understanding of how dopants, defects, or alloying elements modulate the local electronic

environment. These modifications adjust the adsorption energies of key intermediates and can lower reaction energy barriers, thus optimizing catalytic performance [73, 74].

DFT simulations have served as a crucial tool for exploring the impact of structural modifications such as strain, doping, and alloying on HER catalysis. Applying strain to the surface of a catalyst can shift the d-band center and alter adsorption energies, with a tendency to enhance catalytic activity by preferentially adsorbing hydrogen [75]. Doping with heteroatoms or alloying adds new electronic states and modifies the local electronic structure, which can facilitate or weaken hydrogen adsorption. For example, it has been reported that doping g-C_3N_4 with transition metals Re, Rh, or Ru creates under-coordinated sites that can adsorb more than one hydrogen atom and thus enhance HER activity beyond that expected from single hydrogen adsorption models [74]. Alloying also generates synergistic effects by combining metals of different electronic properties in order to fine-tune the adsorption characteristics of the catalyst. Some of the high-performance alloy catalysts with ΔG_H^* near zero have been reported by DFT studies, confirming the success of such an approach [69]. Overall, DFT modeling provides a remarkable, atomistic-scale tool kit for predicting and describing HER catalytic activity by: (i) calculating hydrogen adsorption free energies (ΔG_H^*) as a primary activity descriptor; (ii) analyzing electronic structure features such as the d-band center and charge transfer to understand adsorption processes; and (iii) exploration of the influence of strain, doping, and alloying on the tuning of adsorption energies and catalytic activity.

3.2. Machine learning and high-throughput screening

The quest for highly efficient and affordable catalysts for HER has been significantly boosted by the integration of machine learning (ML) methods with high-throughput computational screening. The synergistic strategy is transforming the practice of catalyst design by substantially minimizing the time and effort required to discover candidate materials. ML provides a dependable framework for examining intricate relationships between catalyst properties and their HER activity. Conventional approaches, i.e., DFT, although precise and reliable, are computationally demanding and time-consuming when dealing with a large number of potential catalysts. Conventional DFT calculations for 2D semiconductors like MoS_2 and g-C_3N_4 often neglect charge states, which can result in inaccurate predictions of HER activity. Charge states significantly affect electronic structure, adsorption energies, and catalytic reaction pathways. Recent studies reveal that understanding the relationship between charge states and HER performance is crucial for accurately modeling and optimizing these materials for high-efficiency HER applications [76]. Charge modulation influences the hydrogen adsorption Gibbs free energy (ΔG_H^*) and alters active site availability by impacting surface electronic states. For example, charged defects or doping can tune the catalytic sites' electron density, optimizing intermediate binding strengths. Explicit inclusion of charge states in

computational models thus improves the predictive power for catalytic activity and facilitates rational design of 2D semiconductor-based HER catalysts with superior efficiency.

Tran et al. [77] proposed an ML model that combines feature selection, model training, and high-throughput screening for identifying optimal catalyst candidates, as shown in Fig. 8. By training on large datasets of known catalytic activity, ML can predict the performance of new materials with little requirement for time-consuming trial experiments. This approach enables researchers to efficiently search the extensive chemical space and discover catalysts with desired characteristics for HER. ML models, trained on existing DFT datasets, can predict key catalytic descriptors like the hydrogen adsorption free energy (ΔG_H^*) with remarkable speed and accuracy. Recent work has yielded machine learning models based on a limited number of physically meaningful features, e.g., the composite energy feature Nd_0^2/ψ_0, for predicting ΔG_H^* across a wide variety of catalyst types, encompassing intermetallic compounds, perovskites, and single-atom catalysts [78, 79]. These models have achieved prediction accuracies with R^2 above 0.9 and mean absolute errors as low as 0.039 eV, which is comparable to the accuracy of DFT calculations but at a tenth of the computational cost. Zhang et al. [80] review the integration of ML with DFT for fast HER electrocatalyst discovery. Authors detail the ML workflow involving data collection, feature selection of key structural and electronic descriptors, model training with algorithms like Gradient Boosting and Random Forests, and model validation. Their review highlights HER's relatively simple reaction mechanism and the reliability of Gibbs free energy of hydrogen adsorption (ΔG_H) as a descriptor, enabling accurate ML predictions. ML-enhanced DFT screening drastically reduces computational cost, allowing rapid identification of promising catalysts, including alloys, 2D materials, and single/dual atom catalysts. Key findings emphasize charge transfer, adsorption energy, and d-band center as critical descriptors impacting HER activity. Challenges remain in realistic environment modelling and feature selection, but ML shows strong potential to guide rational catalyst design.

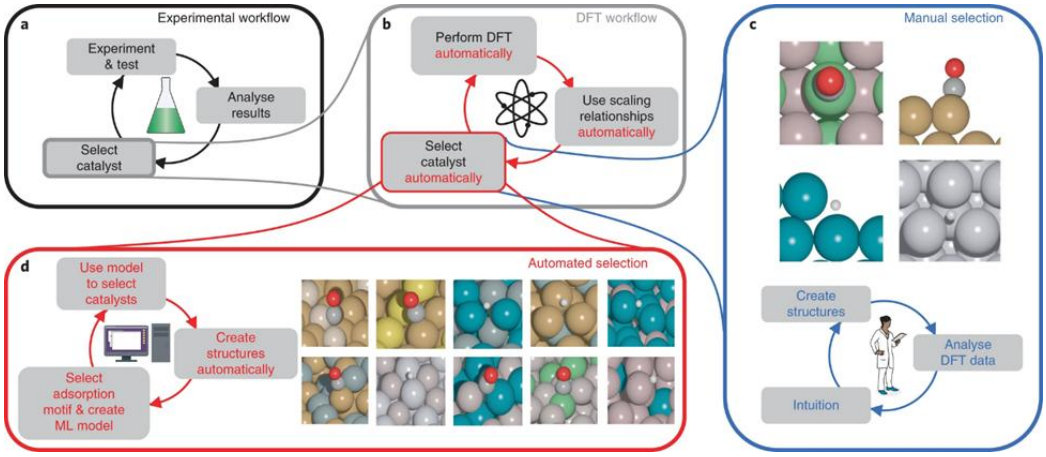


Fig. 8. A schematic representation of a machine learning workflow designed for the discovery of catalysts for hydrogen evolution reactions. This process encompasses key stages such as feature selection, model training, and

high-throughput screening. This method speeds up the process of identifying potential catalyst candidates, reproduced with permission from [77].

Recent advances illustrate the power of machine learning ML to accelerate HER catalyst discovery and optimization. For instance, researchers employed data-driven ML models combined with DFT calculations to predict and synthesize new catalysts with enhanced HER activity, demonstrating accelerated screening and rational material design [69, 81-83]. For example, Abraham et al. [82] integrated ML with DFT and high-throughput experimentation to identify MXenes with Nb, Mo and Cr metals with O functionalization that are discovered to be highly stable and active for catalysis, surpassing commercially available platinum-based counterparts. Another successful example of ML and DFT combination demonstrated efficient screening of two-dimensional materials supported by SACs on various active sites of graphitic carbon nitride [83]. It was found that the ML model based on support vector regression (SVR) exhibits the best performance to accurately and rapidly predict ΔG_H with a lower mean absolute error and a high coefficient of determination of 0.08 eV and 0.95, respectively. The authors of the presented work highlighted that proposed and screened catalysts could be considered as a promising replacement for platinum for large-scale industrial hydrogen generation. The recent developments in ML for low-dimensional electrocatalysts, including zero-dimension nanoparticles and nanoclusters, one-dimensional nanotubes and nanowires, two-dimensional nanosheets, as well as other electrocatalysts, were summarized by Li et al. [84]. Authors pointed out that HER electrocatalytic activity depends not only on the atomic-scale electronic and geometric structures of active sites but also on macroscopic factors such as solvents and electric fields, highlighting the need for cross-scale models that integrate experimental and environmental parameters to enhance the predictive design of efficient HER electrocatalysts. The study by Jyothirmai et al. [85] highlights how the integration of ML and DFT enables efficient exploration of transition-metal intercalated g-C_3N_4/MX_2 (M = Mo, W; X = S, Se, Te) heterostructures, revealing their structural stability and tunable electronic properties for enhanced HER performance. By combining high-throughput DFT screening with ML-driven prediction and SHAP-based interpretability, the approach identifies Sc- and Ti-intercalated systems with optimized hydrogen adsorption on N sites as highly active and stable HER catalysts, demonstrating the effectiveness of this cross-scale computational strategy in guiding the rational design of next-generation electrocatalysts. These representative cases underscore the transformative role of ML in accelerating electrocatalyst development from screening to mechanistic understanding, guiding iterative cycles of computational prediction and experimental validation.

It must be especially emphasized that one of the primary advantages of applying ML in HER electrocatalyst design is its remarkable speed in screening and predicting promising catalytic materials. ML predictions can be up to 200,000 times quicker than DFT computations, allowing for the swift evaluation of thousands of potential materials. Such efficiency enables researchers to quickly pinpoint promising

catalysts like Ir@SV-BN, Mo@SV-BN, and Pt@SV-BN, which demonstrate nearly optimal hydrogen adsorption energies and consequently exhibit high hydrogen evolution reaction activity [86]. The ML models are capable of identifying the most active adsorption sites on these catalysts, which helps to enhance the search for optimal performance [69, 87]. Additionally, ML algorithms such as Extremely Randomized Trees, random forests, and neural networks have been specifically designed to understand the nuanced physicochemical effects, including ligand and coordination environments, alloying, and doping, that impact catalytic behavior. This capability broadens the horizons of catalyst discovery, moving beyond individual material families to explore a wider chemical landscape, thereby addressing the constraints of conventional screening methods [69, 87]. It needs to be highlighted that the effectiveness of ML-driven catalyst discovery is significantly dependent on the availability of extensive and high-quality datasets.

Admit that recent ML studies accentuate the critical role of physicochemical descriptors in predicting and optimizing HER catalyst activity. Atomic radii influence the spatial arrangement and surface strain effects on active sites, while electronegativity impacts the electron density and adsorption strength of H* intermediates. Coordination numbers describe local atomic environments, influencing orbital overlaps and reaction energetics. Advanced ML models integrate these basic descriptors with electronic structure parameters such as d-band center and ΔG_H, improving prediction accuracy and mechanistic interpretability [88]. For example, Ding et al. show that models including electronegativity and coordination environment descriptors can efficiently screen transition metal catalysts and tailor electronic properties for optimal hydrogen adsorption [88]. Sinha et al. also highlight the importance of atomic radius and electronegativity in predicting alloy catalysts' ΔG_H, enabling targeted design of highly active bimetallic HER catalysts [89].

Public databases like the ***Materials Project*** and ***NOMAD (Novel Materials Discovery)*** are essential resources that offer a wealth of information on computed material properties. These include details on crystal structures, electronic properties, and adsorption energies obtained from DFT calculations.

The ***Materials project*** database offers comprehensive insights into a vast array of materials, encompassing intermetallics, oxides, and complex compounds. This allows researchers to utilize precomputed properties and structural data, facilitating the training of ML models and the screening of candidates for HER catalysis. For instance, the ML model referenced earlier utilized data from the ***Materials Project*** to forecast ΔG_H^* values for 132 varied catalysts, which were subsequently confirmed through DFT calculations [69].

NOMAD repository brings together computational data from numerous research groups around the globe, providing a valuable and consistent dataset for training ML algorithms. The open-access nature of this resource encourages collaboration and speeds up the creation of predictive models for designing catalysts. Researchers can effectively utilize these databases to merge data-driven methods with experimental and theoretical knowledge, allowing them to investigate extensive chemical landscapes. The

collaboration of high-throughput screening, ML, and extensive databases is advancing the field of HER catalyst discovery, enhancing the speed, cost-efficiency, and systematic approach of the process [86, 90]. The combination of ML with high-throughput computational screening and extensive materials databases is significantly changing the field of HER catalyst development. This approach enables scientists to swiftly discover and refine new catalysts with specific characteristics, greatly reducing the time it takes to move from theoretical predictions to real-world applications.

Finally, it is worth mentioning that while ML has significantly advanced the prediction and design of efficient HER catalysts by enabling rapid screening across vast chemical spaces, several limitations remain important to acknowledge [84, 91, 92]. The predictive accuracy of ML models heavily depends on the quality, diversity, and size of the training datasets, which can limit applicability when faced with scarce or biased experimental data. The development of accurate and generalizable ML models is hindered by the scarcity of high-quality, standardized experimental and computational datasets, as well as the variability and sensitivity of catalytic processes to experimental parameters. Data bias arising from selective reporting of successful results further complicates model reliability, while limited kinetic and excited-state data constrain the application of ML to dynamic reaction mechanisms. Descriptor selection remains a significant bottleneck, as simple, interpretable, and computable descriptors that capture complex catalytic phenomena are difficult to establish. Additionally, deep learning approaches, though powerful in generating latent representations, face interpretability issues that limit their practical adoption. Transferability of models across different catalyst systems or reaction conditions can be challenging, as ML algorithms may not generalize well beyond the domain of their training data. Moreover, while ML can identify promising candidates and structure-property correlations, these predictions require careful experimental validation to confirm catalytic performance under real operating conditions. Addressing these challenges involves integrating high-quality experimental data, improving model interpretability, and combining ML with physics-based simulations to build more robust, transferable, and reliable catalyst discovery frameworks.

3.3. Multiscale modeling

Multiscale modeling has emerged as a powerful approach to deepen our understanding and improve predictions of HER catalysts by bridging atomic-level phenomena with macroscopic reaction kinetics. By integrating multiple computational techniques, researchers can capture the complex behavior of HER under realistic conditions. This holistic framework enhances the accuracy of performance predictions and also guides the rational design of more efficient catalysts.

DFT provides detailed atomic-scale insights into the energetics of fundamental reaction steps on catalyst surfaces, such as hydrogen adsorption, proton-electron transfer, and hydrogen desorption. However, DFT alone cannot directly predict overall reaction rates or catalytic turnover frequencies due to

the inherently multistep and competitive nature of HER, which involves various active sites operating under dynamic conditions.

To overcome this limitation, microkinetic modeling plays a crucial role. Microkinetic models employ energetic parameters derived from DFT, such as activation barriers and adsorption free energies, to construct a comprehensive network of elementary reaction steps. By solving the coupled kinetic equations, these models yield quantitative predictions of hydrogen evolution rates and current densities, accounting for experimental variables including electrode potential, *pH*, and temperature.

The synergy between DFT and microkinetic modeling enables identification of the rate-determining steps and surface intermediates, as well as evaluation of how catalyst surface structure, composition, and adsorbate coverage influence activity. For example, studies integrating DFT-calculated adsorption energies with microkinetic simulations have explored HER on transition metal complexes and nanostructured catalysts. These investigations reveal how subtle modifications in surface chemistry can profoundly impact overall reaction kinetics and catalytic efficiency [93-95]. This integrated multiscale approach effectively links fundamental atomic-scale properties with experimentally measurable catalytic performance.

Recent studies have demonstrated the power and efficiency of a closed-loop approach that integrates theoretical prediction (ML, DFT calculations, microkinetic modeling), material synthesis, and experimental validation for HER catalysts [96-98]. For example, the work published by Hosseini et al. [96] considered DFT calculations and ML prediction to explore reaction mechanisms across multiple metal combinations, followed by microkinetic modeling to predict Tafel behavior and catalytic activity, which were subsequently confirmed through experimental electrochemical testing. Similarly, the study of Jia et al. [98] implemented a computational screening framework to identify stable and low-cost bifunctional metal oxide catalysts, which were then synthesized and experimentally characterized, validating the computational predictions. Together, these studies clearly illustrate that such closed-loop strategies not only exist but also provide an efficient pathway to accelerate the discovery and optimization of high-performance HER catalysts, bridging computational insights with experimental reality.

Fig. 9 highlights the important function of multiscale-coupled heterogeneous catalysts (MCHCs) in addressing the inherent challenges faced by single-component catalysts in water electrolysis, particularly regarding the HER and oxygen evolution reaction (OER) [99]. Figs. 9(a,b) illustrate volcano-shaped activity plots that connect catalytic performance with the adsorption energies of important reaction intermediates (H*, OH*, O*). This representation emphasizes the classical Sabatier principle, which suggests that optimal binding corresponds to peak activity. Nonetheless, these plots highlight the limitations set by linear scaling relationships (LSRs) among chemically similar intermediates. These constraints hinder the ability to independently adjust adsorption energies, ultimately affecting catalytic efficiency. Fig. 9c illustrates the concept of interface engineering, which brings together various active components into a

cohesive multiscale-coupled catalyst system. This approach allows for the independent adjustment of intermediate binding strengths. This method challenges the LSR constraints, as shown in Figs. 9(d,e), where the integration of components with complementary properties creates a balance between water dissociation and the steps of intermediate desorption. In particular, component A, such as Pt or Cu, facilitates a favorable process for intermediate desorption, whereas component B, like $Ni(OH)_2$ or Ru, improves the kinetics of water dissociation. Their collaborative interaction moves the catalyst system closer to the peak of the volcano, enhancing overall effectiveness.

Additionally, Fig. 9e shows how multiscale coupling disrupts the linear relationships between the adsorption energies of OH* and OOH* intermediates, which represents a significant challenge in acidic OER catalysis. The variation from LSRs in dual-component systems is due to distinct adsorption geometries, like bidentate binding at interfaces, which allow for enhanced OOH* stabilization while maintaining OH* binding integrity. This effect results in notably lower overpotentials and improved catalytic performance, as demonstrated by the Ga-O-Ir interface, which aids in the dynamic movement of intermediates and the dissociation of water.

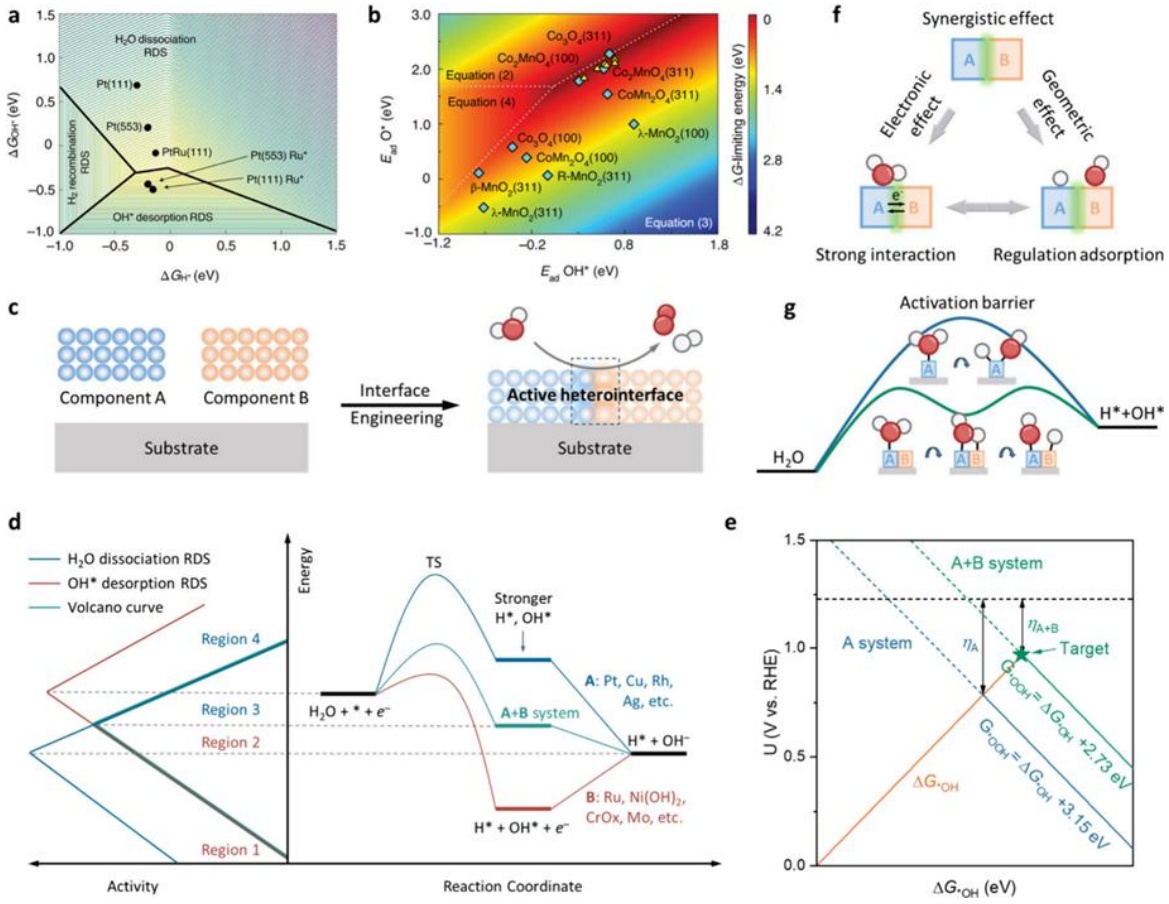


Fig. 9. The strategies for multiscale modeling and interface engineering aimed at enhancing the performance of water electrolysis catalysts: (a) a volcano plot that showcases alkaline hydrogen evolution reaction activity

concerning hydrogen (H*) and hydroxyl (OH*) binding energies, emphasizing the Sabatier principle for achieving optimal adsorption, (b) a two-dimensional activity map for OER illustrating the relationship with the adsorption energies of OH* and O* intermediates, (c) a schematic representation illustrating the engineering of heterointerfaces to create multiscale-coupled heterogeneous catalysts (MCHCs), which allows for the independent adjustment of intermediate binding strengths, (d) volcano-shaped activity trends illustrate how the integration of active components with varying water adsorption properties, weak (A) and strong (B), strikes a balance between water dissociation and intermediate desorption, thereby enhancing the kinetics of the HER, (e) scaling relationship plots are presented to compare single-component (A) and dual-component (A+B) systems, (f) these plots illustrate how the linear scaling relationships (LSRs) are disrupted in multiscale-coupled catalysts, resulting in lower overpotentials and improved OER performance, and the roles of MCHCs in enhancing the kinetics of water dissociation, and (g) illustrations of the reaction pathways for water dissociation on single-component (A) and multiscale-coupled (A+B) catalysts; reproduced with permission from [99].

Fig. 9 illustrates the significant potential of multiscale modeling and interface engineering in the development of advanced catalysts. This approach goes beyond conventional boundaries, offering a thoughtful strategy for the rational optimization of HER and OER catalysts in realistic operating conditions [99]. While DFT and microkinetic models primarily focus on the catalyst surface and reaction intermediates, it is essential to acknowledge the significant influence of the surrounding environment, particularly the solvent, on HER. In aqueous electrolytes, solvent molecules, predominantly water, play a critical role in facilitating proton transport, stabilizing charged intermediates, and shaping the structure and dynamics of the electric double layer at the electrode-electrolyte interface. Molecular dynamics (MD) simulations provide a powerful tool to model the interactions between solvent molecules, ions, and catalyst surfaces over time. By simulating atomic motions governed by interatomic potentials, MD can effectively capture: (i) the organization and behavior of water molecules at the catalyst interface; and (ii) the rearrangement of solvent molecules and hydrogen-bond networks that support proton transfer. Additionally, MD simulations reveal how electrolyte composition, *pH*, and applied potential affect the interfacial structure.

These insights are crucial because the solvent environment strongly influences reaction energetics and pathways, often in ways that differ from vacuum or implicit solvent models typically used in DFT. For example, MD studies have demonstrated that water molecules form hydrogen-bonded chains that facilitate efficient proton transfer to active sites, thereby enhancing HER kinetics. By integrating MD with surface models derived from DFT, researchers can construct more realistic representations of the catalytic interface, leading to improved accuracy in predicting reaction mechanisms and rates [95, 100]. This multiscale perspective underscores the interplay between catalyst surface chemistry and solvent dynamics that governs HER under practical conditions. Summarizing, multiscale modeling of HER catalysts involves: (i) DFT calculations to elucidate atomic-level energetics of reaction intermediates and transition states; (ii)

microkinetic modeling to translate these energetic parameters into reaction rates and identify kinetic bottlenecks; and (iii) molecular dynamics simulations to capture solvent effects and interfacial structure. Together, these complementary approaches establish a comprehensive framework for predicting and optimizing HER catalytic performance, ultimately guiding the rational design of efficient and durable catalysts for sustainable hydrogen production.

4. Key structure-property relationships in HER catalysts

4.1. HER catalysts in acidic media

HER in acidic media is predominantly driven by the direct reduction of protons (H^+) from the acidic electrolyte to produce hydrogen gas. This process is characterized by relatively fast kinetics because protons are readily available as the reactant, which simplifies the reaction mechanism to mainly involve hydrogen adsorption and desorption on the catalyst surface. The key challenge in acidic HER catalysis lies in identifying materials that combine high intrinsic activity, durability in corrosive acidic environments, and cost-effectiveness [101].

Platinum (Pt) and Pt-based noble metals are widely recognized as the benchmark catalysts for acidic HER due to their optimal hydrogen binding energy that balances adsorption and desorption steps, leading to minimal overpotentials and exceptional catalytic efficiency. Pt catalysts exhibit the lowest overpotential, high exchange current densities, and excellent long-term stability in acidic electrolytes, setting the standard for activity in this environment [102]. Nonetheless, the scarcity and cost of platinum motivate ongoing research into alternative catalysts. Recent advances have focused on the development of non-precious metal catalysts and atomically dispersed SACs to replace or reduce noble metal content [103]. SACs, where isolated metal atoms (such as Co, Ni, Fe, or Mo) are anchored on conductive supports like doped carbon, demonstrate maximized atomic efficiency and tunable electronic properties tailored for acidic HER. These catalysts create unique local coordination environments that facilitate proton-electron transfer and optimize hydrogen adsorption energies, thereby approaching the performance of platinum-based catalysts [104].

Additionally, defect engineering, such as the introduction of vacancies or heteroatom dopants into catalyst lattices, has been shown to significantly enhance acidic HER activity by modulating the electronic structure and providing more active sites for hydrogen adsorption. Carbon-based materials doped with nitrogen, phosphorus, or sulfur have emerged as promising metal-free or hybrid catalysts, exhibiting reasonable catalytic activity along with high chemical and mechanical stability in acidic media [105].

Despite these promising developments, challenges remain in ensuring the long-term durability and resistance to corrosion of non-noble catalysts under strongly acidic conditions. Active research seeks to improve their stability through protective coatings, strong metal-support interactions, and optimized synthesis strategies. It could be summarized that acidic HER catalysis prioritizes catalysts that can

effectively adsorb and desorb hydrogen intermediates while withstanding harsh acidic environments. Pt and Pt alloys continue to dominate, but advances in SACs, defect-rich materials, and doped carbon matrices pave the way for sustainable and cost-effective alternatives in this crucial domain of hydrogen production.

4.1.1. Noble metal-based catalysts (Pt, Pd, etc.)

The catalytic performance of noble metal-based HER catalysts, such as those utilizing platinum (Pt), ruthenium (Ru), and iridium (Ir), is strongly governed by their structural and electronic characteristics. By influencing catalytic activity, stability, and cost-effectiveness, these structure–property relationships play a vital role in advancing materials for sustainable hydrogen generation.

This section explores how crystal facets, nanoparticle morphology, alloying strategies, and single-atom architectures impact HER activity. The surface structure of noble metal nanoparticles, in particular, plays a critical role in determining both the density and accessibility of active sites. For instance, among platinum facets, Pt(111) exhibits a less negative hydrogen adsorption free energy (ΔG_H^*) than Pt(100), indicating weaker H binding that is closer to the thermoneutral value ($\Delta G_H^* \approx 0$). This optimal adsorption energetics enhances HER kinetics under acidic conditions [106].

Atomic-scale interactions further highlight the significance of surface structure. For example, studies of Pt surfaces interacting with iodine species offer a detailed view of the structure-property relationship [107]. Fig. 10 presents transition state (TS) structures associated with iodine desorption at CH_3CN/Pt interfaces across Pt(111), Pt(100), and Pt(411) facets. The Pt–I bond lengths are found to be 4.20 Å, 4.48 Å, and 4.49 Å, respectively, with iodine atoms (***I****) surrounded by CH_3CN molecules. Charge density difference maps indicate electron accumulation near iodine and depletion at platinum atoms, confirming the ionic nature of the Pt–I bond, characterized by negligible orbital overlap.

Bader charge analysis reveals a partial negative charge on ***I**** at the transition state, which varies slightly with the surface orientation. Desorption energy barriers ($\boldsymbol{E_a^{des}}$) correlate with iodine adsorption energies ($\boldsymbol{E_{ad}^{I}}$), showing the lowest barrier on Pt(111) at 0.39 eV and the highest on Pt(100) at 0.74 eV. Corresponding Gibbs free energy profiles at standard and equilibrium voltages indicate that the overall iodine reduction reaction (IRR) activity follows the trend: Pt(111) > Pt(411) > Pt(100), primarily due to differences in the iodine desorption step.

These findings underscore how atomic-scale surface structure modulates both adsorption strength and desorption kinetics, directly impacting catalytic efficiency. A detailed understanding of such mechanisms is essential for the rational design of high-performance noble metal catalysts, offering pathways to improved activity and durability [107].

It should be emphasized that iodine desorption studies can serve as a proxy for evaluating the strength of hydrogen binding on catalyst surfaces. This approach is based on the well-documented competitive

adsorption between halogen species and hydrogen on Pt(100), which indicates that both adsorbates occupy similar surface sites [108]. Therefore, analyzing the desorption energy and behavior of iodine helps infer the catalyst's hydrogen adsorption and desorption properties, which are crucial for HER activity. In HER, achieving an optimal balance between hydrogen adsorption and desorption is vital: too strong adsorption causes site poisoning and slows hydrogen release, while too weak adsorption results in inadequate proton reduction [109]. Hence, iodine adsorption and desorption studies indirectly reveal the hydrogen binding characteristics of the surface, guiding catalyst design by identifying ideal binding strengths that enhance HER efficiency. Although iodine is not directly involved in HER, its desorption studies provide valuable mechanistic insights that complement conventional HER activity measurements.

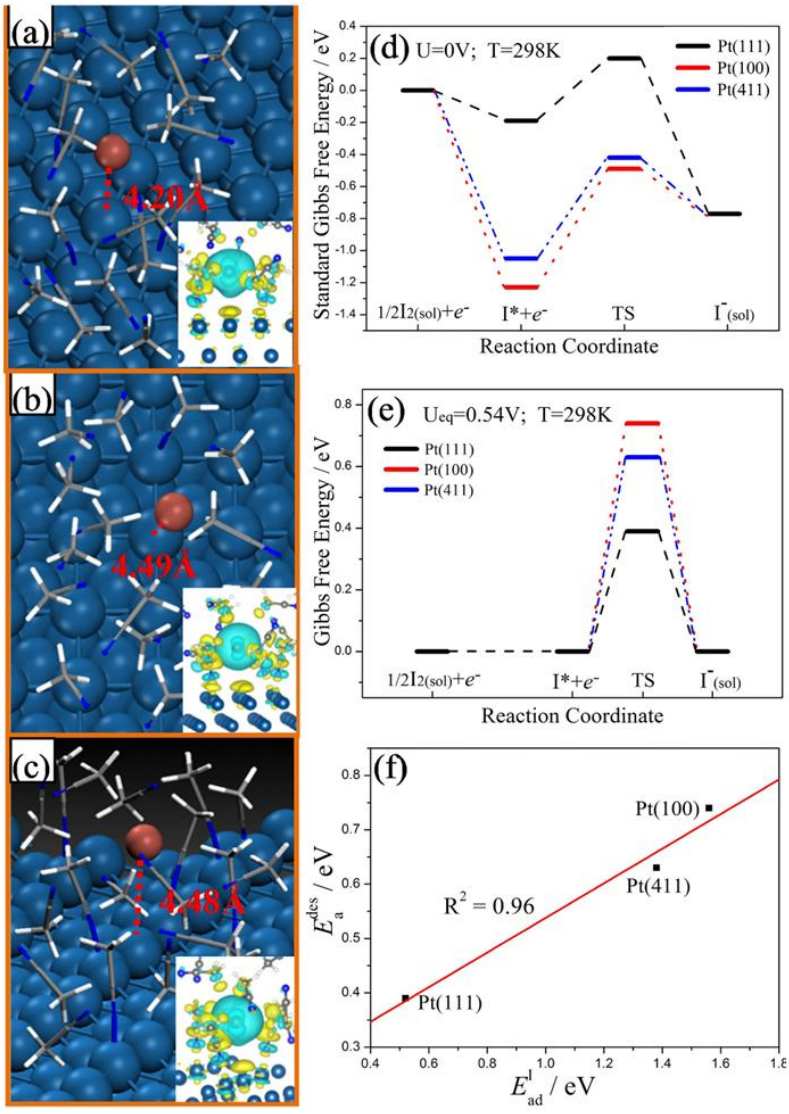


Fig. 10. The transition state structures and energy profiles associated with iodine desorption at CH_3CN/Pt interfaces on the Pt(111), Pt(100), and Pt(411) surfaces: **(a,b,c)** the geometries of TS along with charge density difference maps that highlight the ionic bonding between Pt and I, **(d)** standard Gibbs free energy profiles for the iodine reduction

reaction (IRR) at zero electrode potential, and **(e)** free energy profiles at the I_3^-/I^- equilibrium voltage (0.54 V). A linear correlation exists between iodine desorption barriers and adsorption energies, illustrating the influence of surface atomic structure on essential catalytic processes in noble metal-based HER catalysts; reproduced with permission from [107].

Admit also that facet engineering extends beyond platinum. For instance, introducing Ni into ruthenium (Ru) nanocrystals enables precise facet engineering, particularly exposing the highly active Ru (101) facet, which significantly enhances HER in acidic media. This facet modulation optimizes the hydrogen adsorption free energy, accelerating charge transfer kinetics and resulting in extraordinarily low overpotentials of 21.1 mV at 10 $mA \cdot cm^{-2}$, outperforming the benchmark Pt/C catalyst in acidic conditions [110].

It is well established that the size and morphology of noble metal nanoparticles critically influence their HER catalytic performance. Reducing particle size increases the surface-to-volume ratio, thereby exposing more active sites, which enhances catalytic activity [111]. Porous or dendritic nanostructures, such as iridium nanosheets, improve charge transport and electrolyte diffusion, lowering the overpotential during HER [111]. However, ultrasmall nanoparticles (<2 nm) often face agglomeration due to high surface energy, requiring stabilizers or supports, such as carbon-based materials, to maintain dispersion and catalytic stability [112].

Alloying is another effective strategy to tailor the properties of HER electrocatalysts. Combining noble metals with abundant transition metals such as nickel, molybdenum, or zinc can modify the electronic structure and reduce costs [111, 113]. For instance, Pt–Ni alloys shift the d-band center of Pt, tuning hydrogen adsorption and desorption kinetics [~~75~~ 113]. SACs, such as Ir_1/Co_3O_4, exhibit electronic structures similar to isolated atoms, resulting in lower activation barriers for water dissociation and enhanced charge transfer during HER [112, 114, 115]. SACs also demonstrate superior resistance to sintering and leaching compared to traditional nanoparticles, improving long-term stability [112].

Integrating these strategies, such as alloying with facet engineering or anchoring single atoms on high-surface-area supports, offers a pathway to high-performance, durable, and scalable HER catalysts. Advanced characterization methods, including in situ TEM and XAS, are indispensable for probing the dynamic structural and electronic changes that occur under operational HER conditions [116]. Future research should prioritize scalable synthesis techniques and mechanistic studies that bridge the gap between laboratory-scale innovations and real-world industrial deployment [111, 117].

4.2. HER catalysts in alkaline media

The hydrogen evolution reaction in alkaline media is mechanistically more complex than in acidic media, due to the necessity of water molecule dissociation as the primary source of protons [14]. The

additional water dissociation step introduces an energy barrier that significantly slows down the overall reaction kinetics, resulting in higher overpotentials and lower intrinsic catalytic activity compared to acidic conditions [118]. Overcoming this kinetic limitation is a central challenge in designing efficient alkaline HER catalysts.

Catalysts tailored for alkaline HER thus require bifunctional properties: the ability to efficiently dissociate water molecules and the ability to adsorb and desorb hydrogen intermediates effectively. Transition metal compounds, such as phosphides (Ni_2P, CoP), sulfides (MoS_2, WS_2), carbides, and nitrides, have emerged as leading candidates due to their favorable electronic structures, which promote both water activation and hydrogen evolution [119]. These materials often exhibit robust stability and scalability, making them promising alternatives to precious metals in alkaline electrolyzers. Interface and hybrid catalysts have attracted significant attention in alkaline HER due to their ability to combine complementary functionalities. By constructing heterostructures that couple catalytic materials with conductive supports or metal oxides/hydroxides, synergistic effects arise that enhance overall activity. In these systems, metal hydroxides provide active sites for the water dissociation step, while adjacent metal or metal compound domains facilitate hydrogen adsorption and molecular hydrogen formation. Such interface engineering improves charge transfer, modulates electronic states, and creates active sites that lower the energy barriers for both water cleavage and hydrogen evolution steps [120, 121]. Recent studies report core–shell structures, metal/metal-oxide heterojunctions, and nanoscale hybrid catalysts that deliver superior HER performance with low overpotentials and enhanced stability under alkaline conditions [122-124].

Despite these advances, challenges persist in fully elucidating the reaction mechanisms and developing catalysts that combine earth-abundant materials with industrial-scale durability and activity in alkaline electrolytes. Continued research in defect engineering, strain modulation, and theoretical modeling is essential to tailor catalysts that meet these demands. Alkaline HER catalysts are distinguished by their need to bridge water dissociation and hydrogen evolution steps, demanding multifunctional active sites and sophisticated interface designs. Transition metal compounds, hybrid interfaces, and SACs represent forefront strategies to address kinetic bottlenecks and propel alkaline hydrogen production technologies toward commercial viability.

4.2.1. Transition metal compounds (sulfides, phosphides, carbides, nitrides)

The HER activity of transition metal compounds, including sulfides, phosphides, carbides, and nitrides, is primarily dictated by the interplay between their atomic structures and electronic properties. These materials offer tunable properties that impact the kinetics of intermediate adsorption/desorption and the efficiency of charge transfer. Through targeted strategies such as anion selection and defect engineering, the performance of these catalysts can be significantly enhanced. Anion selection (e.g., *S*, *P*, *C*, or *N*) is

particularly critical, as it alters the d-band structure and influences charge distribution within the metal centers. Let's consider the most common anions and the possibility of their combination.

Sulfides: The high electronegativity of sulfur (2.58) creates electron-deficient metal centers, as observed in MoS_2, where catalytic activity is localized at edge sites while the basal plane remains largely inert. Engineering heterostructures such as MoS_2-Ni_3S_2 enables synergistic enhancements: MoS_2 contributes active edge sites, while Ni_3S_2 provides improved electrical conductivity [125]. Fig. 11 illustrates the electronic structure of a 1T-MoS_2/NiS heterostructure, revealing that heterojunction formation shifts the projected density of states near the Fermi level [126]. This shift reflects enhanced electronic conductivity and a favorable alignment of the d-band center, which together improve charge transfer and optimize the hydrogen adsorption free energy (ΔG_H^*). Charge density difference analysis further shows significant electron migration from NiS to MoS_2, enriching Mo centers with electrons while preserving structural stability. This interfacial charge redistribution lowers the energy barriers for hydrogen adsorption and desorption, facilitating the Volmer step and enhancing overall HER kinetics [126].

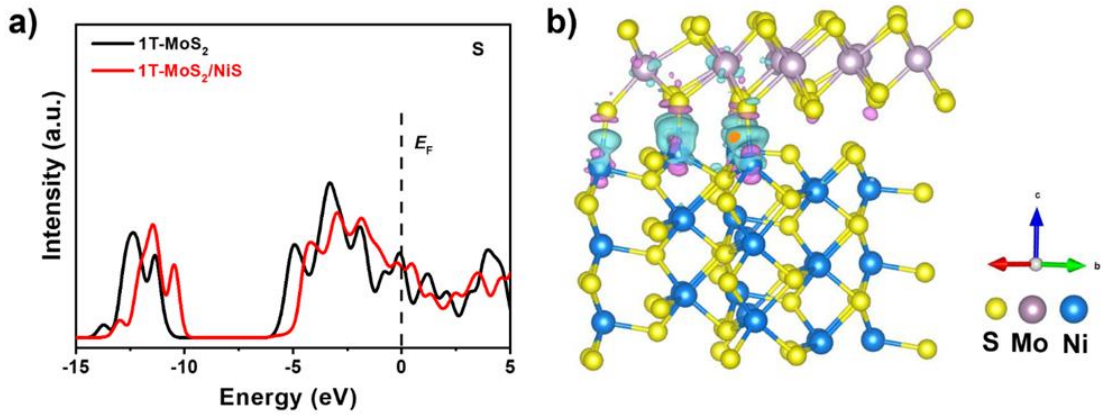


Fig. 11. The electronic structure and charge transfer analysis of the 1T-MoS_2/NiS heterostructure: (a) the projected density of states illustrates a comparison among pristine 1T-MoS_2, NiS, and the heterostructure. This analysis reveals an increase in electronic states close to the Fermi level, which contributes to improved conductivity and catalytic activity. The charge density difference map illustrates the transfer of electrons from NiS to MoS_2. This process enhances the electron density at the Mo active sites, thereby optimizing hydrogen adsorption and improving the kinetics of the HER, and (b) the design of the heterostructure skillfully merges the high catalytic activity found at the edges of MoS_2 with the excellent conductivity of NiS, leading to a notable improvement in HER performance; reproduced with permission from [126].

Phosphides: The lower electronegativity of phosphorus (2.19) relative to sulfur or nitrogen allows for greater electron donation to metal centers. In cobalt phosphide (CoP) catalysts, this electron redistribution at Co sites lowers ΔG_H^*, thus improving hydrogen binding characteristics and catalytic performance [127].

Carbides: The incorporation of carbon into transition metals such as molybdenum contracts the metal's d-band, producing an electronic configuration similar to that of platinum. Molybdenum carbide (Mo_2C),

for example, exhibits HER activity comparable to Pt due to its optimal hydrogen binding energy and favorable reaction kinetics [128].

Nitrides: Nitrogen, with its high electronegativity (3.04), plays a key role in modifying oxidation states and facilitating metal-to-ligand charge transfer. Transition metal nitrides such as titanium nitride (TiN) exhibit improved electrical conductivity, chemical stability, and corrosion resistance compared to their metallic counterparts, contributing to enhanced catalytic performance [129].

Multi-Anion Systems: Introducing multiple anionic species can further enhance catalytic behavior via synergistic electronic modulation. For instance, N/P/S co-doped Mo_2C demonstrates a remarkably low overpotential of 53 mV at 20 mA/cm² in acidic media, outperforming single-anion doped variants. This enhancement arises from the coordinated tuning of electronic properties in both the Mo centers and the carbon matrix, resulting in improved active site functionality and charge mobility [130].

Recent theoretical and experimental studies converge on a synergistic interaction between heteroatoms in multi-doped Mo_2C catalysts that improves HER activity. The work based on DFT has shown that co-dopants can redistribute electron density around Mo centers and shift the d-band characteristics, thereby tuning H-adsorption energetics; for example, P and transition-metal co-doping has been shown to act as complementary anion/cation dopants that decrease the negative H-binding energy of Mo_2C [131]. Experimental studies on N,P,S multi-doped Mo_2C/C and on N,P/N,S co-doped Mo_2C/C corroborate these findings, reporting improved HER metrics and attributing the enhancement to electronic-configuration modulation of both Mo_2C and the carbon matrix. XPS, EPR and MAS-NMR measurements (and complementary electrochemical characterization) indicate dopant-induced shifts in Mo electronic states and ligand environments that stabilize active sites and optimize proton–electron transfer. Together, these DFT and operando/ensemble characterizations underscore the power of multi-heteroatom engineering for precisely tuning Mo electronic structure toward superior HER performance [130, 132].

The rational design of transition metal compound catalysts through heterostructuring, anion tailoring, and multi-element doping provides a versatile platform for achieving high HER efficiency. These strategies highlight the importance of understanding structure-property relationships at the atomic and electronic levels for the development of next-generation electrocatalysts.

The intentional introduction of vacancies is a powerful strategy to tune local electronic environments in HER catalysts. For example, sulfur vacancies in MoS_2 expose under-coordinated Mo sites and introduce defect states that both increase active-site density and lower the barrier for water dissociation, enhancing HER reactivity [133, 134]. Nitrogen vacancies in transition-metal nitrides (e.g., VN) similarly modify local charge density and can markedly improve H-adsorption energetics, especially when combined with conductive supports or metal species [135, 136]. In transition-metal phosphides, phosphorus vacancies often accelerate in-situ surface reconstruction (formation of Co-oxyhydroxide-like species), which can

generate highly active surface phases under operating conditions [137, 138]. Beyond vacancies, substitutional heteroatom doping provides precise control over charge transfer and orbital hybridization. Cation substitution (for example, transition-metal doping of Mo_2C) and anion doping (S, P, N into Mo_2C or M-N-C sites) both alter d-band characteristics and hydrogen binding energies; in some cases, sulfur or phosphorus incorporation weakens Mo–H binding and improves HER kinetics [130, 139].

Dual and multi-anion doping strategies (e.g., N/P or N/P/S in Mo_2C) can be especially effective by creating charge-compensated electronic configurations and faster kinetics (for example, N,P,S-multi-doped Mo_2C/C achieves one of the lower Tafel slopes reported among doped Mo_2C catalysts) [130]. Nonetheless, deconvoluting dopant vs. defect effects in multi-component systems remains challenging and requires operando/ in-situ spectroscopies together with theoretical descriptors and data-driven synthesis approaches to identify causal structure–function relations [127, 140].

4.2.2. Hybrid and interface-engineered catalysts

Hybrid and interface-engineered catalysts have become a key class of HER materials, providing significant benefits by leveraging synergistic interactions at material interfaces to overcome the limitations of individual components and achieve superior catalytic performance. The effectiveness of these systems heavily depends on the relationship between atomic-scale structures and electrochemical properties. By intentionally designing interfaces and composite architectures, researchers can utilize synergistic electronic effects and optimized active site arrangements to greatly improve catalytic activity.

One illustrative example is the MoS_2/graphene hybrid, which demonstrates how interfacial interactions can transform the catalytic behavior of inherently limited materials [141]. While pristine MoS_2 suffers from low electrical conductivity and largely inert basal planes, integration with graphene introduces efficient charge-transfer pathways, thereby enhancing electron mobility and overall catalytic performance [141, 142].

This effect is further magnified through defect engineering. The introduction of sulfur vacancies (V_S) and Mo-on-S antisite defects (Mo_{S_2}) results in localized electron-rich regions that effectively lower the hydrogen adsorption free energy (ΔG_H^*) to values near thermoneutral [141]. Additionally, the application of biaxial tensile strain (up to about 5 %) has been shown to synergistically interact with these defects by modulating the d-band center of Mo atoms, thus optimizing the binding strength of hydrogen intermediates. Strained V_S sites can achieve a theoretical $\Delta G_H \approx 0$ eV, a hallmark of ideal HER catalysts [141].

Beyond electronic enhancements, the graphene substrate provides structural benefits by preventing MoS_2 restacking, maintaining high surface area, and forming strong interfacial bonds that improve catalyst durability [142]. This is illustrated in Fig. 12a, which shows the superior HER activity of MoS_2 nanoparticles supported on reduced graphene oxide (RGO) compared to either component alone. The

improved performance is attributed to the chemical and electronic coupling at the MoS_2/RGO interface, which not only promotes rapid charge transport but also prevents MoS_2 aggregation, increasing the number of accessible catalytic edge sites [143]. Furthermore, Fig. 12b highlights the exceptional electrochemical durability of the MoS_2/RGO hybrid catalyst. After 1,000 continuous HER cycles, the catalyst retains its activity with negligible current loss, underscoring the role of graphene in preserving structural integrity and ensuring long-term operational stability [143].

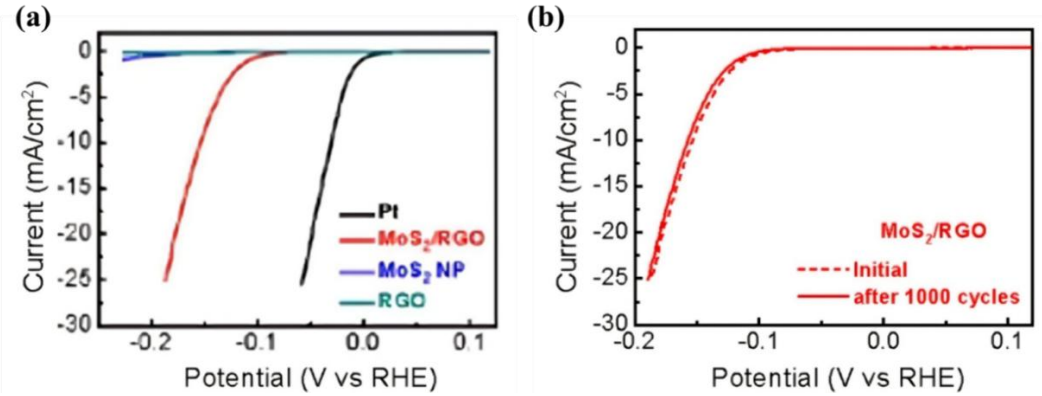


Fig. 12. (a) Comparison of HER activity for free MoS_2, RGO, and MoS_2/RGO hybrid catalysts. The MoS_2/RGO hybrid exhibits dramatically superior HER performance, attributed to strong electronic coupling at the interface, which facilitates rapid electron transfer and maximizes the exposure of active edge sites for catalysis, and **(b)** cycling stability of the MoS_2/RGO hybrid catalyst over 1,000 cycles. The negligible change in performance confirms the role of graphene in preventing MoS_2 restacking and maintaining catalyst durability during prolonged HER operation; reproduced with permission from [143].

Direct evidence of interfacial electronic coupling in MoS_2/RGO composites has been shown using advanced spectroscopic and theoretical techniques. XPS studies display clear shifts in the binding energy in the Mo 3d and S 2p spectra after integration with reduced graphene oxide, indicating charge transfer and strong interfacial interactions [144]. Near-edge X-ray absorption fine structure (NEXAFS) and resonant Auger spectroscopy measurements further reveal changes in unoccupied electronic states near the Fermi level, reflecting alterations in the local electronic environment at the MoS_2–RGO interface [144]. Complementary DFT charge-density-difference analyses demonstrate significant electron redistribution localized at the interface, supporting the experimental results [145]. Collectively, these characterizations confirm the important role of interfacial electronic coupling in enhancing HER activity, as observed in Fig. 12.

Heterostructure architectures and synergistic interfacial effects can be intentionally designed to improve catalytic performance beyond that of individual components, as summarized in Table 3. Such composite catalysts utilize interfacial electron redistribution, enabling more favorable electronic structures

and enhanced active site exposure. For example, in the MoS_2–g–$CuNi_2S_4$ nanocomposite, the addition of copper and nickel dopants increases the electron density at sulfur sites, while graphene anchoring helps expose more catalytic edge sites [142]. XPS analysis confirms an increased fraction of metal-bonded sulfur species from 40.02 % in the MoS_2–$CuNi_2S_4$ composite to 48.83 % in the graphene-integrated MoS_2–g–$CuNi_2S_4$, indicating a higher proportion of catalytically active sulfide species. This hybridization also slightly raises the total surface sulfur content (from 15.95 % to 17.04 %), supporting improved active site exposure [142]. This dual-modification approach, combining heteroatom doping and interfacial engineering, achieves platinum-like HER activity with earth-abundant materials. The key performance metrics for various HER catalysts are detailed in Table 4.

Table 3. Heterostructure architectures and synergistic effects in composite catalysts.

Material system	Key synergistic effect	HER performance metric
MoS_2-graphene-$CuNi_2S_4$ [142]	Charge transfer from Cu/Ni dopants to MoS_2	Tafel slope: 29.3 mV/dec
B,N-doped CNS-hBN [146]	hBN edge sites activate the carbon framework	Onset potential: -50 mV vs RHE
Pt/TiO_2 [40]	SMSI modulates Pt oxidation state	10x current density vs bulk Pt

Table 4. Comparative HER performance metrics of representative catalysts.

Type	Catalyst	Overpotential 10 mA/cm^2 (mV)	Tafel slope (mV/dec)	Exchange current density (mA/cm^2)	Stability (hours)/cycles	pH	Refs.
Noble Metal	Pt/C	~20	~30	High	>100 h /10000	Acidic (0.5 M H_2SO_4)	[11, 147]
Transition Metal Phosphide	Ni_2P	~50 – 150	~40 – 70	~10^{-3} – 10^{-1}	tens to > 50 h /500	Acidic (0.5 M H_2SO_4) Alkaline (1 M KOH)	[148-150]
Transition Metal Sulfide	MoS_2	~31 – 210	~40 – 120	~10^{-4} – 10^{-1}	14–100 h/ 1000	Alkaline (1 M KOH)	[151-155]
Single-Atom Catalyst	Pt-SAC on graphene	~19 – 50	~25 – 40	~10^{-3} up to ~1	Tens → >100 h/ 1000	Acidic (0.5 M H_2SO_4)	[156-158]
Hybrid Catalyst	N-doped graphene supported MoS_2	112	44	-	-/1000	Acidic (0.5 M H_2SO_4)	[159]
Hybrid Catalyst	Pt/α-MoC	- (125 mV to achieve a current density of 1000 mA cm^{-2})	-	-	300 h/-	pH universal	[160]
Metal Carbide	Mo_2C-embedded nitrogen-doped	45 86	46 62	1.14	-	1 M KOH	[161]

	porous carbon nanosheets (Mo_2C@2D-NPCs)					0.5 M H_2SO_4	
Metal Sulphide	VS_2 nanostructures on Mo/Co	63	50	-	35 h/-	1 M KOH	[162, 163]
Transition Metal Carbide	W_2C	130 173	100 86	0.438 0.194	20 h/-	1 M KOH 0.5 M H_2SO_4	[164]
Transition Metal Phosphide	CoP	94	42	-	25 h/-	1 M KOH	[165]
Non-metallic Catalyst	Boron Carbonitride (BCN) with tunable B/N Lewis acid/base	~100	61.3	-	48 h/2000	1 M KOH	[166]
Transition Metal Oxide	NiO/Ni@NCNTs	87.5	80	-	24 h/-	1 M KOH	[30]

According to strategies for modulating electronic structure, three main approaches have been identified for tuning catalytic centers at the atomic level: (i) ***Defect engineering*** involves creating sulfur vacancies in MoS_2, which not only increases the number of exposed active sites but also causes localized lattice strain, thereby boosting catalytic activity [141]; (ii) ***Doping*** effects occur when transition metal dopants such as copper and nickel are introduced, altering the d-band electron distribution, which effectively weakens the hydrogen binding energy (ΔG_H) and enhances HER kinetics [142, 167]; and (iii) ***Interfacial charge transfer*** involves electron withdrawal by a graphene substrate from the MoS_2 layer, creating electronically activated regions, especially at phase or domain boundaries [168, 169].

Collectively, these atomic-level modifications reduce kinetic barriers associated with both the Volmer-Heyrovsky and Volmer-Tafel mechanisms. DFT calculations support these findings, reporting energy barriers of less than 1 eV in optimally engineered heterostructures [170, 171].

4.3. HER catalysts in acidic/alkaline media

While HER catalysis in acidic and alkaline media inherently involves different reaction pathways and kinetic challenges, some catalysts show strong and efficient activity in both environments. Catalysts with a wide pH range usability are essential for flexible electrolyzer design, allowing operation under various conditions and supporting cost-effective hydrogen production. Platinum and other Pt-group metals remain benchmark catalysts with outstanding performance due to their near-ideal hydrogen binding energies, which favor both proton reduction in acidic media and effective water splitting and hydrogen adsorption in alkaline conditions. However, the high cost and limited availability of these noble metals drive ongoing research into alternative catalysts that can work efficiently in both acidic and alkaline electrolytes. Transition metal

compounds, such as phosphides, sulfides, and carbides, have gained attention for their promising bifunctional abilities, providing solid HER activity across a broad pH range. Their catalytic features can be precisely adjusted through heteroatom doping, defect engineering, and nanostructuring to optimize electronic states and surface chemistries suited for dual-environment catalysis [172, 173].

Carbon-based materials doped with heteroatoms such as N, P, B or S also demonstrate promising HER performance across both acidic and alkaline media [174-178]. Adjusting their electronic structure, surface functionalities, and active site distributions enhances their catalytic activity in various environments. When combined with metallic components in hybrid structures, these catalysts benefit from synergistic effects that enhance charge transfer and facilitate the adsorption and desorption of reaction intermediates. Interface and hybrid catalyst designs, which incorporate strong metal-support interactions and heterostructured phases, are becoming key to achieving multifunctionality. For such catalysts, it is necessary to modify local electronic environments and support efficient catalytic cycles for both proton reduction and water dissociation, addressing the mechanistic differences in acidic and alkaline HER reactions.

The development of pH-universal HER catalysts is a burgeoning area of research, driven by the demand for versatile hydrogen production technologies. Designing such catalysts requires addressing the distinct mechanistic and energetic challenges posed by different proton sources and reaction intermediates in various pH environments. Bifunctional active sites that facilitate both proton reduction and water dissociation are central to this goal [179]. Interface engineering, forming heterostructures that combine metals with oxides or carbides, adjusts adsorption energies and accelerates charge transfer, enabling effective catalysis under all pH conditions [123, 168]. Single-atom catalysts also exhibit promising universal activity by precisely tuning local coordination and electronic structure to balance adsorption and desorption kinetics [180]. Notable examples include subnanometric Pt/α-MoC catalysts demonstrating low overpotentials and high current densities in acidic and alkaline media, highlighting the synergy between metal components for proton reduction and carbide phases promoting water dissociation [160]. Surface defect engineering and heteroatom doping further enhance the robustness and adaptable performance of pH-universal HER catalysts, enabling efficient activity across acidic, neutral, and alkaline environments [168, 179]. Table 5 summarizes some of the most efficient pH-universal HER catalysts with key quantitative characteristics and literature references.

Table 5. Representative pH-universal HER catalysts with key structural features and electrochemical performance.

Catalyst	Structure / Type	Electrolyte	Overpotential @ 10 mA/cm² (mV)	Tafel Slope (mV/dec)	Key Feature	Refs.
Pt/α-MoC	Subnanometric metal/carbidic hybrid	Acidic & Alkaline	22.2 -	22 -	Synergy: Pt for proton	[160]

					reduction, MoC for water dissociation	
1T0.81-MoS_2@Ni_2P	Multi-heterojunction interfaces	Acidic & Alkaline	38.9 95	41 42	Bifunctional active sites, enhanced conductivity	[168]
Rh NP/PC (porous carbon)	Supported metal nanoparticle catalysts	Acidic & Alkaline	21 33	34 -	Interface engineering, high active site density	[180]
Rh_2P/NPC	Metal phosphide/graphene hybrid	Acidic & Alkaline	40 17	- -	Interface engineering, high active site density	[180]
N–Co_2P/CC (carbon cloth)	N-atom doping to tailor the electronic structure	Acidic & Alkaline	27 34	45 51	Enhanced intrinsic activity, fast charge transfer, and mechanical and chemical stability	[180]
MoS_2/Mo_2C	Heterostructured Interface Catalyst	Acidic & Alkaline	- -	40 43	Improved interfacial mass transfer, robust pH-universal activity	[179]

Despite significant progress, fundamental challenges persist in fully elucidating the universal catalytic mechanisms and achieving long-term operational stability under industrially relevant conditions. Continued efforts integrating atomic-scale engineering, operando characterization, and advanced computational modeling are essential to accelerate the rational design of next-generation pH-universal HER electrocatalysts. Such approaches will enable the development of flexible, durable, and scalable systems for the sustainable production of green hydrogen.

4.3.1. Carbon-based and non-metallic catalysts

Carbon-based and other non-metallic materials have recently gained significant attention as promising classes of catalysts for HER owing to their tunable electronic structures, high structural versatility, and cost-

effectiveness. These materials encompass a wide spectrum of systems, ranging from heteroatom-doped carbons to truly metal-free two-dimensional compounds.

Truly metal-free catalysts are composed entirely of non-metal elements and exhibit intrinsic catalytic activity without the participation of metal centers. Representative examples include hexagonal boron nitride (h-BN) and phosphorene. Hexagonal boron nitride, a two-dimensional material analogous to graphene but composed of alternating boron and nitrogen atoms, possesses a wide bandgap and excellent chemical stability. Its catalytic activity toward HER has been attributed to defect-induced electronic states and reactive edge sites that enable favorable proton adsorption and electron transfer, even in the absence of metal species [181].

Similarly, phosphorene, an atomically thin allotrope of black phosphorus, exhibits tunable electronic and chemical properties that facilitate hydrogen adsorption and reduction through its anisotropic surface structure and adjustable bandgap. These features allow phosphorene to catalyze HER via purely non-metallic pathways [182].

While materials like h-BN and phosphorene exemplify non-metallic systems with intrinsic catalytic potential, carbon allotropes such as graphene and carbon nanotubes (CNTs) represent another crucial category of HER catalysts, offering highly conductive, chemically tunable frameworks that can be tailored for enhanced reactivity. Heteroatom-doped carbon materials, including those doped with nitrogen, sulfur, phosphorus, or boron, have been widely studied for HER applications [183]. Doping introduces heteroatoms into the carbon lattice, altering its electronic configuration and creating localized charge redistribution that improves proton adsorption and promotes electron transfer during hydrogen evolution [184, 185]. However, many synthesis routes for these doped carbons involve metal-containing precursors or catalysts, which can leave trace metal residues in the final material. These metallic impurities introduced isolated metal atoms in SACs can significantly contribute to the overall catalytic activity, making it difficult to classify such systems as entirely metal-free.

It should be highlighted that graphene and CNTs serve as promising platforms for HER due to their: (i) exceptional electrical conductivity arising from sp^2-hybridized carbon networks, (ii) high surface area with abundant edge sites and defect structures, and (iii) chemical tunability through functional group modification or heteroatom doping. While pristine graphene's basal planes are generally catalytically inert, edge defects and vacancies can be activated through targeted functionalization strategies. For instance, ***nitrogen doping*** introduces asymmetric charge distributions across the graphene lattice, creating electron-rich regions that promote proton adsorption and thereby enhance HER activity [186].

Recent studies increasingly support that ***sulfur doping*** creates defect/strain-induced structural distortions in carbon materials, enhances conductivity and modifies adsorption properties [187, 188]. However, direct observations in sulfur-doped CNTs that quantify changes in work function or curvature

strain in relation to HER remain rare. Existing works often involve co-doping, hybrid structures, or use analogous carbon frameworks (e.g., S-doped carbon nanofibers, S-doped g-C_3N_4) or include metal components.

The incorporation of heteroatoms such as N, S, and P into the carbon lattice enables the creation of tailored active sites with specific electronic properties, as summarized in Table 6. In particular, ***dual-doping strategies*** produce synergistic electronic effects: for example, ***N/S co-doped carbon materials*** exhibited superior performance for electrocatalytic oxygen evolution reaction [189]; ***N/P co-doped graphene*** achieves an improvement in HER efficiency in comparison with single (N or P)-doped materials, confirming the synergistic coupling effect in N,P-graphene [190]. Additionally, the calculated hydrogen adsorption energy (−0.117 to −0.173 eV) on heteroatom ***B/N-doped porous graphene*** lies within the optimal range (−0.1 to −0.2 eV) for high-performance adsorbents, indicating that both the structural porosity and the presence of heteroatom dopants play a critical role in enhancing H_2 adsorption [191].

Table 6. Effects of heteroatom doping on metal-free carbon-based catalysts for HER.

Dopant	Electronegativity	Effect on carbon structure	HER performance impact
Nitrogen	3.04	Formation of pyridinic, pyrrolic, and graphitic N; introduces localized electron-rich sites; modifies charge distribution	Enhances proton adsorption, improves electron transfer, increases HER activity; secondary heteroatoms can further boost activity [183-186]
Phosphorus	2.19	Distorts carbon lattice; induces charge redistribution; adjusts bandgap and local electronic environment	Facilitates hydrogen adsorption; synergistic dual-doping (N/P) improves HER efficiency [182, 190]
Sulfur	2.58	Creates defects, strain, and curvature in carbon lattice; improves surface hydrophilicity and electron mobility, induces spin density redistribution, creating active sites for intermediate adsorption, which is crucial for efficient HER, especially at edge sites	Enhances proton adsorption and electron transfer; boosts HER performance; co-doping can create synergistic effects [183, 187, 188]

While heteroatom doping tailors the electronic structure of carbon-based metal-free catalysts to enhance proton adsorption and electron transfer, further improvements in HER performance can be achieved through defect engineering (Fig. 13) [192]. Controlled generation of structural defects amplifies catalytic activity through several mechanisms: (i) ***Edge site exposure*** – The formation of zigzag or armchair edges in graphene introduces unsaturated carbon atoms that serve as highly active sites for hydrogen adsorption, these edge sites have been shown to significantly enhance HER performance [192]; (ii) ***Vacancy formation*** – The removal of carbon atoms induces localized charge polarization, particularly at pyridinic nitrogen-vacancy sites, which significantly lowers the hydrogen adsorption free energy (ΔG_H^*) to near-thermoneutral levels, thereby facilitating HER kinetics [192]; (iii) ***Pore architecture*** – Engineering hierarchical pore structures in 3D graphene frameworks enhances mass transport while exposing a greater number of internal active sites [192].

Experimental evidence supports these effects: sulfur vacancies in carbon-sulfur composites have been shown to reduce the energy barrier for the Volmer step by approximately 40 %, while nitrogen vacancies in carbon nitrides enable the development of metal-free catalysts with turnover frequencies comparable to those of platinum [192].

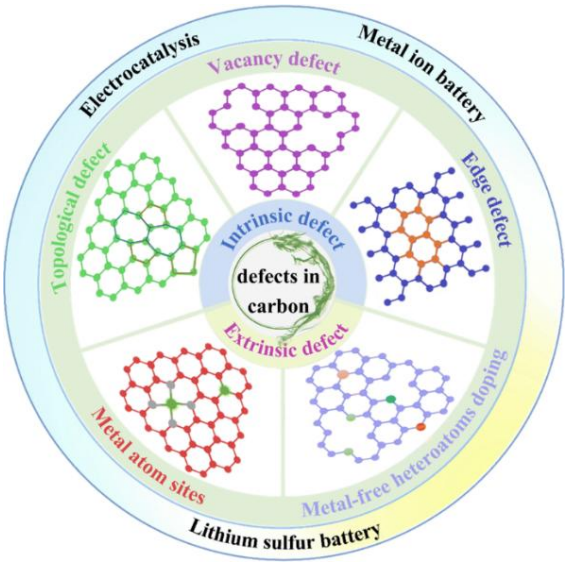


Fig. 13. A schematic of defect engineering in carbon for energy storage and conversion, reproduced with permission from [192].

Recent studies have revealed several key structure-property relationships that inform the rational design of high-performance HER and oxygen reduction reaction (ORR) catalysts for efficient hydrogen generation. These include: (i) ***Charge density modulation*** – The strategic placement of dopant atoms, such as graphitic nitrogen, when coordinated with pentagon defects, optimize the density of states near the Fermi level, leading to optimized binding energies with oxygen-containing intermediates that assiste four-electron ORR activity in both alkaline and acidic media [193]; (ii) ***Dopant coordination control*** – for metal-free carbon-based catalysts, the term "dopant coordination control" usually refers to the strategic arrangement of heteroatoms (like N, P, S, or B) within the carbon lattice to create specific local electronic environments that optimize HER activity, even in the absence of metal centers [192]; (iii) ***Defect-dopant synergy*** – Combining phosphorus doping with mesoporous architectures in carbon frameworks significantly boosts HER performance. For example, P-doped carbon with mesopores ensures the sufficient exposure and availability of catalytic sites to realize considerable catalytic activity and facilitate the movement of the reactants (H_2O), producing efficient HER kinetics [194].

It needs to be emphasized that carbon-based and other non-metallic catalysts demonstrate immense potential for efficient and sustainable HER catalysis due to their tunable electronic structures, structural versatility, and metal-free active sites. By integrating heteroatom doping, defect engineering, and pore

architecture optimization, these materials achieve precise control over charge distribution and active site density, thereby advancing the development of next-generation, high-efficiency, and environmentally sustainable electrocatalysts.

4.3.2. MXenes as Emerging HER Electrocatalysts

MXenes, a rapidly expanding family of two-dimensional transition metal carbides, nitrides, and carbonitrides ($M_{n+1}X_nT_x$, where T_x represents surface terminations such as –O, –OH, and –F), have emerged as one of the most promising classes of materials for HER electrocatalysis [195, 196]. Their exceptional metallic conductivity, adjustable surface chemistry, and structural robustness make them highly suitable for facilitating fast charge transfer and efficient hydrogen adsorption. Typically derived from the selective etching of MAX phases followed by delamination, MXenes offer large accessible surface areas and tunable electronic structures that can be precisely engineered to optimize catalytic activity.

The catalytic behavior of MXenes is largely dictated by their surface terminations and compositional versatility. Recent studies have demonstrated that the modification of surface groups and heteroatom incorporation can dramatically alter the hydrogen adsorption free energy (ΔG_H^*), thereby tuning the intrinsic catalytic properties. For instance, computational analyses and machine-learning-assisted screening have revealed that the composition and surface terminations of 2D MXene ordered binary alloys can effectively modulate the hydrogen adsorption free energy (ΔG_H^*), enabling the rational design of highly active MXene-based catalysts for HER [197].

Experimentally, Luxa et al. reported that $Mo_2TiC_2T_x$ MXene derived from Mo_2TiAlC_2 exhibited enhanced HER activity attributed to dynamic surface reconstruction and the in situ generation of MoO_2 species during operation, which created a synergistic interface that enhances charge transport and catalytic kinetics [198]. Similarly, heteroatom doping has proven effective in adjusting electronic states; for example, Zr-doped MXenes, such as Ti_3C_2 and Ti_3CN, achieved near-thermoneutral ΔG_H^* values of 0.18-0.16 eV, conditions ideal for efficient hydrogen adsorption and desorption, which significantly boost HER performance [199]. Moreover, expanding the MXene family beyond traditional $M_{n+1}X_n$ compositions, such as introducing M_5X_4 and TMA+-intercalated Mo_4VC_4 variants, has shown promise in improving electrochemical stability due to increased interlayer spacing that enhances proton accessibility [200].

Although pristine MXenes exhibit moderate HER activity, their catalytic performance can be greatly enhanced through hybridization and compositing strategies. Integration with other catalytic materials, such as transition metal dichalcogenides (TMDs), metal–organic frameworks (MOFs), and single-atom catalysts, has yielded remarkable synergies [201-205]. For example, the MXene hybrid nanosheet composed of WS_2/Ti_3C_2 has been demonstrated to be an efficient electrocatalyst for HER [201]. In this hybrid system, WS_2 contributes a high surface area and abundant active sites for electrocatalytic activity, while the MXene

Ti_3C_2 enhances charge transfer efficiency. Another representative example is the $Ti_3C_2T_x$-engineered MoS_2/SiNWs multifunctional photocathode, which has been identified as a suitable candidate for photoelectrochemical hydrogen generation [202]. This photocathode exhibited a current density of –0.10 mA/cm² at 0 V versus RHE, with a resistance of 102 Ω, indicating its efficient photoelectrochemical performance. Zhang et al. demonstrated that the synergistic coupling among $Mo_2TiC_2T_x$ MXene, Ni_2S, and MoS_2 significantly enhances HER performance [203]. The MoNiS/$Mo_2TiC_2T_x$ catalyst, tested in 1 M KOH solution, exhibited remarkable HER activity with a low overpotential of 153 mV to achieve a current density of 10 $mA \cdot cm^{-2}$ and a small Tafel slope of 92 $mV \cdot dec^{-1}$. Furthermore, the catalyst displayed excellent stability, maintaining its activity for at least 12 hours without noticeable degradation.

Luo et al. achieved excellent HER catalytic activity through the synergistic combination of small-sized Ru nanoparticles, leaf-shaped ZIF-L(Co) nanosheets with abundant active sites, and the high electrical conductivity of MXene [206]. The resulting Ru@ZIF-L(Co)/FL-$Ti_3C_2T_x$ nanocomposite exhibited outstanding HER performance, requiring only a low overpotential of 16.2 mV to reach a current density of 10 $mA \cdot cm^{-2}$, along with a small Tafel slope of 21.0 $mV \cdot dec^{-1}$ and remarkable stability in 1.0 M KOH solution. Pandey et al. revealed that integrating $Ti_3C_2T_x$ MXene with α-Fe_2O_3 into a nanocomposite represents a promising strategy for enhancing catalytic performance [207]. This synergistic combination effectively addresses the individual limitations of each component by improving stability, electrical conductivity, and interfacial charge dynamics. Furthermore, the authors provided a comprehensive summary of representative MXene-based catalysts, highlighting several with outstanding HER performance, as presented in Table 7.

Table 7. Comparative Electrocatalytic Performance of $Ti_3C_2T_x$-Derived Catalysts for HER. Data extracted from Ref. [207].

Catalyst	Electrolyte	Tafel slope ($mVdec^{-1}$)	Overpotential @ 10 $mAcm^{-2}$ (mV)
$Pt_3Ti/Ti_3C_2T_x$	0.1 M HClO4	32	33
$Mo_2TiC_2T_x$-Pt_{SA}	0.5 M H_2SO_4	30	30
$Pd_{NPS}/Ti_3C_2T_x$/ CNTs	0.1 M KOH	50	158
$CoP/Ti_3C_2T_x$	1 M KOH	57	113
$Ti_3C_2T_x$- N_6	1 M KOH	61	119
1 T/2H-$MoSe_2$/ Ti_3C_2	1 M KOH	91	95

When considering efficient MXene-based HER catalysts, it is important to highlight single-atom catalysts immobilized on layered MXene nanosheets. A notable example is iodine single atoms supported

on MXene [205]. This material exhibits a remarkably low overpotential of 190 mV at a current density of 10 $mA \cdot cm^{-2}$, along with an improved Tafel slope of 69 $mV \cdot dec^{-1}$. In addition, the catalyst demonstrates a high turnover frequency and excellent stability, making it a promising candidate for practical HER applications. A systematic analysis of SACs supported on MXene-based materials has been conducted by Wang et al. [208]. Their study emphasizes the prominent role of noble-metal SACs on MXene, highlighting their exceptional catalytic performance and significance in HER applications.

Despite remarkable progress, several challenges continue to hinder the large-scale application of MXene-based catalysts for HER [196]. One major limitation is surface oxidation, where MXenes, particularly $Ti_3C_2T_x$, tend to form oxide layers such as TiO_2 during electrochemical cycling or storage, leading to decreased electrical conductivity and degradation of active sites. In addition, the strong van der Waals interactions between adjacent nanosheets promote restacking, which restricts ion diffusion and reduces the accessible surface area. To overcome this, various strategies such as introducing interlayer spacers, heteroatom doping, or constructing three-dimensional porous architectures have been utilized to preserve open frameworks and enhance mass transport. Moreover, scalable and environmentally benign synthesis routes capable of precisely controlling surface terminations, defect densities, and layer thicknesses remain underdeveloped. Understanding the true nature of active sites and their dynamic behavior during HER also requires advanced in situ and operando characterization techniques.

Nevertheless, MXenes remain a highly tunable and promising platform for next-generation HER electrocatalysts. Their intrinsic metallic conductivity, compositional flexibility, and chemically modifiable surfaces provide unique opportunities to design high-performance, earth-abundant, and durable catalytic systems. Continued advancements in surface engineering, heterostructure design, and real-time structural analysis are expected to unlock their full potential in HER applications.

5. Challenges and future perspectives

5.1 Remaining knowledge gaps

Despite notable advancements in HER catalysis, several critical knowledge gaps remain unresolved. A major limitation lies in the insufficient resolution of current in situ and operando characterization techniques, which struggle to fully capture the dynamic transformations of catalyst surfaces during actual electrochemical operation. Many catalytic processes involve fleeting intermediates and subtle electronic restructuring that conventional ex-situ approaches fail to detect. Although advanced operando techniques, such as in situ XAS, electrochemical Raman spectroscopy, and SEM, have shown promise, further methodological improvements are necessary to achieve real-time, atomic-level visualization of active site evolution and reaction intermediates under realistic working conditions [209, 210].

A second critical issue is the limited understanding of degradation mechanisms that compromise catalyst durability. While some materials, such as MoS_2, demonstrate commendable stability, others undergo dissolution, surface reconstruction, or poisoning during extended HER operation. Although quantitative indicators, such as the stability number, have been introduced to evaluate catalyst longevity, the underlying atomic-scale degradation pathways, particularly under industrially relevant and fluctuating conditions, remain poorly understood [211]. Gaining detailed insight into these mechanisms is essential for developing catalysts that maintain high activity and structural integrity over prolonged operational lifetimes.

5.2. Design strategies for next-generation HER catalysts

To address current limitations and accelerate the development of efficient HER catalysts, future research must utilize rational design strategies that tightly integrate experimental insights with theoretical modeling. Computational tools such as DFT, microkinetic simulations, and emerging machine learning algorithms enable the prediction of active site geometries, adsorption energies, and reaction pathways. These insights inform the targeted synthesis of materials with optimized electronic structures and catalytic performance [66, 212]. When coupled with advanced characterization techniques, this integrated approach significantly enhances the precision and efficiency of catalyst design and optimization.

Equally important is the advancement of scalable, cost-effective synthesis techniques tailored for industrial-scale applications. Many high-performing HER catalysts are currently produced through complex, low-throughput processes, which hinder their practical implementation. Scalable methods such as hydrothermal synthesis, electrodeposition, and solution-phase chemical reduction have shown promise for fabricating catalysts like NiMo-based electrodes capable of withstanding industrial-level current densities. These techniques offer pathways to reproducible, large-scale production while maintaining the nanoscale structural features essential for catalytic activity [213]. Future research should focus on developing synthesis protocols that balance scalability, cost-efficiency, and structural precision to ensure the commercial viability of next-generation HER electrocatalysts.

5.3. Integration with full water-splitting systems

For practical hydrogen production, HER catalysts must operate in tandem with OER catalysts to achieve overall water splitting. This integration presents significant challenges, as the optimal electrochemical conditions for HER and OER often diverge. Successful system integration requires careful alignment of catalyst compatibility, operating *pH*, and electrolyte composition to ensure efficient, stable performance across both half-reactions. A detailed understanding of how *pH* and electrolyte properties influence reaction kinetics, intermediate adsorption, and catalyst degradation is essential. For instance, in

neutral or alkaline environments, sluggish water dissociation can reduce hydrogen coverage on active sites, limiting HER efficiency [66]. The kinetics of the Volmer step critically influence HER efficiency, especially in neutral and alkaline environments where water decomposition is necessary for creating adsorbed hydrogen intermediates. Systematic electrochemical and microkinetic studies reveal that in alkaline and neutral media, the additional energy barrier associated with water dissociation can serve as a key kinetic bottleneck in the Volmer step, resulting in generally slower HER kinetics compared to acidic conditions [214, 215]. This *pH* dependence arises because protons are abundant in acidic electrolytes, while water molecules serve as proton sources in neutral/alkaline media, necessitating cleavage steps that tend to limit general reaction speed.

To regulate and improve HER kinetics in alkaline media, catalyst design approaches focus on engineering active sites that work in a complex manner: lowering the water dissociation barrier, improving and balancing hydrogen adsorption, and facilitating the subsequent *H** combination. Common strategies pair oxophilic sites ($Ni(OH)_2$, metal oxides/hydroxides, etc.) that accelerate H–O–H cleavage with hydrogen-binding sites (Pt, single-atom noble metals, doped TMDs, etc.), implemented as heterostructures, noble-atom decoration or single-atom catalysts to lower the water-dissociation barrier and balance *H** adsorption for better and faster H* combination [123, 216]. For example, dual-site and interface engineering ($Ni(OH)_2$–Pt, Co-doped WO_2/Co_xW, Pt–Ru/RuO_2 with Pt single atoms) and doping/defect strategies in TMDs have been shown to kinetically accelerate water dissociation and enhance alkaline HER activity [123, 215, 216].

Additionally, electrolyte effects, including cation identity and concentration, significantly modulate HER kinetics by influencing water structure, double layer configuration and charge transfer at the interface [217-219]. By integrating catalyst surface engineering with electrolyte optimization, it is possible to mitigate *pH*-related kinetic constraints and enhance overall HER performance in neutral and alkaline systems, promoting practical and sustainable hydrogen production.

While traditional HER catalyst evaluations often focus on current densities around 10 mA/cm², industrial water electrolysis demands robust catalyst performance at significantly higher currents, commonly exceeding 500 mA/cm². Operating at such elevated current densities introduces multiple practical challenges, including intensified hydrogen bubble formation that blocks active sites, increased ohmic losses due to mass transport limitations, and higher thermal loads on electrodes. To address these issues, advanced catalyst architectures featuring three-dimensional, porous, and hierarchical structures have been developed [220]. These morphologies facilitate efficient gas bubble detachment, improve reactant diffusion, and maintain catalyst accessibility under vigorous gas evolution. Additionally, catalyst supports with high electrical conductivity and stability help sustain activity and durability during prolonged high-current operation. Emerging studies underscore the importance of evaluating catalysts under these practical

conditions. For example, UP-RuNiSAs/C and $MoO_2/MoSi_2$ ceramic electrodes have shown promising stability and activity at current densities beyond 500 mA/cm² [221, 222]. These insights inform design principles tailored for scalable and durable HER electrocatalysis, critical for advancing green hydrogen production technologies.

Beyond catalyst design, device engineering is critical to addressing mass transport limitations, enhancing gas bubble release, and maintaining high electrical conductivity. Advanced electrolyzer architectures that incorporate superaerophobic and superhydrophilic surfaces help alleviate gas bubble accumulation at high current densities, thus preserving catalytic efficiency and operational stability [213]. Future research should prioritize the co-design of catalysts and electrolyzer components to enable seamless integration, balancing electrochemical activity with structural durability. This includes the development of bifunctional catalysts, hybrid systems, and modular electrolyzer designs tailored to industrial-scale hydrogen generation.

Unlocking the full potential of HER technologies demands a multidisciplinary approach bridging fundamental knowledge gaps through operando studies, advancing theory-guided catalyst design, scaling up cost-effective synthesis methods, and seamlessly integrating materials into optimized water-splitting systems. Collectively, these strategies will accelerate the development of economically viable and sustainable hydrogen energy solutions.

5.4 Sustainability considerations in HER catalysts

Achieving truly sustainable hydrogen evolution catalysis requires a holistic assessment encompassing techno-economic feasibility, environmental impacts, resource availability, and practical operational considerations beyond mere catalyst activity or cost. This multidimensional perspective is critical to advancing green hydrogen technologies at scale in alignment with global climate goals. Below, the most important aspects of sustainability assessment will be considered point by point.

Resource availability and supply risk: Noble metals such as platinum, iridium and similar remain benchmark catalysts for HER due to their outstanding activity and stability, but face limitations from scarcity and geopolitical risks. This concern motivates the exploration of earth-abundant alternatives such as transition metal carbides, nitrides, sulfides, and phosphides, which are more sustainably sourced and exhibit promising catalytic properties [10, 22, 68, 129, 135, 172, 173]. Sustainable catalyst development must prioritize materials with low criticality while maintaining or improving performance.

Scalability of synthesis routes: The large-scale practicality of catalyst synthesis is strongly influenced by the chosen fabrication method. Techniques such as hydrothermal synthesis, chemical vapor deposition, molten salt synthesis, and pyrolysis differ significantly in terms of energy consumption, solvent usage, process complexity, and environmental footprint. For instance, high-temperature vapor-phase techniques

can produce high-quality materials with excellent crystallinity and purity, but often at the expense of higher carbon emissions and operational costs. In contrast, aqueous-phase or solution-based routes are generally more scalable and environmentally benign, though they may offer less precise control over morphology or composition. Comprehensive techno-economic analysis and LCA are therefore essential to balance catalyst performance with energy efficiency and material sustainability [223].

Environmental footprint and life cycle impacts: LCA provides a comprehensive evaluation of greenhouse gas emissions, water consumption, toxicity, and waste generation across the entire lifecycle of a catalyst from production and operation to end-of-life management. For example, carbon-based catalysts derived from biomass waste offer notable environmental advantages by valorizing residual biomass and reducing dependence on fossil-derived carbon blacks [224]. In contrast, precious metal catalysts typically exhibit higher initial environmental burdens; however, their extended durability and recyclability can partially offset these impacts over the full lifecycle.

Corrosion and stability in realistic electrolytes: Stability under realistic HER operating conditions, including acidic, neutral, and alkaline electrolytes, profoundly affects catalyst lifespan and net environmental impact [225]. Corrosion resistance ensures consistent catalytic performance and reduces resource consumption and waste from frequent catalyst replacement. Understanding degradation mechanisms through operando characterization helps design more robust catalytic systems that minimize environmental and economic burdens.

Circularity and recyclability: Incorporating circular economy principles, catalyst recycling and recovery methods enable reclamation of scarce or hazardous materials, closing resource loops and limiting environmental impact. Developing catalysts with inherent recyclability or designing systems compatible with efficient material recovery fosters sustainable hydrogen production infrastructure [226, 227].

Thus, the integration of material criticality assessment, scalable and green synthesis strategies, rigorous life cycle environmental impact analysis, durability evaluation under practical conditions, and circularity considerations forms a comprehensive sustainability framework. This framework guides the rational design and deployment of HER electrocatalysts that are not only high-performing but also material- and environmentally responsible, ultimately supporting the sustainable scale-up of green hydrogen technologies.

5.5 Stability Testing and Benchmarking

Rigorous stability testing is essential to complement overpotential measurements and fully assess catalyst durability under operating conditions. The most widely recommended protocols include: ***(i) Chronoamperometry (CA) and chronopotentiometry (CP)***: These methods measure current or potential at a fixed applied voltage or current density over extended durations (typically 10–50 hours or longer),

simulating continuous operation and revealing temporal performance decay [147]; ***(ii) Accelerated Stress Tests (ASTs)***: Repetitive cyclic voltammetry scanning between defined potential windows (e.g., −0.35 to 0.4 V vs RHE) at fast rates (50–100 mV/s) for several thousand cycles, subjecting catalysts to accelerated aging, highlighting degradation mechanisms [228]; ***(iii) Complementary post-mortem or in situ characterization***: Surface-sensitive techniques such as XPS, XRD, TEM and FT-IR before and after stability tests help identify structural and compositional changes responsible for activity loss [229].

To illustrate the state of the art, two representative catalyst systems can be considered. The first example is a Ru–N coupling catalyst supported on nitrogen-doped carbon [230]. In this case, HER is efficiently catalyzed by Ru–N coupling in defect-rich Ru/g-C_3N_4 nanosheets. The reported material achieves overpotentials as low as 27 mV in acidic and 34 mV in alkaline media at 10 mA cm^{-2} and demonstrates stability over at least 10,000 CV cycles and 20 h of steady-state operation [230]. These findings indicate that favorable Ru–N bonding and high active-site exposure can enable both exceptional catalytic activity and operational durability, establishing a valuable benchmark for future HER catalyst design.

The second example is a non-precious PGM-free alloy/oxide system for high current density in AEM-electrolyzers [231]. An oxide-promoted, self-supported Ni_4Mo catalyst for high current density anion exchange membrane water electrolysis presents a self-supported Ni_4Mo–MoO_x catalyst fabricated via electrodeposition. The catalyst enables an AEM water-electrolyzer to operate stably at 3 A cm^{-2} with a cell voltage of 2 V, exceeding previous PGM-free benchmarks in both activity and stability. The presented study further applies operando X-ray diffraction and absorption spectroscopy to confirm the active phase and elucidate how the surface MoO_x species enhance the Volmer step, yielding robust operation at industrially-relevant currents.

Together, these examples underscore that durability cannot be decoupled from activity: a catalyst with ultra-low overpotential but rapid decay offers little practical value, whereas a slightly higher overpotential but exceptional long-term stability may prove more viable for real-world deployment. Therefore, when benchmarking HER catalysts, researchers should aim to report: overpotentials at defined current densities (e.g., 10 mA, 100 mA cm^{-2}); stability tests under chronoamperometry/chronopotentiometry at fixed current densities for durations beyond 10 h (and preferably hundreds of hours); accelerated stress tests protocols of several thousand CV cycles, and pre- and post-test characterization (e.g., XPS, TEM, XRD) to identify structural or compositional changes responsible for decay. The inclusion of such comprehensive data will strengthen the reliability of claims of “high performance” and facilitate meaningful comparison across studies.

6. Conclusions

The catalytic activity of HER materials is fundamentally governed by the interplay between atomic structure, electronic configuration, and interfacial dynamics. Specific structural modifications, such as sulfur vacancies in MoS_2, create under-coordinated Mo sites and localized electronic states, lowering hydrogen adsorption energy ($\Delta G_H \approx 0$ eV) and enhancing conductivity. Nitrogen and phosphorus vacancies in transition metal compounds and carbon frameworks modulate charge density and facilitate favorable hydrogen binding, mimicking Pt-like behavior. Dual-heteroatom doping strategies (e.g., N/P in graphene) induce synergistic charge redistribution, achieving overpotentials as low as 53 mV at 10 mA cm^{-2}. In hybrid systems such as MoS_2/RGO, strain engineering (4–6 %) and defect-rich interfaces shift d-band centers and promote active basal plane sites, significantly improving activity and long-term stability over 1,000 cycles.

Moreover, structural features such as mesoporosity, defect-dopant coordination, and heterostructure interfaces (e.g., MoS_2–g-$CuNi_2S_4$) enhance mass transport, interfacial electron transfer, and active site exposure, driving current densities and turnover frequencies comparable to noble metals. Multiscale modeling confirms that these atomic- to mesoscale designs reduce energy barriers for both the Volmer and Heyrovsky/Tafel steps. Collectively, these findings underscore that tailoring catalyst structure across length scales is essential for optimizing HER performance and for designing durable, scalable systems for sustainable hydrogen production.

Looking forward, the development of bifunctional catalysts capable of efficiently catalyzing both HER and OER represents a critical frontier for sustainable and economically viable water electrolysis. Such catalysts can simplify electrolyzer design and reduce costs by enabling integrated, reversible, or hybrid electrochemical systems. The pursuit of catalysts that maintain high performance at industrially relevant current densities is increasingly important, emphasizing the need for stability under harsh operating conditions and scalable synthesis strategies. Emerging trends also highlight the role of advanced nanostructuring, interface engineering, and AI (machine learning)-guided catalyst design in accelerating discovery and optimization. Coupling electrocatalyst innovations with evolving electrolyzer technologies and renewable energy integration will be pivotal for achieving cost-competitive, green hydrogen production at scale, ultimately advancing the global hydrogen economy and supporting climate goals.

References

[1] A. Mehtab, S.A. Ali, I. Sadiq, S. Shaheen, H. Khan, M. Fazil, N.A. Pandit, F. Naaz, T. Ahmad, Hydrogen Energy as Sustainable Energy Resource for Carbon-Neutrality Realization, ACS Sustain. Resour. Manag. 1 (2024) 604-620. https://doi.org/10.1021/acssusresmgt.4c00039.

[2] T. Gao, Q. An, X. Tang, Q. Yue, Y. Zhang, B. Li, P. Li, Z. Jin, Recent progress in energy-saving

electrocatalytic hydrogen production via regulating the anodic oxidation reaction, Phys. Chem. Chem. Phys. 26 (2024) 19606-19624. https://doi.org/10.1039/D4CP01680G.

[3] S. Attarilar, J. Yang, M. Ebrahimi, Q. Wang, J. Liu, Y. Tang, J. Yang, The Toxicity Phenomenon and the Related Occurrence in Metal and Metal Oxide Nanoparticles: A Brief Review From the Biomedical Perspective, Front. Bioeng. Biotechnol. 8 (2020). https://doi.org/10.3389/fbioe.2020.00822.

[4] M.G. Idris, H.Y. Hafeez, J. Mohammed, A.B. Suleiman, C.E. Ndikilar, A review on recent development in the spinel ferrites-based materials for efficient solar fuel (hydrogen) generation via photocatalytic water-splitting, Appl. Surf. Sci. Adv. 18 (2023) 100468. https://doi.org/10.1016/j.apsadv.2023.100468.

[5] Electrochemical Water Electrolysis:Fundamentals and Technologies, Ebrary.Net |. (n.d.).

[6] Z. Li, X. Liu, Q. Yu, X. Qu, J. Wan, Z. Xiao, J. Chi, L. Wang, Recent advances in design of hydrogen evolution reaction electrocatalysts at high current density: A review, Chinese J. Catal. 63 (2024) 33-60. https://doi.org/10.1016/S1872-2067(24)60076-8.

[7] S.O. Akpasi, I.M. Smarte Anekwe, E.K. Tetteh, U.O. Amune, S.I. Mustapha, S.L. Kiambi, Hydrogen as a clean energy carrier: advancements, challenges, and its role in a sustainable energy future, Clean Energy. 9 (2025) 52-88. https://doi.org/10.1093/ce/zkae112.

[8] M.R.G. de Chialvo, A.C. Chialvo, Hydrogen evolution reaction: Analysis of the Volmer-Heyrovsky-Tafel mechanism with a generalized adsorption model, J. Electroanal. Chem. 372 (1994) 209-223. https://doi.org/10.1016/0022-0728(93)03043-O.

[9] F. Bao, E. Kemppainen, I. Dorbandt, R. Bors, F. Xi, R. Schlatmann, R. van de Krol, S. Calnan, Understanding the Hydrogen Evolution Reaction Kinetics of Electrodeposited Nickel-Molybdenum in Acidic, Near-Neutral, and Alkaline Conditions, ChemElectroChem. 8 (2021) 195-208. https://doi.org/10.1002/celc.202001436.

[10] C. Li, H. Gao, W. Wan, T. Mueller, Mechanisms for hydrogen evolution on transition metal phosphide catalysts and a comparison to Pt(111), Phys. Chem. Chem. Phys. 21 (2019) 24489-24498. https://doi.org/10.1039/C9CP05094A.

[11] T. Shinagawa, A.T. Garcia-Esparza, K. Takanabe, Insight on Tafel slopes from a microkinetic analysis of aqueous electrocatalysis for energy conversion, Sci. Rep. 5 (2015) 13801. https://doi.org/10.1038/srep13801.

[12] C. Wan, Y. Ling, S. Wang, H. Pu, Y. Huang, X. Duan, Unraveling and Resolving the Inconsistencies in Tafel Analysis for Hydrogen Evolution Reactions, ACS Cent. Sci. 10 (2024) 658-665. https://doi.org/10.1021/acscentsci.3c01439.

[13] A. Lasia, Mechanism and kinetics of the hydrogen evolution reaction, Int. J. Hydrogen Energy 44,

36 (2019) 19484-19518. https://doi.org/10.1016/j.ijhydene.2019.05.183.

[14] S. Anantharaj, S. Noda, V.R. Jothi, S.C. Yi, M. Driess, P.W. Menezes, Strategies and Perspectives to Catch the Missing Pieces in Energy-Efficient Hydrogen Evolution Reaction in Alkaline Media, Angew. Chem. 60, 35 (2021) 18981-19006. https://doi.org/10.1002/anie.202015738.

[15] Y. Zhu, L. Li, H. Cheng, J. Ma, Alkaline Hydrogen Evolution Reaction Electrocatalysts for Anion Exchange Membrane Water Electrolyzers: Progress and Perspective, ACS Au 4, 12 (2024) 4639-4654. https://doi.org/10.1021/jacsau.4c00898.

[16] P.S. Lamoureux, A.R. Singh, K. Chan, pH Effects on Hydrogen Evolution and Oxidation over Pt(111): Insights from First-Principles, ACS Catal. 9, 7 (2019) 6194-6201. https://doi.org/10.1021/acscatal.9b00268.

[17] N. Podrojková, A. Gubóová, M. Streckova, R. Oriňaková, A study of the mechanism of the hydrogen evolution reaction catalysed by molybdenum phosphide in different media, Mater. Today Sustain., 31 (2025) 101141.

[18] M. Lao, P. Li, Y. Jiang, H. Pan, S.X. Dou, W. Sun, From fundamentals and theories to heterostructured electrocatalyst design: An in-depth understanding of alkaline hydrogen evolution reaction, Nano Energy 98 (2022) 107231. https://doi.org/10.1016/j.nanoen.2022.107231.

[19] A.R. Zeradjanin, P. Narangoda, J. Masa, On the Origins of Intrinsic Limitations of Electrocatalytic Hydrogen Evolution in Alkaline Media, ChemCatChem 16, 18 (2024) e202400634. https://doi.org/10.1002/cctc.202400634.

[20] J.D. Wiensch, J. John, J.M. Velazquez, D.A. Torelli, A.P. Pieterick, M.T. McDowell, K. Sun, X. Zhao, B.S. Brunschwig, N.S. Lewis, Comparative Study in Acidic and Alkaline Media of the Effects of pH and Crystallinity on the Hydrogen-Evolution Reaction on MoS_2 and $MoSe_2$, ACS Energy Lett. 2, 10 (2017) 2234-2238. https://doi.org/10.1021/acsenergylett.7b00700.

[21] K. Song, X. Feng, X. Ju, D. Ma, S. Wang, J.-W. Shi, Poisoning mechanism of potassium and calcium on a Mn-based quasi-MOF de-NOx catalyst, J. Hazard. Mater. 497 (2025) 139714. https://doi.org/10.1016/j.jhazmat.2025.139714.

[22] Y. Sim, Y. Chae, S.-Y. Kwon, Recent advances in metallic transition metal dichalcogenides as electrocatalysts for hydrogen evolution reaction, iScience 25, 10 (2022) 105098. https://doi.org/10.1016/j.isci.2022.105098.

[23] R. Wu, J. Xu, C.-L. Zhao, X.-Z. Su, X.-L. Zhang, Y.-R. Zheng, F.-Y. Yang, X.-S. Zheng, J.-F. Zhu, J. Luo, W.-X. Li, M.-R. Gao, S.-H. Yu, Dopant triggered atomic configuration activates water splitting to hydrogen, Nat. Commun. 14 (2023) 2306. https://doi.org/10.1038/s41467-023-37641-3.

[24] F. Wang, L. Xie, N. Sun, T. Zhi, M. Zhang, Y. Liu, Z. Luo, L. Yi, Q. Zhao, L. Wang, Deformable Catalytic Material Derived from Mechanical Flexibility for Hydrogen Evolution Reaction, Nano-

Micro Lett. 16 (2024) 32. https://doi.org/10.1007/s40820-023-01251-x.

[25] J. Zhang, T. Wang, D. Pohl, B. Rellinghaus, R. Dong, S. Liu, X. Zhuang, X. Feng, Interface Engineering of MoS_2/Ni_3S_2 Heterostructures for Highly Enhanced Electrochemical Overall-Water-Splitting Activity, Angew. Chemie Int. Ed. 55 (2016) 6702-6707. https://doi.org/10.1002/anie.201602237.

[26] P. Tang, P.-Y. Huang, J.E.N. Swallow, C. Wang, D. Gianolio, H. Guo, J.H. Warner, R.S. Weatherup, M. Pasta, Structure-Property Relationship of Defect-Trapped Pt Single-Site Electrocatalysts for the Hydrogen Evolution Reaction, ACS Catal. 13 (2023) 9558-9566. https://doi.org/10.1021/acscatal.3c01513.

[27] L.J. Moriau, A. Hrnjić, A. Pavlišič, A.R. Kamšek, U. Petek, F. Ruiz-Zepeda, M. Šala, L. Pavko, V.S. Šelih, M. Bele, P. Jovanovič, M. Gatalo, N. Hodnik, Resolving the nanoparticles' structure-property relationships at the atomic level: a study of Pt-based electrocatalysts, IScience. 24 (2021) 102102. https://doi.org/10.1016/j.isci.2021.102102.

[28] J. Wei, Q.D. Wang, M. Ebrahimi, L. Zhang, D.D. Yin, H.Y. Jiang, W.J. Ding, Experimental Study on the Elastic-plastic Transitions of the Hetero-structured High Pressure Die Casting Mg-Al-RE Alloy, Exp. Mech. 61 (2021) 1143-1152. https://doi.org/10.1007/s11340-021-00724-7.

[29] X.-F. Yang, A. Wang, B. Qiao, J. Li, J. Liu, T. Zhang, Single-Atom Catalysts: A New Frontier in Heterogeneous Catalysis, Acc. Chem. Res. 46 (2013) 1740-1748. https://doi.org/10.1021/ar300361m.

[30] M.N. Hossain, L. Zhang, R. Neagu, S. Sun, Exploring the properties, types, and performance of atomic site catalysts in electrochemical hydrogen evolution reactions, Chem. Soc. Rev. 54 (2025) 3323-3386. https://doi.org/10.1039/D4CS00333K.

[31] H. Jin, K. Zhou, R. Zhang, H. Cui, Y. Yu, P. Cui, W. Song, C. Cao, Regulating the electronic structure through charge redistribution in dense single-atom catalysts for enhanced alkene epoxidation, Nat. Commun. 14 (2023) 2494. https://doi.org/10.1038/s41467-023-38310-1.

[32] W. Yang, X. Liu, X. Chen, Y. Cao, S. Cui, L. Jiao, C. Wu, C. Chen, D. Fu, I.D. Gates, Z. Gao, H. Jiang, A Sulfur-Tolerant MOF-Based Single-Atom Fe Catalyst for Efficient Oxidation of NO and Hg^0, Adv. Mater. 34 (2022). https://doi.org/10.1002/adma.202110123.

[33] S. Attarilar, C. Gode, M.H. Mashhuriazar, M. Ebrahimi, Tailoring twist extrusion process; the better strain behavior at the lower required loads, J. Alloys Compd. 859 (2021) 157855. https://doi.org/10.1016/j.jallcom.2020.157855.

[34] M. Ebrahimi, L. Zhang, Q. Wang, H. Zhou, W. Li, Damping performance of SiC nanoparticles reinforced magnesium matrix composites processed by cyclic extrusion and compression, J. Magnes. Alloy. (2021). https://doi.org/10.1016/j.jma.2021.07.024.

[35] D. Voiry, H. Yamaguchi, J. Li, R. Silva, D.C.B. Alves, T. Fujita, M. Chen, T. Asefa, V.B. Shenoy, G. Eda, M. Chhowalla, Enhanced catalytic activity in strained chemically exfoliated WS_2 nanosheets for hydrogen evolution, Nat. Mater. 12 (2013) 850-855. https://doi.org/10.1038/nmat3700.

[36] J. Wang, S. Dou, X. Wang, Structural tuning of heterogeneous molecular catalysts for electrochemical energy conversion, Sci. Adv. 7 (2021). https://doi.org/10.1126/sciadv.abf3989.

[37] S. Attarilar, F. Djavanroodi, M. Ebrahimi, K.J. Al-Fadhalah, L. Wang, M. Mozafari, Hierarchical Microstructure Tailoring of Pure Titanium for Enhancing Cellular Response at Tissue-Implant Interface, J. Biomed. Nanotechnol. 17 (2021) 115-130. https://doi.org/10.1166/jbn.2021.3015.

[38] S. Attarilar, M.T. Salehi, K.J. Al-Fadhalah, F. Djavanroodi, M. Mozafari, Functionally graded titanium implants: Characteristic enhancement induced by combined severe plastic deformation, PLoS One. 14 (2019) 1-18. https://doi.org/10.1371/journal.pone.0221491.

[39] D. Cao, H. Xu, H. Li, C. Feng, J. Zeng, D. Cheng, Volcano-type relationship between oxidation states and catalytic activity of single-atom catalysts towards hydrogen evolution, Nat. Commun. 13 (2022) 5843. https://doi.org/10.1038/s41467-022-33589-y.

[40] Y. Shi, Z.-R. Ma, Y.-Y. Xiao, Y.-C. Yin, W.-M. Huang, Z.-C. Huang, Y.-Z. Zheng, F.-Y. Mu, R. Huang, G.-Y. Shi, Y.-Y. Sun, X.-H. Xia, W. Chen, Electronic metal-support interaction modulates single-atom platinum catalysis for hydrogen evolution reaction, Nat. Commun. 12 (2021) 3021. https://doi.org/10.1038/s41467-021-23306-6.

[41] W. Wei, F. Guo, C. Wang, L. Wang, Z. Sheng, X. Wu, B. Cai, A. Eychmüller, Strain Effects in Ru-Au Bimetallic Aerogels Boost Electrocatalytic Hydrogen Evolution, NanoMicroSmall 20, 25 (2024) 2310603. https://doi.org/10.1002/smll.202310603.

[42] J. Hu, C. Zhang, P. Yang, J. Xiao, T. Deng, Z. Liu, B. Huang, M.K.H. Leung, S.Yang, Kinetic-Oriented Construction of MoS_2 Synergistic Interface to Boost pH-Universal Hydrogen Evolution, Adv. Funct. Mater. 30, 6 (2020) 1908520. https://doi.org/10.1002/adfm.201908520.

[43] R. Liu, M. Sun, X. Liu, Z. Lv, X. Yu, J. Wang, Y. Liu, L. Li, X. Feng, W. Yang, B. Huang, B. Wang, Enhanced Metal-Support Interactions Boost the Electrocatalytic Water Splitting of Supported Ruthenium Nanoparticles on a Ni_3N/NiO Heterojunction at Industrial Current Density, Angew. Chem. Int. Ed. 62 (2023) e202312644. https://doi.org/10.1002/anie.202312644.

[44] T. Wu, M.-Z. Sun, B.-L. Huang, Non-noble metal-based bifunctional electrocatalysts for hydrogen production, Rare Met. 41 (2022) 2169-2183. https://doi.org/10.1007/s12598-021-01914-x.

[45] M. Chen, Y. Yang, Y. Ding, J. Liu, Toward a molecular-scale picture of water electrolysis: mechanistic insights, fundamental kinetics and electrocatalyst dynamic evolution, Coordination Chemistry Reviews 536 (2025) 216651. https://doi.org/10.1016/j.ccr.2025.216651.

[46] F. Dionigi, Z. Zeng, I. Sinev, T. Merzdorf, S. Deshpande, M.B. Lopez, S. Kunze, I. Zegkinoglou,

H. Sarodnik, D. Fan, A. Bergmann, J. Drnec, J.F. de Araujo, M. Gliech, D. Teschner, J. Zhu, W.-X. Li, J. Greeley, B.R. Cuenya, P. Strasser. In-situ structure and catalytic mechanism of NiFe and CoFe layered double hydroxides during oxygen evolution. Nat Commun. 11, 1 (2020) 2522. https://doi.org/10.1038/s41467-020-16237-1.

[47] Y. Zhang, J. Pan, G. Gong, R. Song, Y. Yuan, M. Li, W. Hu, P. Fan, L. Yuan, L. Wang, In Situ Surface Reconstruction of Catalysts for Enhanced Hydrogen Evolution, Catalysts. 13 (2023) 120. https://doi.org/10.3390/catal13010120.

[48] D.D. Megersa, G.T. Gudena, Y. Kim, H.K. Yu, Chemical Vapor Deposition of Ru/$RuSe_2$ Catalyst for Electrolytic Hydrogen Evolution Reaction, Adv. Sustain. Syst. 7 (2023). https://doi.org/10.1002/adsu.202300257.

[49] R. Schlögl, Chapter 5 X-ray Diffraction, in: 2009: pp. 273-338. https://doi.org/10.1016/S0360-0564(08)00005-9.

[50] M. Vega-Paredes, C. Scheu, R. Aymerich-Armengol, Expanding the Potential of Identical Location Scanning Transmission Electron Microscopy for Gas Evolving Reactions: Stability of Rhenium Molybdenum Disulfide Nanocatalysts for Hydrogen Evolution Reaction, ACS Appl. Mater. Interfaces. 15 (2023) 46895-46901. https://doi.org/10.1021/acsami.3c09188.

[51] F. Djavanroodi, M. Daneshtalab, M. Ebrahimi, A novel technique to increase strain distribution homogeneity for ECAPed materials, Mater. Sci. Eng. A. 535 (2012) 115-121. https://doi.org/10.1016/j.msea.2011.12.050.

[52] A. Prajapati, C. Hahn, I.M. Weidinger, Y. Shi, Y. Lee, A.N. Alexandrova, D. Thompson, S.R. Bare, S. Chen, S. Yan, N. Kornienko, Best practices for in-situ and operando techniques within electrocatalytic systems, Nat. Commun. 16 (2025) 2593. https://doi.org/10.1038/s41467-025-57563-6.

[53] V.M. V, G. Nageswaran, Operando X-Ray Spectroscopic Techniques: A Focus on Hydrogen and Oxygen Evolution Reactions, Front. Chem. 8 (2020). https://doi.org/10.3389/fchem.2020.00023.

[54] X. Sun, M. Ebrahimi, S. Attarilar, The decisive impact of microstructure on the machinability of pure copper, Arch. Civ. Mech. Eng. 21 (2021) 136. https://doi.org/10.1007/s43452-021-00290-8.

[55] M. Chen, D. Liu, L. Qiao, P. Zhou, J. Feng, K.W. Ng, Q. Liu, S. Wang, H. Pan, In-situ/operando Raman techniques for in-depth understanding on electrocatalysis, Chem. Eng. J. 461 (2023) 141939. https://doi.org/10.1016/j.cej.2023.141939.

[56] A. Nsabimana, Y. Guan, G. Xu, In situ and operando characterization techniques for nanocatalyst-based electrochemical hydrogen evolution reactions, J. Electrochem. Sci. Eng. 15, 1 (2025) 2526. https://doi.org/10.5599/jese.2526.

[57] W. Liao, S. Wang, H. Su, Y. Zhang, Application of in situ/operando characterization techniques in

heterostructure catalysts toward water electrolysis. Nano Res. 16 (2023) 1984-1991. https://doi.org/10.1007/s12274-022-5048-1.

[58] Q. Fu, L.W. Wong, F. Zheng, X. Zheng, C.S. Tsang, K.H. Lai, W. Shen, T.H. Ly, Q. Deng, J. Zhao, Unraveling and leveraging in situ surface amorphization for enhanced hydrogen evolution reaction in alkaline media. Nat Commun 14 (2023) 6462. https://doi.org/10.1038/s41467-023-42221-6.

[59] E.B. Creel, X. Lyu, G. McCool, R.J. Ouimet, A. Serov, Protocol for Screening Water Oxidation or Reduction Electrocatalyst Activity in a Three-Electrode Cell for Alkaline Exchange Membrane Electrolysis, Front. Energy Res. 10 (2022). https://doi.org/10.3389/fenrg.2022.871604.

[60] M. Mazzucato, C. Durante, Comparative Analysis of Rotating Electrode and Gas Diffusion Electrode Methods for Assessing Activity and Stability of Fe-N-C Based Catalysts in ORR, Electrochim. Acta. 463 (2023) 142801. https://doi.org/10.1016/j.electacta.2023.142801.

[61] N. Bhuvanendran, S. Ravichandran, Q. Xu, T. Maiyalagan, H. Su, A quick guide to the assessment of key electrochemical performance indicators for the oxygen reduction reaction: A comprehensive review, Int. J. Hydrogen Energy. 47 (2022) 7113-7138. https://doi.org/10.1016/j.ijhydene.2021.12.072.

[62] S. Anantharaj, S. Kundu, Do the Evaluation Parameters Reflect Intrinsic Activity of Electrocatalysts in Electrochemical Water Splitting?, ACS Energy Lett. 4 (2019) 1260-1264. https://doi.org/10.1021/acsenergylett.9b00686.

[63] M.A. Qadeer, X. Zhang, M.A. Farid, M. Tanveer, Y. Yan, S. Du, Z.-F. Huang, M. Tahir, J.-J. Zou, A review on fundamentals for designing hydrogen evolution electrocatalyst, J. Power Sources. 613 (2024) 234856. https://doi.org/10.1016/j.jpowsour.2024.234856.

[64] X.-M. Lin, X.-T. Wang, Y.-L. Deng, X. Chen, H.-N. Chen, P.M. Radjenovic, X.-G. Zhang, Y.-H. Wang, J.-C. Dong, Z.-Q. Tian, J.-F. Li, In Situ Probe of the Hydrogen Oxidation Reaction Intermediates on PtRu a Bimetallic Catalyst Surface by Core–Shell Nanoparticle-Enhanced Raman Spectroscopy, Nano Lett. 22 (2022) 5544-5552. https://doi.org/10.1021/acs.nanolett.2c01744.

[65] M. Ebrahimi, M. Shamsborhan, Monotonic and dynamic mechanical properties of PTCAE aluminum, J. Alloys Compd. 705 (2017) 28-37. https://doi.org/10.1016/j.jallcom.2017.02.109.

[66] Y. Luo, Y. Zhang, J. Zhu, X. Tian, G. Liu, Z. Feng, L. Pan, X. Liu, N. Han, R. Tan, Material Engineering Strategies for Efficient Hydrogen Evolution Reaction Catalysts, Small Methods. 8 (2024). https://doi.org/10.1002/smtd.202400158.

[67] Y. Han, H. Xu, Q. Li, A. Du, X. Yan, DFT-assisted low-dimensional carbon-based electrocatalysts design and mechanism study: a review, Front. Chem. 11 (2023). https://doi.org/10.3389/fchem.2023.1286257.

[68] X. Jiang, G. Liu, L. Zhang, Z. Hu, Integrating Density Functional Theory Calculations and Machine

Learning to Identify Conduction Band Minimum as a Descriptor for High-Efficiency Hydrogen Evolution Reaction Catalysts in Transition Metal Dichalcogenides, Catalysts. 15 (2025) 309. https://doi.org/10.3390/catal15040309.

[69] C. Wang, B. Wang, C. Wang, A. Li, Z. Chang, R. Wang, A machine learning model with minimize feature parameters for multi-type hydrogen evolution catalyst prediction, Npj Comput. Mater. 11 (2025) 111. https://doi.org/10.1038/s41524-025-01607-4.

[70] V. Fung, G. Hu, P. Ganesh, B.G. Sumpter, Machine learned features from density of states for accurate adsorption energy prediction, Nat. Commun. 12 (2021) 88. https://doi.org/10.1038/s41467-020-20342-6.

[71] S.R. Kandavalli, Q. Wang, M. Ebrahimi, C. Gode, F. Djavanroodi, S. Attarilar, S. Liu, A Brief Review on the Evolution of Metallic Dental Implants: History, Design, and Application, Front. Mater. 8 (2021). https://doi.org/10.3389/fmats.2021.646383.

[72] A. Pei, R. Xie, Y. Zhang, Y. Feng, W. Wang, S. Zhang, Z. Huang, L. Zhu, G. Chai, Z. Yang, Q. Gao, H. Ye, C. Shang, B.H. Chen, Z. Guo, Effective electronic tuning of Pt single atoms via heterogeneous atomic coordination of $(Co,Ni)(OH)_2$ for efficient hydrogen evolution, Energy Environ. Sci. 16 (2023) 1035-1048. https://doi.org/10.1039/D2EE02785B.

[73] R. Jindal, V. Sharma, A. Shukla, Density functional theory study of the hydrogen evolution reaction in haeckelite boron nitride quantum dots, Int. J. Hydrogen Energy. 47 (2022) 41783-41794. https://doi.org/10.1016/j.ijhydene.2022.06.216.

[74] H. Li, Z. Zhang, Z. Liu, Non-Monotonic Trends of Hydrogen Adsorption on Single Atom Doped g-C_3N_4, Catalysts. 9 (2019) 84. https://doi.org/10.3390/catal9010084.

[75] M. Schalenbach, R. Tesch, P.M. Kowalski, R.-A. Eichel, The electrocatalytic activity for the hydrogen evolution reaction on alloys is determined by element-specific adsorption sites rather than d-band properties, Phys. Chem. Chem. Phys. 26 (2024) 14171-14185. https://doi.org/10.1039/D4CP01084A.

[76] J. Zhang, D. Li, L. Ju, G. Yang, D. Yuan, Z. Fengd, W. Wang, The charge effects on the hydrogen evolution reaction activity of the defected monolayer MoS_2, Phys. Chem. Chem. Phys. 25 (2023) 10956-10965. https://doi.org/10.1039/D2CP05927D.

[77] K. Tran, Z.W. Ulissi, Active learning across intermetallics to guide discovery of electrocatalysts for CO_2 reduction and H_2 evolution, Nat. Catal. 1 (2018) 696-703. https://doi.org/10.1038/s41929-018-0142-1.

[78] M. Ebrahimi, C. Gode, S. Attarilar, R. Berjis, Concurrent Enhancement of Strength and Corrosion Resistance in Ultrafine-grained Al6063 Tubes, Trans. Indian Inst. Met. 74 (2021) 753-766. https://doi.org/10.1007/s12666-021-02204-x.

[79] S. Attarilar, F. Djavanroodi, O.M. Irfan, F.A. Al-Mufadi, M. Ebrahimi, Q.D. Wang, Strain uniformity footprint on mechanical performance and erosion-corrosion behavior of equal channel angular pressed pure titanium, Results Phys. 17 (2020) 103141. https://doi.org/10.1016/j.rinp.2020.103141.

[80] Y. Zhang, X. Liu, W. Wang, Theoretical Calculation Assisted by Machine Learning Accelerate Optimal Electrocatalyst Finding for Hydrogen Evolution Reaction, ChemElectroChem 11, 13 (2024) e202400084. doi.org/10.1002/celc.202400084.

[81] U. Baeck, M.-C. Kim, D.N. Nguyen, J. Kim, J. Lim, Y. Chae, N. Shin, H. Choi, J.Y. Kim, C.-H. Chung, W.-S. Choe, H.S. Park, U. Sim, J.K. Kim, Machine-Learning-Assisted Design and Optimization of Single-Atom Transition Metal-Incorporated Carbon Quantum Dot Catalysts for Electrocatalytic Hydrogen Evolution Reaction, Carbon Energy 7, 7 (2025) e70006. https://doi.org/10.1002/cey2.70006.

[82] B.M. Abraham, P. Sinha, P. Haldera, J.K. Singh, Fusing a machine learning strategy with density functional theory to hasten the discovery of 2D MXene-based catalysts for hydrogen generation, J. Mater. Chem. A 11 (2023) 8091-8100. https://doi.org/10.1039/D3TA00344B.

[83] M. V. Jyothirmai, D. Roshini, B.M. Abraham, J.K. Singh, Accelerating the Discovery of g-C_3N_4-Supported Single Atom Catalysts for Hydrogen Evolution Reaction: A Combined DFT and Machine Learning Strategy, ACS Appl. Energy Mater. 6, 10 (2023) 5598-5606. https://doi.org/10.1021/acsaem.3c00835.

[84] J. Li, N. Wu, J. Zhang, H.-H. Wu, K. Pan, Y. Wang, G. Liu, X. Liu, Z. Yao, Q. Zhang, Machine Learning-Assisted Low-Dimensional Electrocatalysts Design for Hydrogen Evolution Reaction, Nano-Micro Lett. 15 (2023) 227. https://doi.org/10.1007/s40820-023-01192-5.

[85] M.V. Jyothirmai, R. Dantuluri, P. Sinha, B.M. Abraham, J.K. Singh, Machine-Learning-Driven High-Throughput Screening of Transition-Metal Atom Intercalated g-C_3N_4/MX_2 (M = Mo, W; X = S, Se, Te) Heterostructures for the Hydrogen Evolution Reaction, ACS Appl. Mater. Interfaces 16, 10 (2024) 12437-12445. https://doi.org/10.1021/acsami.3c17389.

[86] H. Park, D.-M. Geum, H.J. Kim, Accelerating hydrogen evolution catalyst discovery via data-driven strategy for high-performance single-atom catalysts embedded in h-BN, J. Energy Chem. 107 (2025) 750-758. https://doi.org/10.1016/j.jechem.2025.04.002.

[87] C. Martínez-Alonso, V. Vassilev-Galindo, B.M. Comer, F. Abild-Pedersen, K.T. Winther, J. LLorca, Application of machine learning to discover new intermetallic catalysts for the hydrogen evolution and the oxygen reduction reactions, Catal. Sci. Technol. 14 (2024) 3784-3799. https://doi.org/10.1039/D4CY00491D.

[88] R. Ding, J. Chen, Y. Chen, J. Liu, Y. Bandoe, X. Wang, Unlocking the potential: machine learning

applications in electrocatalyst design for electrochemical hydrogen energy transformation, Chem. Soc. Rev. 53 (2024) 11390. https://doi.org/10.1039/d4cs00844h.

[89] P. Sinha, M.V. Jyothirmai, B.Moses Abraham, Jayant K. Singh, Machine learning driven advancements in catalysis for predicting hydrogen evolution reaction activity, Mater. Chem. Phys. 326 (2024) 129805. https://doi.org/10.1016/j.matchemphys.2024.129805.

[90] G. Yin, H. Zhu, S. Chen, T. Li, C. Wu, S. Jia, J. Shang, Z. Ren, T. Ding, Y. Li, Machine Learning-Assisted High-Throughput Screening for Electrocatalytic Hydrogen Evolution Reaction, Molecules 30 (2025) 759. https://doi.org/10.3390/molecules30040759.

[91] M.N.I. Salehmin, S.K. Tiong, H. Mohamed, D.A. Umar, K.L. Yu, H.C. Ong, S. Nomanbhay, S.S. Lim, Navigating challenges and opportunities of machine learning in hydrogen catalysis and production processes: Beyond algorithm development, J. Energy Chem. 99 (2024) 223-252. https://doi.org/10.1016/j.jechem.2024.07.045.

[92] Y. Guan, D. Chaffart, G. Liu, Z. Tan, D. Zhang, Y. Wang, J. Li, L. Ricardez-Sandoval, Machine learning in solid heterogeneous catalysis: Recent developments, challenges and perspectives, Chem. Eng. Sci. 248, Part A (2022) 117224. https://doi.org/10.1016/j.ces.2021.117224.

[93] D. Senthilnathan, P. Giunta, V. Vetere, A. Kachmar, P. Maldivi, A.A. Franco, An efficient and cyclic hydrogen evolution reaction mechanism on $[Ni(PH_2NH_2)_2]^{2+}$ catalysts: a theoretical and multiscale simulation study, RSC Adv. 4 (2014) 5177. https://doi.org/10.1039/c3ra44896g.

[94] S. Deo, W. Sun, T. Chatterjee, T. Moore, M. Yuan, S. Akhade, M. Mcnenly, G. Bucci, Cross-scale catalyst modeling framework: A case study of H_2 storage and release via formic acid, (2024). https://doi.org/10.26434/chemrxiv-2024-rhm2t.

[95] Y. Wang, ed., Multiscale Modeling of Electrochemical Reactions and Processes, AIP Publishing LLCMelville, New York, 2021. https://doi.org/10.1063/9780735422377.

[96] H. Hosseini, C.J. Herring, C.F. Nwaokorie, G.A. Sulley, M.M. Montemore, Computational Design of Catalysts with Experimental Validation: Recent Successes, Effective Strategies, and Pitfalls, J. Phys. Chem. C 128, 43 (2024) 18144-18157. https://doi.org/10.1021/acs.jpcc.4c04949.

[97] X. Cao, S. Xing, D. Ma, Y. Tan, Y. Zhu, J. Hu, Y. Wang, X. Chen, Z. Chen, Design of high-performance ion-doped CoP systems for hydrogen evolution: From multi-level screening calculations to experiment, Journal of Energy Chemistry 82 (2023) 307-316, https://doi.org/10.1016/j.jechem.2023.03.043.

[98] X. Jia, Z. Zhou, F. Liu, T. Wang, Y. Wang, D. Zhang, H. Liu, Y. Wang, S. Ye, K. Amezawa, L. Wei, H. Li, Closed-Loop Framework for Discovering Stable and Low-Cost Bifunctional Metal Oxide Catalysts for Efficient Electrocatalytic Water Splitting in Acid, J. Am. Chem. Soc. 147, 26 (2025) 22642-22654. https://doi.org/10.1021/jacs.5c04079.

[99] H. Jin, X. Chen, Y. Da, L. Fan, R. Jiang, W. Chen, Advancing Multiscale-Coupled Heterointerface Catalysts for Enhanced Water Electrolysis, Accounts Mater. Res. 6 (2025) 648-660. https://doi.org/10.1021/accountsmr.5c00055.

[100] V. Sinha, D. Sun, E.J. Meijer, T.J.H. Vlugt, A. Bieberle-Hütter, A multiscale modelling approach to elucidate the mechanism of the oxygen evolution reaction at the hematite-water interface, Faraday Discuss. 229 (2021) 89-107. https://doi.org/10.1039/C9FD00140A.

[101] Q. Zhang, Y. Li, F. Luo, Z. Yang, Navigating the energy crisis: design principles and challenges in the development of high-performance catalysts for electrolytic water splitting, Chem. Commun. 61 (2025) 10747-10763. https://doi.org/10.1039/D5CC02288F.

[102] V.A. Kiliyankil, W. Mao, Y. Takahashi, W. Gong, S. Kabayama, Y. Hamasaki, K. Fukutani, H. Matsuzaki, I. Sakata, K. Takeuchi, M. Endo, B. Fugetsu, Edge sites on platinum electrocatalysts are responsible for discharge in the hydrogen evolution reaction, J. Mater. Chem. A 12 (2024) 28731-28743. https://doi.org/10.1039/D4TA04887C.

[103] H. Liu, X. Peng, X. Liu, Single-Atom Catalysts for the Hydrogen Evolution Reaction, ChemElectroChem 5, 20 (2018) 2963-2974. https://doi.org/10.1002/celc.201800507.

[104] Z. Pu, I.S. Amiinu, R. Cheng, P. Wang, C. Zhang, S. Mu, W. Zhao, F. Su, G. Zhang, S. Liao, S. Sun, Single-Atom Catalysts for Electrochemical Hydrogen Evolution Reaction: Recent Advances and Future Perspectives. Nano-Micro Lett. 12 (2020) 21. https://doi.org/10.1007/s40820-019-0349-y.

[105] K. Ahmed, S. Hameed, K. Patchigolla, N. Dawood, Z.K. Ghouri, Carbon-based electrocatalysts for hydrogen evolution reaction, Energy Convers. Manage.: X 26 (2025) 100892, https://doi.org/10.1016/j.ecmx.2025.100892.

[106] Q. Shi, R. Sun, Adsorption manners of hydrogen on Pt(100), (110) and (111) surfaces at high coverage, Comput. Theor. Chem. 1106 (2017) 43-49. https://doi.org/10.1016/j.comptc.2017.02.024.

[107] B. Zhang, D. Wang, Y. Hou, S. Yang, X.H. Yang, J.H. Zhong, J. Liu, H.F. Wang, P. Hu, H.J. Zhao, H.G. Yang, Facet-Dependent Catalytic Activity of Platinum Nanocrystals for Triiodide Reduction in Dye-Sensitized Solar Cells, Sci. Rep. 3 (2013) 1836. https://doi.org/10.1038/srep01836.

[108] N. Garcia-Araez, J.J. Lukkien, M.T.M. Koper, J.M. Feliu, Competitive adsorption of hydrogen and bromide on Pt(100): Mean-field approximation vs. Monte Carlo simulations, Journal of Electroanalytical Chemistry 588, 1 (2006) 1-14. https://doi.org/10.1016/j.jelechem.2005.11.034.

[109] F. Li, G.-F. Han, H.-J. Noh, J.-P. Jeon, I. Ahmad, S. Chen, C. Yang, Y. Bu, Z. Fu, Y. Lu, J.-B. Baek, Balancing hydrogen adsorption/desorption by orbital modulation for efficient hydrogen evolution catalysis, Nat. Commun. 10 (2019) 4060. https://doi.org/10.1038/s41467-019-12012-z.

[110] Q.-Q. Pang, X. Bai, X. Du, S. Zhang, Z.-Y. Liu, X.-Z. Yue, Facet modulation of nickel-ruthenium

nanocrystals for efficient electrocatalytic hydrogen evolution, Journal of Colloid and Interface Science 633 (2023) 275-283, https://doi.org/10.1016/j.jcis.2022.11.082.

[111] C. Li, J.-B. Baek, Recent Advances in Noble Metal (Pt, Ru, and Ir)-Based Electrocatalysts for Efficient Hydrogen Evolution Reaction, ACS Omega. 5 (2020) 31-40. https://doi.org/10.1021/acsomega.9b03550.

[112] J. Cai, R. Javed, D. Ye, H. Zhao, J. Zhang, Recent progress in noble metal nanocluster and single atom electrocatalysts for the hydrogen evolution reaction, J. Mater. Chem. A. 8 (2020) 22467-22487. https://doi.org/10.1039/D0TA06942F.

[113] H. Niu, Q. Wang, C. Huang, M. Zhang, Y. Yan, T. Liu, W. Zhou, Noble Metal-Based Heterogeneous Catalysts for Electrochemical Hydrogen Evolution Reaction, Appl. Sci. 13 (2023) 1-17. https://doi.org/10.3390/app13042177.

[114] M.I. Hussain, M.U. Farooq, M. Xia, X. Ren, R.R. Zairov, M. Harb, Single-atom catalysts for electrocatalytic applications: Synthetic strategies, in-situ characterization, and future challenges, Appl. Mater. Today. 36 (2024) 102037. https://doi.org/10.1016/j.apmt.2023.102037.

[115] X. Qiu, R. Ren, B. Wang, R. Wang, I. Kozhevnikov, Advancements and insights into single-atom catalysts for environmental and energy applications, Renew. Sustain. Energy Rev. 218 (2025) 115842. https://doi.org/10.1016/j.rser.2025.115842.

[116] Z. Chen, P. Zhang, Electronic Structure of Single-Atom Alloys and Its Impact on The Catalytic Activities, ACS Omega. 7 (2022) 1585-1594. https://doi.org/10.1021/acsomega.1c06067.

[117] X. Wang, R. Su, H. Aslan, J. Kibsgaard, S. Wendt, L. Meng, M. Dong, Y. Huang, F. Besenbacher, Tweaking the composition of NiMoZn alloy electrocatalyst for enhanced hydrogen evolution reaction performance, Nano Energy. 12 (2015) 9-18. https://doi.org/10.1016/j.nanoen.2014.12.007.

[118] Y. Zheng, Y. Jiao, A. Vasileff, S.-Z. Qiao, The Hydrogen Evolution Reaction in Alkaline Solution: From Theory, Single Crystal Models, to Practical Electrocatalysts, Angewandte Chemie 57, 26 (2018) 7568-7579. https://doi.org/10.1002/anie.201710556.

[119] J. Shi, Y. Bao, R. Ye, J. Zhong, L. Zhou, Z. Zhao, W. Kang, S.B. Aidarova, Recent progress and perspective of electrocatalysts for the hydrogen evolution reaction, Catal. Sci. Technol. 15 (2025) 2104-2131. https://doi.org/10.1039/D4CY01449A.

[120] H. Wang, W. Fu, X. Yang, Z. Huang, J. Li, H. Zhang, Y. Wang, Recent advancements in heterostructured interface engineering for hydrogen evolution reaction electrocatalysis, J. Mater. Chem. A 8 (2020) 6926-6956. https://doi.org/10.1039/C9TA11646J.

[121] Y. Li, L. Feng, Recent Advances and Perspectives in Ru Hybrid Electrocatalysts for the Hydrogen Evolution Reaction, Energy Fuels 37, 12 (2023) 8079-8098. https://doi.org/10.1021/acs.energyfuels.3c00749.

[122] J. Liang, Y. Liu, Z. Wang, Y. Jia, Z. Ding, L. Gao, Ni_3S_2@MoO_3@Co_3O_4@AMO/NF core–shell heterostructure for high performance alkaline overall water splitting, Discover Nano 20 (2025) 112. https://doi.org/10.1186/s11671-025-04283-x.

[123] Y. Zhu, M. Klingenhof, C. Gao, T. Koketsu, G. Weiser, Y. Pi, S. Liu, L. Sui, J. Hou, J. Li, H. Jiang, L. Xu, W.-H. Huang, C.-W. Pao, M. Yang, Z. Hu, P. Strasser, J. Ma. Facilitating alkaline hydrogen evolution reaction on the hetero-interfaced Ru/RuO_2 through Pt single atoms doping, Nat. Commun. 15 (2024) 1447. https://doi.org/10.1038/s41467-024-45654-9.

[124] J. Yan, R. Wu, G. Jin, L. Jia, G. Feng, X. Tong, The hybrid Pt nanoclusters/Ru nanowires catalysts accelerating alkaline hydrogen evolution reaction, Advanced Powder Materials 3, 5 (2024) 100214, https://doi.org/10.1016/j.apmate.2024.100214.

[125] A. Song, S. Song, M. Duanmu, H. Tian, H. Liu, X. Qin, G. Shao, G. Wang, Recent Progress of Non-Noble Metallic Heterostructures for the Electrocatalytic Hydrogen Evolution, Small Sci. 3, 9 (2023) 2300036. https://doi.org/10.1002/smsc.202300036.

[126] H. Wei, A. Tan, W. Liu, J. Piao, K. Wan, Z. Liang, Z. Xiang, Z. Fu, Interface Engineering-Induced 1T-MoS_2/NiS Heterostructure for Efficient Hydrogen Evolution Reaction, Catalysts. 12 (2022) 947. https://doi.org/10.3390/catal12090947.

[127] V. Giulimondi, S. Mitchell, J. Pérez-Ramírez, Challenges and Opportunities in Engineering the Electronic Structure of Single-Atom Catalysts, ACS Catal. 13 (2023) 2981-2997. https://doi.org/10.1021/acscatal.2c05992.

[128] M. Miao, J. Pan, T. He, Y. Yan, B.Y. Xia, X. Wang, Molybdenum Carbide-Based Electrocatalysts for Hydrogen Evolution Reaction, Chemistry 23, 46 (2017) 10947-10961. https://doi.org/10.1002/chem.201701064.

[129] H.-M. Zhang, J.-J. Wang, Y. Meng, F. Lu, M. Ji, C. Zhu, J. Xu, J. Sun, Review on Intrinsic Electrocatalytic Activity of Transition Metal Nitrides on HER, Energy Mater. Adv. 2022 (2022). https://doi.org/10.34133/energymatadv.0006.

[130] J. Xu, L. Ge, Y. Zhou, G. Jiang, L. Li, Y. Li, Y. Li, Insights into N, P, S multi-doped Mo_2C/C composites as highly efficient hydrogen evolution reaction catalysts, Nanoscale Adv. 2 (2020) 3334-3340. https://doi.org/10.1039/D0NA00335B.

[131] Z. Li, S. Xu, K. Chu, G. Yao, Y. Xu, P. Niu, Y. Yang, F. Zheng, Synergistic Tuning of the Electronic Structure of Mo_2C by P and Ni Codoping for Optimizing Electrocatalytic Hydrogen Evolution, Inorg Chem 59, 18 (2020) 13741-13748. https://doi.org/10.1021/acs.inorgchem.0c02103.

[132] D. Wang, T. Liu, J. Wang, Z. Wu, N, P (S) Co-doped Mo_2C/C hybrid electrocatalysts for improved hydrogen generation, Carbon 139 (2018) 845-852. https://doi.org/10.1016/j.carbon.2018.07.043.

[133] L. Li, Z. Qin, L. Ries, S. Hong, T. Michel, J. Yang, C. Salameh, M. Bechelany, P. Miele, D. Kaplan,

M. Chhowalla, D. Voiry, Role of Sulfur Vacancies and Undercoordinated Mo Regions in MoS_2 Nanosheets toward the Evolution of Hydrogen, ACS Nano 13, 6 (2019) 6824-6834. https://doi.org/10.1021/acsnano.9b01583.

[134] B.-A. Chen, A.J.E. Rowberg, T.A. Pham, T. Ogitsu, P.V. Kamat, S. Ptasinska, Reactivity of Sulfur Vacancy-Rich MoS_2 to Water Dissociation, J. Phys. Chem. C 128, 25 (2024) 10379-10387. https://doi.org/10.1021/acs.jpcc.4c01677.

[135] S. Tang, Z. Zhang, J. Xiang, X. Yang, X. Shen, F. Song, Recent advances in transition metal nitrides for hydrogen electrocatalysis in alkaline media: From catalyst design to application, Front Chem. 10 (2022) 1073175. https://doi.org/10.3389/fchem.2022.1073175.

[136] H. Shen, S. Liang, S. Adimi, X. Guo, Y. Zhu, H. Guo, T. Thomas, J.P. Attfield, M. Yang, Supporting nickel on vanadium nitride for comparable hydrogen evolution performance to platinum in alkaline solution, J. Mater. Chem. A 9 (2021) 19669-19674. https://doi.org/10.1039/D1TA02760C.

[137] L. Su, X. Cui, T. He, L. Zeng, H. Tian, Y. Song, K. Qia, B.Y. Xia, Surface reconstruction of cobalt phosphide nanosheets by electrochemical activation for enhanced hydrogen evolution in alkaline solution, Chem. Sci. 10 (2019) 2019-2024. https://doi.org/10.1039/C8SC04589E.

[138] F. Luo, X. Shu, X. Jiang, Y. Liu, J. Zhang, S. Chen, Accelerating the surface reconstruction of cobalt phosphide via dual-doping engineering for high-performance water electrolysis, Journal of Power Sources 551 (2022) 232181. https://doi.org/10.1016/j.jpowsour.2022.232181.

[139] J.Y. Kim, P. Lindgren, Y.-J. Zhang, S.K. Kim, T.M. Valentin, H.-T. Jung, A.A. Peterson, Sulfur promotes hydrogen evolution on molybdenum carbide catalysts, Cite this: Mater. Adv. 2 (2021) 4867. https://doi.org/10.1039/d1ma00281c.

[140] D.K. Perivoliotis, J. Ekspong, X. Zhao, G. Hu, T. Wågberg, E. Gracia-Espino, Recent progress on defect-rich electrocatalysts for hydrogen and oxygen evolution reactions, Nano Today 50 (2023) 101883. https://doi.org/10.1016/j.nantod.2023.101883.

[141] Z. Yang, J. Zhu, X. Xu, L. Wang, G. Zhou, Z. Yang, Y. Zhang, Defect and strain engineered MoS_2/graphene catalyst for an enhanced hydrogen evolution reaction, RSC Adv. 13 (2023) 4056-4064. https://doi.org/10.1039/D2RA07363C.

[142] P.S. Adarakatti, M. Mahanthappa, J.P. Hughes, S.J. Rowley-Neale, G.C. Smith, S. Ashoka, C.E. Banks, MoS_2-graphene-$CuNi_2S_4$ nanocomposite an efficient electrocatalyst for the hydrogen evolution reaction, Int. J. Hydrogen Energy. 44 (2019) 16069-16078. https://doi.org/10.1016/j.ijhydene.2019.05.004.

[143] Y. Li, H. Wang, L. Xie, Y. Liang, G. Hong, H. Dai, MoS_2 Nanoparticles Grown on Graphene : An Advanced Catalyst for Hydrogen Evolution Reaction, J. Am. Chem. Soc. 133, 19 (2011) 7296-7299. https://doi.org/10.1021/ja201269b.

[144] S. Kumar, P.K. Sahoo, A.K. Satpati, Electrochemical and SECM Investigation of MoS_2/GO and MoS_2/rGO Nanocomposite Materials for HER Electrocatalysis, ACS Omega 2, 11 (2017) 7532-7545. https://doi.org/10.1021/acsomega.7b00678.

[145] Y. Garcia-Basabe, G.F. Peixoto, D. Grasseschi, E.C. Romani, F.C. Vicentin, C.E.P. Villegas, A.R. Rocha, D.G. Larrude, Phase transition and electronic structure investigation of MoS_2-reduced graphene oxide nanocomposite decorated with Au nanoparticles, Nanotechnology 30 (2019) 475707. https://doi.org/10.1088/1361-6528/ab3c91.

[146] S. Ozden, S. Bawari, S. Vinod, U. Martinez, S. Susarla, C. Narvaez, J. Joyner, C.S. Tiwary, T.N. Narayanan, P.M. Ajayan, Interface and defect engineering of hybrid nanostructures toward an efficient HER catalyst, Nanoscale. 11 (2019) 12489-12496. https://doi.org/10.1039/C9NR01321K.

[147] W. Zhai, Y. Ma, D. Chen, J.C. Ho, Z. Dai, Y. Qu, Recent progress on the long-term stability of hydrogen evolution reaction electrocatalysts, InfoMat 4, 9 (2022) e12357. https://doi.org/10.1002/inf2.12357.

[148] A. Shahroudi, S. Habibzadeh, Enhanced hydrogen evolution reaction activity through samarium-doped nickel phosphide (Ni_2P) electrocatalyst. Sci Rep 14 (2024) 16818. https://doi.org/10.1038/s41598-024-66775-7.

[149] A. Han, S. Jin, H. Chen, H. Ji, Z. Suna, P. Du, A robust hydrogen evolution catalyst based on crystalline nickel phosphide nanoflakes on three-dimensional graphene/nickel foam: high performance for electrocatalytic hydrogen production from pH 0–14, J. Mater. Chem. A 3 (2015) 1941-1946. https://doi.org/10.1039/C4TA06071G.

[150] E.J. Popczun, J.R. McKone, C.G. Read, A.J. Biacchi, A.M. Wiltrout, N.S. Lewis, R.E. Schaak, Nanostructured Nickel Phosphide as an Electrocatalyst for the Hydrogen Evolution Reaction, J. Am. Chem. Soc. 135, 25 (2013) 9267-9270. https://doi.org/10.1021/ja403440e.

[151] J. Zhang, W. Cui, Y. Ni, W. Chen, D. You, A MoS_2/$Cu_{1.8}S$/NiS@MoSX heterostructured electro-catalyst for high-efficiency hydrogen evolution in alkaline solution, International Journal of Hydrogen Energy 51 (2024) 1577-1585. https://doi.org/10.1016/j.ijhydene.2023.08.018.

[152] X. Zhang, S. Hua, L. Lai, Z. Wang, T. Liao, L. He, H. Tang, X. Wan, Strategies to improve electrocatalytic performance of MoS_2-based catalysts for hydrogen evolution reactions, RSC Adv. 12 (2022) 17959-17983. https://doi.org/10.1039/d2ra03066g.

[153] T.F. Jaramillo, K.P. Jørgensen, J. Bonde, J.H. Nielsen, S. Horch, I. Chorkendorff, Identification of Active Edge Sites for Electrochemical H_2 Evolution from MoS_2 Nanocatalysts, Science 317, 5834 (2007) 100-102. https://doi.org/10.1126/science.1141483.

[154] A.K Kunhiraman, A. Prabhu S, M.R. Puthalath, A. Rakkesh R, A. Hochgesang, Hydrogen evolution reaction catalyzed by MoS_2/CoS_2 supported on nanocarbon hybrid in acidic medium, Surfaces and

Interfaces 42, Part A (2023) 103366. https://doi.org/10.1016/j.surfin.2023.103366.

[155] J.L. Zhu, J.X. Zhang, J. Liu, Z. Liu, Y.D. He, A.X. Wei, Electrocatalytic performance of MoS_2 nanosheets grown on a carbon nanotubes/carbon cloth substrate for the hydrogen evolution reaction, Dig. J. Nanomater. Bios. 17, 3 (2022) 799-810. https://doi.org/10.15251/DJNB.2022.173.799.

[156] S. Fang, X. Zhu, X. Liu, J. Gu, W. Liu, D. Wang, W. Zhang, Y. Lin, J. Lu, S. Wei, Y. Li, T. Yao, Uncovering near-free platinum single-atom dynamics during electrochemical hydrogen evolution reaction, Nat. Commun. 11 (2020) 1029. https://doi.org/10.1038/s41467-020-14848-2.

[157] N. Cheng, S. Stambula, D. Wang, M.N. Banis, J. Liu, A. Riese, B. Xiao, R. Li, T.-K. Sham, L.-M. Liu, G.A. Botton, X. Sun, Platinum single-atom and cluster catalysis of the hydrogen evolution reaction, Nat. Commun. 7 (2016) 13638. https://doi.org/10.1038/ncomms13638.

[158] F. Guo, T.J. Macdonald, A.J. Sobrido, L. Liu, J. Feng, G. He, Recent Advances in Ultralow-Pt-Loading Electrocatalysts for the Efficient Hydrogen Evolution, Advanced Science 10, 21 (2023) 2301098. https://doi.org/10.1002/advs.202301098.

[159] H. Dong, C. Liu, H. Ye, L. Hu, B. Fugetsu, W. Dai, Y. Cao, X. Qi, H. Lu, X. Zhang, Three-dimensional Nitrogen-Doped Graphene Supported Molybdenum Disulfide Nanoparticles as an Advanced Catalyst for Hydrogen Evolution Reaction, Sci. Rep. 5 (2015) 17542. https://doi.org/10.1038/srep17542.

[160] W. Liu, A. Wang, J. Zhang, S. Yu, M. Wang, S. Tian, H. Tang, Z. Zhao, X. Ren, Y. Guo, D. Ma, Pt/α-MoC Catalyst Boosting pH-Universal Hydrogen Evolution Reaction at High Current Densities, ACS Nano 19, 10 (2025) 10038-10047. https://doi.org/10.1021/acsnano.4c16678.

[161] C. Lu, D. Tranca, J. Zhang, F.R. Hernández, Y. Su, X. Zhuang, F. Zhang, G. Seifert, X. Feng, Molybdenum Carbide-Embedded Nitrogen-Doped Porous Carbon Nanosheets as Electrocatalysts for Water Splitting in Alkaline Media, ACS Nano 11, 4 (2017) 3933-3942. https://doi.org/10.1021/acsnano.7b00365.

[162] V.K. Singh, U.T. Nakate, P. Bhuyan, J. Chen, D.T. Tran, S. Park, Mo/Co doped 1T-VS_2 nanostructures as a superior bifunctional electrocatalyst for overall water splitting in alkaline media, J. Mater. Chem. A 10 (2022) 9067-9079. https://doi.org/10.1039/D2TA00488G.

[163] Haoyu Li, Juan Wu, Mengyao Li, Yude Wang, Recent Advances in Vanadium-Based Electrocatalysts for Hydrogen and Oxygen Evolution Reactions: A Review, Catalysts 14, 6 (2024) 368. https://doi.org/10.3390/catal14060368.

[164] S. Hussain, D. Vikraman, A. Feroze, W. Song, K.-S. An, H.-S. Kim, S.-H. Chun, J. Jung, Synthesis of Mo_2C and W_2C Nanoparticle Electrocatalysts for the Efficient Hydrogen Evolution Reaction in Alkali and Acid Electrolytes, Front. Chem. 7 (2019) 716. https://doi.org/10.3389/fchem.2019.00716.

[165] S.J. Yoon, S.J. Lee, M.H. Kim, H.A. Park, H.S. Kang, S.-Y. Bae, I.-Y. Jeon, Recent Tendency on Transition-Metal Phosphide Electrocatalysts for the Hydrogen Evolution Reaction in Alkaline Media, Nanomaterials 13, 18 (2023) 2613. https://doi.org/10.3390/nano13182613.

[166] D. Shi, B. Chang, Z. Ai, H. Jiang, F. Chen, Y. Shao, J. Shen, Y. Wu, X. Hao, Boron carbonitride with tunable B/N Lewis acid/base sites for enhanced electrocatalytic overall water splitting, Nanoscale 13 (2021) 2849-2854. https://doi.org/10.1039/D0NR06857H.

[167] M. Hakala, R. Kronberg, K. Laasonen, Hydrogen adsorption on doped MoS_2 nanostructures, Scientific Reports 7 (2017) 15243. https://doi.org/10.1038/s41598-017-15622-z.

[168] M. Liu, J.-A. Wang, W. Klysubun, G.-G. Wang, S. Sattayaporn, F. Li, Y.-W. Cai, F. Zhang, J. Yu, Y. Yang, Interfacial electronic structure engineering on molybdenum sulfide for robust dual-pH hydrogen evolution, Nature Communications 12 (2021) 5260. https://doi.org/10.1038/s41467-021-25647-8.

[169] A.K.R. Robledo, M.F. Salazar, B.A.M. Martínez, Á.A. Torres-Rosales, H.F. Lara-Alfaro, O. Del Pozo-Zamudio, E.A. Cerda-Méndez, S. Jiménez-Sandoval, A. De Luna Bugallo, Interlayer charge transfer in supported and suspended MoS_2/Graphene/MoS_2 vertical heterostructures, PLoS ONE 18, 7 (2023) e0283834. https://doi.org/10.1371/journal.pone.0283834.

[170] S.Ø. Hanslin, H. Jónsson, J. Akola, Sulfur-deficient edges as active sites for hydrogen evolution on MoS_2, Phys. Chem. Chem. Phys. 25 (2023) 32541-32548. https://doi.org/10.1039/D3CP04198K.

[171] F. Keivanimehr, S. Habibzadeh, A. Baghban, A. Esmaeili, A. Mohaddespour, A.H. Mashhadzadeh, M.R. Ganjali, M.R. Saeb, V. Fierro, A. Celzard, Electrocatalytic hydrogen evolution on the noble metal-free MoS_2/carbon nanotube heterostructure: a theoretical study, Scientific Reports 11 (2021) 3958. https://doi.org/10.1038/s41598-021-83562-w.

[172] H. Zhao, Z.-Y. Yuan, Engineering of transition metal phosphide-based heterostructures for electrocatalytic water splitting, Smart Mater Devices. 1 (2025) 202521. https://doi.org/10.70401/smd.2025.0013.

[173] Z.H. Tan, X.Y. Kong, B.-J. Ng, H.S. Soo, A.R. Mohamed, S.-P. Chai, Recent Advances in Defect-Engineered Transition Metal Dichalcogenides for Enhanced Electrocatalytic Hydrogen Evolution: Perfecting Imperfections, ACS Omega 8, 2 (2023) 1851-1863. https://doi.org/10.1021/acsomega.2c06524.

[174] S. Lakshmanaperumal, H.P. Somasundharam, S.M.S. Kumar, In-situ dual engineering strategy for the development of Metallic 1T-MoS_2 decorated over N, S – Heteroatom doped hollow carbon spheres for enhanced hydrogen evolution reaction, Int. J. Hydrogen Energy 138 (2025) 434-444. https://doi.org/10.1016/j.ijhydene.2025.05.132.

[175] R. Zhang, Y. Zhu, Y. Cheng, J. Guan, Q. Zou, B. Guo, M. Zhang. Ru-modified cobalt phosphide

nanoparticles on N-doped carbon nanofibers for efficient hydrogen evolution reaction in alkaline media, J. Alloys Compd. 968 (2023) 171889. https://doi.org/10.1016/j.jallcom.2023.171889.

[176] C. Renugadevi, L. Cindrella, Nanoscale Pd-Co alloy supported on dual heteroatoms doped carbon – An efficient electrocatalyst for hydrogen evolution and oxygen reduction reactions, J. Alloys Compd. 1022 (2025) 179990. https://doi.org/10.1016/j.jallcom.2025.179990.

[177] D. Manoj, L. Gnanasekaran, S. Rajendran, T.K.A. Hoang, A.A. Jalil, M. Soto-Moscoso, A review on metallic carbides/phosphides embedded in N-doped porous carbon as highly efficiency electrocatalyst for hydrogen evolution reactions in alkaline medium, Int. J. Hydrogen Energy 54 (2024) 316-326. https://doi.org/10.1016/j.ijhydene.2023.04.010.

[178] J. Cencerrero, P. Sánchez, A. de Lucas-Consuegra, A.R. de la Osa, A. Romero, Influence of boron doping level and calcination temperature on hydrogen evolution reaction in acid medium of metal-free graphene aerogels, Heliyon 9, 10 (2023) e20748, https://doi.org/10.1016/j.heliyon.2023.e20748.

[179] Y. Luo, L. Tang, U. Khan, Q. Yu, H.-M. Cheng, X. Zou, B. Liu. Morphology and surface chemistry engineering toward pH-universal catalysts for hydrogen evolution at high current density, Nature Communications volume 10 (2019) 269. https://doi.org/10.1038/s41467-018-07792-9.

[180] J. Lin, X. Wang, Z. Zhao, D. Chen, R. Liu, Z. Ye, B. Lu, Y. Hou, J. Lu, Design of pH-universal electrocatalysts for hydrogen evolution reaction, Carbon Energy 6, 11 (2024) e555. https://doi.org/10.1002/cey2.555.

[181] M.Z. Rahman, M.G. Kibria, C.B. Mullins, Metal-free photocatalysts for hydrogen evolution, Chem. Soc. Rev. 49 (2020) 1887-1931. https://doi.org/10.1039/C9CS00313D.

[182] Y. Cai, J. Gao, S. Chen, Q. Ke, G. Zhang, Y.-W. Zhang, Design of Phosphorene for Hydrogen Evolution Performance Comparable to Platinum, Chem. Mater. 31, 21 (2019) 8948-8956. https://doi.org/10.1021/acs.chemmater.9b03031.

[183] M. Cai, L. Xu, J. Guo, X. Yang, X. He, Peng Hu, Recent advances in metal-free electrocatalysts for the hydrogen evolution reaction, J. Mater. Chem. A 12 (2024) 592-612. https://doi.org/10.1039/D3TA05901D.

[184] K. Qu, Y. Zheng, X. Zhang, K. Davey, S. Dai, S.Z. Qiao, Promotion of Electrocatalytic Hydrogen Evolution Reaction on Nitrogen-Doped Carbon Nanosheets with Secondary Heteroatoms, ACS Nano 11, 7 (2017) 7293-7300. https://doi.org/10.1021/acsnano.7b03290.

[185] Tewodros Asefa, Dr. Xiaoxi Huang, Heteroatom-Doped Carbon Materials for Electrocatalysis, ChemEurJ 23, 45 (2017) 10703-10713. https://doi.org/10.1002/chem.201700439.

[186] Y. Fujimoto, Formation, Structure, Electronic, and Transport Properties of Nitrogen Defects in Graphene and Carbon Nanotubes, Micromachines (Basel). 15, 9 (2024) 1172.

https://doi.org/10.3390/mi15091172.

[187] F.A. Alharthi, I. Hasan, Improved Photocatalytic Hydrogen Evolution using Sulfur-Doped Graphite-like Carbon Nitride (S-G-C_3N_4) Photocatalyst, ChemistrySelect 8, 34 (2023) e202302369. https://doi.org/10.1002/slct.202302369.

[188] Z. Zhang, C. Song, J. Fan, Z. Fang, H. Wang, J. Zou, Morphology and doping engineering of sulfur-doped g-C_3N_4 hollow nanovesicles for boosting photocatalytic hydrogen production, J. Mater. Chem. A 13 (2025) 6385-6396. https://doi.org/10.1039/D4TA09249J.

[189] J. Yan, F. Ye, Q. Dai, X. Ma, Z. Fang, L. Dai, C. Hu, Recent progress in carbon-based electrochemical catalysts: From structure design to potential applications, Nano Res. Energy. 2 (2023) e9120047. https://doi.org/10.26599/NRE.2023.9120047.

[190] Y. Zheng, Y. Jiao, L.H. Li, T. Xing, Y. Chen, M. Jaroniec, S.Z. Qiao, Toward Design of Synergistically Active Carbon-Based Catalysts for Electrocatalytic Hydrogen Evolution, ACS Nano 8, 5 (2014) 5290-5296. https://doi.org/10.1021/nn501434a.

[191] C.W. Chan, S.Y. Wu, H.T. Chen, The interaction of hydrogen with heteroatoms (B, N)-doped porous graphene: A computational study. Chem. Pap. 76 (2022) 1009-1017. https://doi.org/10.1007/s11696-021-01901-7.

[192] Z. Zhao, H. Chen, W. Zhang, S. Yi, H. Chen, Z. Su, B. Niu, Y. Zhang, D. Long, Defect engineering in carbon materials for electrochemical energy storage and catalytic conversion, Mater. Adv. 4 (2023) 835-867. https://doi.org/10.1039/D2MA01009G.

[193] X. Zhu, Y. Shao, D. Xia, Y. Wei, Z. Li, W. Liu, N. Wang, Q. Wu, F. Ding, J. Li, F. Kang, L. Gan, When Graphitic Nitrogen Meets Pentagons: Selective Construction and Spectroscopic Evidence for Improved Four-Electron Oxygen Reduction Electrocatalysis, Adv. Materials 37, 26 (2025) 2414976. https://doi.org/10.1002/adma.202414976.

[194] H. Chen, X. Luo, S. Huang, F. Yu, D. Li, Y. Chen, Phosphorus-doped activated carbon as a platinum-based catalyst support for electrocatalytic hydrogen evolution reaction, J. Electroanal. Chem. 948 (2023) 117820. https://doi.org/10.1016/j.jelechem.2023.117820.

[195] P. Wana, Q. Tang, Theoretical progress of MXenes as electrocatalysts for the hydrogen evolution reaction, Mater. Chem. Front. 8 (2024) 507-527. https://doi.org/10.1039/D3QM00783A.

[196] L. He, H. Zhuang, Q. Fan, P. Yu, S. Wang, Y. Pang, K. Chen, K. Liang, Advances and challenges in MXene-based electrocatalysts: unlocking the potential for sustainable energy conversion, Mater. Horiz. 11 (2024) 4239-4255. https://doi.org/10.1039/D4MH00845F.

[197] X. Wang, C. Wang, S. Ci, Y. Ma, T. Liu, L. Gao, P. Qian, C. Jif, Y. Su, Accelerating 2D MXene catalyst discovery for the hydrogen evolution reaction by computer-driven workflow and an ensemble learning strategy, J. Mater. Chem. A 8 (2020) 23488-23497.

https://doi.org/10.1039/D0TA06583H.

[198] J. Luxa, P. Kupka, F. Lipilin, J. Šturala, A. Subramani, P. Lazar, Z. Sofer, Hydrogen Evolution Reaction Activity in $Mo_2TiC_2T_x$ MXene Derived from Mo_2TiAlC_2 MAX Phase: Insights from Compositional Transformations, ACS Catal. 14, 20 (2024) 15336-15347. https://doi.org/10.1021/acscatal.4c04099.

[199] S. Dutta, R. Banerjee, Tuning Catalytic Efficiency: Thermodynamic Optimization of Zr-Doped \ce{Ti_3C_2} and \ce{Ti_3CN} MXenes for HER Catalysis. Condensed matter. (2025). https://doi.org/10.48550/arXiv.2501.15092.

[200] P. Devi, M. Downes, S. Pahra, S. Ippolito, R.J. Wang, Y. Gogotsi, Electrocatalytic Performance of M_5X_4 MXenes for Hydrogen Evolution Reaction, N. M. Small 21, 36 (2025) e03947. https://doi.org/10.1002/smll.202503947.

[201] M.A. Tekalgne, H.H. Do, T.V. Nguyen, Q.V. Le, S.H. Hong, S.H. Ahn, S.Y. Kim, MXene Hybrid Nanosheet of WS_2/Ti_3C_2 for Electrocatalytic Hydrogen Evolution Reaction, ACS Omega 8, 44 (2023) 41802-41808. https://doi.org/10.1021/acsomega.3c06403.

[202] S. Sharma, A. Halder, P. Devi, $Ti_3C_2T_x$-engineered MoS_2/SiNWs multifunctional photocathode for Photoelectrochemical hydrogen generation and wastewater remediation, Inorg. Chem. Commun. 182, Part 2 (2025) 115552. https://doi.org/10.1016/j.inoche.2025.115552.

[203] J. Zhang, W. Zhang, J. Zhang, Y. Li, Y. Wang, L. Yang, S. Yin, MOF-derived bimetallic NiMo-based sulfide electrocatalysts for efficient hydrogen evolution reaction in alkaline media, J. Alloys Compd. 935, Part 2 (2023) 167974. https://doi.org/10.1016/j.jallcom.2022.167974.

[204] L. Wang, L. Song, Z. Yang, Y.-M. Chang, F. Hu, L. Li, L. Li, H.-Y. Chen, S. Peng, Electronic Modulation of Metal–Organic Frameworks by Interfacial Bridging for Efficient pH-Universal Hydrogen Evolution, Adv. Funct. Mater. 33, 1 (2023) 2210322. https://doi.org/10.1002/adfm.202210322.

[205] D. Vasu, Y.-T. Huang, S.-H. Chang, M. Pichumani, T.-W. Chiu, Resourceful hydrogen evolution reaction using a high atom-efficiency single-atom catalyst immobilized on layered MXene nanosheets, Int. J. Hydrog. Energy 137 (2025) 406-415. https://doi.org/10.1016/j.ijhydene.2025.05.023.

[206] R. Luo, Z. Li, R. Li, C. Jiang, R. Qi, M. Liu, H. Lin, R. Huang, C. Luo, H. Peng, Ultrafine Ru nanoparticles derived from few-layered $Ti_3C_2T_x$ MXene templated MOF for highly efficient alkaline hydrogen evolution, Int. J. Hydrog. Energy 47, 77 (2022) 32787-32795. https://doi.org/10.1016/j.ijhydene.2022.07.205.

[207] S. Pandey, M. Ghimire, C. Lee, J. Park, M.I.O. Amaya, T.T. Trần, J.-W. Son, Y.J. Yun, Y. Jun, Recent progress on MXene-hematite nanocomposite catalyst for water-splitting applications:

Synthesis strategies, synergetic performance, and future perspectives, Fuel 404, Part B (2026) 136248. https://doi.org/10.1016/j.fuel.2025.136248.

[208] H. Wang, X. Li, Y. Deng, J. Jiang, H. Ma, J. Zou, Advances in MXene-based single-atom catalysts for electrocatalytic applications, Coord. Chem. Rev. 529 (2025) 216462. https://doi.org/10.1016/j.ccr.2025.216462.

[209] A. Nsabimana, Y. Guan, G. Xu, In situ and operando characterization techniques for nanocatalyst-based electrochemical hydrogen evolution reactions, J. Electrochem. Sci. Eng. 15, 1 (2025) 2526. https://doi.org/10.5599/jese.2526.

[210] E. Zhu, W. Hu, J. Dong, J. Chen, Y. Li, L. Wang, Advanced Development of In situ Characterization Technique for Electrocatalytic Hydrogen Evolution Reaction, Adv. Sustain. Syst. (2024). https://doi.org/10.1002/adsu.202400224.

[211] Z. Wang, Y.-R. Zheng, J. Montoya, D. Hochfilzer, A. Cao, J. Kibsgaard, I. Chorkendorff, J.K. Nørskov, Origins of the Instability of Nonprecious Hydrogen Evolution Reaction Catalysts at Open-Circuit Potential, ACS Energy Lett. 6 (2021) 2268-2274. https://doi.org/10.1021/acsenergylett.1c00876.

[212] Z.W. Seh, J. Kibsgaard, C.F. Dickens, I. Chorkendorff, J.K. Nørskov, T.F. Jaramillo, Combining theory and experiment in electrocatalysis: Insights into materials design, Science 355 (2017) eaad4998. https://doi.org/10.1126/science.aad4998.

[213] L. Zhang, Z. Shi, Y. Lin, F. Chong, Y. Qi, Design Strategies for Large Current Density Hydrogen Evolution Reaction, Front. Chem. 10 (2022) 866415. https://doi.org/10.3389/fchem.2022.866415.

[214] L. Tang, J. Yu, Y. Zhang, Z. Tang, Y. Qin, Boosting the hydrogen evolution reaction activity of Ru in alkaline and neutral media by accelerating water dissociation, RSC Adv. 11 (2021) 6107-6113. https://doi.org/10.1039/D0RA09515J.

[215] H. Jung, S. Choung, J.W. Han, Design principles of noble metal-free electrocatalysts for hydrogen production in alkaline media: combining theory and experiment, Nanoscale Adv. 3 (2021) 6797-6826. https://doi.org/10.1039/D1NA00606A.

[216] J. Chen, Q. Jin, Y. Li, Y. Li, H. Cui, C. Wang, Design Superior Alkaline Hydrogen Evolution Electrocatalyst by Engineering Dual Active Sites for Water Dissociation and Hydrogen Desorption, ACS Appl. Mater. Interfaces 11, 42 (2019) 38771-38778. https://doi.org/10.1021/acsami.9b13657.

[217] M.C.O. Monteiro, A. Goyal, P. Moerland, M.T.M. Koper, Understanding Cation Trends for Hydrogen Evolution on Platinum and Gold Electrodes in Alkaline Media, ACS Catal. 11, 23 (2021) 14328-14335. https://doi.org/10.1021/acscatal.1c04268.

[218] L.B.T. de Kam, T.L. Maier, K. Krischer, Electrolyte effects on the alkaline hydrogen evolution reaction: A mean-field approach, Electrochim. Acta 497 (2024) 144530.

https://doi.org/10.1016/j.electacta.2024.144530.

[219] P. Li, Y.-L. Jiang, Y. Men, Y.-Z. Jiao, S. Chen, Kinetic cation effect in alkaline hydrogen electrocatalysis and double layer proton transfer, Nat. Commun. 16 (2025) 1844. https://doi.org/10.1038/s41467-025-56966-9.

[220] S.V. Chauhan, K.K. Joshi, P.M. Pataniya, C.K. Sumesh, Advancing industrial rate current density in water electrolysis for green hydrogen production: catalyst development, benchmarking, and best practices, Sustain. 9 (2025) 3550-3576. https://doi.org/10.1039/D5SE00262A.

[221] R. Yao, K. Sun, K. Zhang, Y. Wu, Y. Du, Q. Zhao, G. Liu, C. Chen, Y. Sun, J. Li, Stable hydrogen evolution reaction at high current densities via designing the Ni single atoms and Ru nanoparticles linked by carbon bridges, Nat. Commun. 15 (2024) 2218. https://doi.org/10.1038/s41467-024-46553-9.

[222] N. Ke, H. Huang, F. Wang, A. Huang, C. Tan, B. Dong, Y. Wu, L. Hao, X. Xu, S. Agathopoulos, Self-Supported MoO_2/$MoSi_2$ Ceramic Electrode for High Current Density Hydrogen Evolution Reaction, ACS Sustainable Chem. Eng. 11, 9 (2023) 3769-3779. https://doi.org/10.1021/acssuschemeng.2c06893.

[223] C. Nelson, M.M. Gui, P.K.J. Robertson, The Environmental Emission and Climate Change Impact of Hydrogen Fuel Derived from Photocatalysis Water-Splitting Reaction, Adv. Energ. Sust. Res. 6, 5 (2025) 2400337. https://doi.org/10.1002/aesr.202400337.

[224] J. Comendador, J. Llanos, Á. Ramírez, M. Muñoz-Morales, E. López-Fernández, Turning Polluted Biomass Waste into Sustainable Carbon-Based Catalysts for Hydrogen Production via Water Electrolysis, Energy Fuels 39, 31 (2025) 15003-15015. https://doi.org/10.1021/acs.energyfuels.5c02282.

[225] R.A. Marquez, J.T. Bender, A.M. Aleman, E. Kalokowski,T.V. Le, C.L. Williamson, M.L. Frederiksen, K. Kawashima, C.E. Chukwuneke, A. Dolocan, D.J. Milliron, J. Resasco, T.F. Jaramillo, C.B. Mullins, Insights into catalyst degradation during alkaline water electrolysis under variable operation, Energy Environ. Sci. 18 (2025) 7170-7187. https://doi.org/10.1039/D5EE02194D.

[226] L. Mirizzi, E. Carena, C. Santoro, V.C.A. Ficca, E. Placidi, E. Berretti, Al. Lavacchi, C. Ferrara, M. Muhyuddin. Many lives of cobalt within electrochemical systems: from waste batteries to efficient hydrogen evolution reaction electrocatalyst. Mater. Renew. Sustain. Energy 14 (2025) 37. https://doi.org/10.1007/s40243-025-00312-y.

[227] Z. Chen, S. Yun, L. Wu, J. Zhang, X. Shi, W. Wei, Y. Liu, R. Zheng, N. Han, B.-J. Ni, Waste-Derived Catalysts for Water Electrolysis: Circular Economy-Driven Sustainable Green Hydrogen Energy. Nano-Micro Lett. 15 (2023) 4. https://doi.org/10.1007/s40820-022-00974-7.

[228] W. Yoshimune, A. Kato, T. Hayakawa, S. Yamaguchi, S. Kato, Simultaneous accelerated stress testing of membrane electrode assembly components in polymer electrolyte fuel cells, npj Mater. Degrad. 8 (2024) 106. https://doi.org/10.1038/s41529-024-00524-z.

[229] W. Shen, Y. Ye, Q. Xia, P. Xi, Progress in in situ characterization of electrocatalysis, EES Catal. 3 (2025) 10-31. https://doi.org/10.1039/D4EY00168K.

[230] D. Li, Y. Liu, Z. Liu, J. Yang, C. Hu, L. Feng, Electrochemical hydrogen evolution reaction efficiently catalyzed by Ru–N coupling in defect-rich Ru/g-C_3N_4 nanosheets, J. Mater. Chem. A 9 (2021) 15019-15026. https://doi.org/10.1039/D1TA03809E.

[231] A. Serban, M.-T. Liu, N. Chen, H.M. Chen, X. Hu, An oxide-promoted, self-supported Ni_4Mo catalyst for high current density anion exchange membrane water electrolysis, Energy Environ. Sci. 18 (2025) 1533-1543. https://doi.org/10.1039/D4EE04528A.

7. Comparative HER performance and derived sustainability indicators for all investigated catalyst samples developed in DEMADES

The sustainability-oriented comparison was based on the electrochemical parameters obtained in WP3. In addition to the experimentally determined or Tafel-derived HER parameters, the HER overpotential-related energy penalty was calculated according to $E_{\eta,H2}=2F\,\eta_{10}$. Relative energy saving was calculated with respect to C-MoFeNiP-1200 in alkaline medium (η_{10}=321 mV). The calculated energy penalty represents only the additional cathodic energy associated with HER overpotential and should not be interpreted as the total energy consumption of water electrolysis.

Table 8. Comparative HER performance and derived sustainability indicators for all investigated catalyst samples.

Catalyst family	Sample	η_{10} (mV)	Tafel slope (mV dec^{-1})	Apparent j_0 (A cm^{-2})	Rct (Ω)	HER energy penalty (kJ mol^{-1} H_2)	Relative energy saving (%)	Evidence score
DES-Ni	2	302.0	153.7	8.39×10^{-5}	–	58.3	5.9	3
	3	271.1	121.6	5.05×10^{-5}	–	52.3	15.5	3
	4	296.1	124.7	4.22×10^{-5}	–	57.1	7.8	3
	5	306.1	115.4	2.23×10^{-5}	–	59.1	4.6	3
	9_2	290.4	123.94	4.54×10^{-5}	–	56.0	9.5	3

	10_2	309.1	92.25	4.46×10^{-6}	–	59.6	3.7	3
	11_2	343.2	104.66	5.26×10^{-6}	–	66.2	−6.9	3
	12_2	312.0	93.8	4.73×10^{-6}	–	60.2	2.8	3
	13_2	278.0	72.0	1.49×10^{-6}	–	53.6	13.4	3
	14_2	287.0	81.1	3.03×10^{-6}	–	55.4	10.6	3
	15_2	300.0	94.6	6.69×10^{-6}	–	57.9	6.5	3
	16_2	259.4	102.7	2.98×10^{-5}	–	50.1	19.2	3
	17_2	274.3	141.8	1.16×10^{-4}	–	52.9	14.5	3
	18_2	285.2	142.1	9.85×10^{-5}	–	55.0	11.2	3
	19_2	**223.0**	134.1	**2.17×10^{-4}**	–	**43.0**	**30.5**	3
Ni/MoS_2	1_1	273.8	107.7	2.76×10^{-5}	–	52.8	14.7	3
	2_1	266.9	95.7	1.58×10^{-5}	–	51.5	16.9	3
	3_1	275.3	107.9	2.62×10^{-5}	–	53.1	14.2	3
	4_1	292.7	105.7	1.72×10^{-5}	–	56.5	8.8	3
	1_2	284.7	105.0	1.77×10^{-5}	–	54.9	11.3	3
	2_2	290.3	130.8	4.90×10^{-5}	–	56.0	9.6	3
	3_2	278.6	121.6	4.30×10^{-5}	–	53.8	13.2	3
	4_2	310.1	95.7	5.71×10^{-6}	–	59.8	3.4	3
	1_3	269.8	113.5	3.74×10^{-5}	–	52.1	16.0	3
	2_3	274.9	134.2	7.21×10^{-5}	–	53.0	14.4	3
	3_3	280.8	120.4	3.98×10^{-5}	–	54.2	12.5	3
	4_3	292.1	141.3	6.37×10^{-5}	–	56.4	9.0	3
	5_3	**259.1**	129.8	**8.80×10^{-5}**	–	**50.0**	**19.3**	3
Ni/MXene	1	271.6	111.0	3.09×10^{-5}	–	52.4	15.4	3
	2	279.9	114.2	2.99×10^{-5}	–	54.0	12.8	3
	3	267.8	93.7	1.26×10^{-5}	–	51.7	16.6	3
	4	283.8	131.9	5.39×10^{-5}	–	54.8	11.6	3
	5	285.2	96.4	9.48×10^{-6}	–	55.0	11.2	3
	6	278.8	113.9	3.03×10^{-5}	–	53.8	13.1	3
	7	289.8	109.7	1.95×10^{-5}	–	55.9	9.7	3
	8	291.2	124.2	3.78×10^{-5}	–	56.2	9.3	3
	9	294.9	101.0	1.05×10^{-5}	–	56.9	8.1	3
	10	282.2	140.6	7.70×10^{-5}	–	54.5	12.1	3
	11	282.20	122.30	4.21×10^{-5}	–	54.5	12.1	3
	12	268.09	127.41	6.32×10^{-5}	–	51.7	16.5	3
	13	266.44	123.10	5.80×10^{-5}	–	51.4	17.0	3

	14	290.78	108.42	1.76×10^{-5}	–	56.1	9.4	3
	15	288.13	117.07	2.86×10^{-5}	–	55.6	10.2	3
	16	231.91	**92.21**	2.90×10^{-5}	–	44.8	27.8	3
	17	232.48	127.65	1.30×10^{-4}	–	44.9	27.6	3
	18	235.88	138.32	1.68×10^{-4}	–	45.5	26.5	3
	19	229.47	141.83	2.04×10^{-4}	–	44.3	28.5	3
	20	**209.52**	137.88	**2.76×10^{-4}**	–	**40.4**	**34.7**	3
C-MoFeNiP	800	522	≈120	2.2×10^{-7}	13.7	100.7	−62.6	4
	1000	349	138	2.8×10^{-5}	9.6	67.3	−8.7	4
	1200	**321**	**93**	3.4×10^{-6}	**5.3**	**61.9**	**0.0**	**5**
Ni–Co sulfides	NiS	279	70	1.1×10^{-6}	19.5	53.8	13.1	4
	$Ni_{0.9}Co_{0.1}S$	320	105	8.6×10^{-6}	9.7	61.8	0.3	4
	$Ni_{0.75}Co_{0.25}S$	422	103	7.8×10^{-7}	27.1	81.4	−31.5	4
	$Ni_{0.6}Co_{0.4}S$	393	113	3.4×10^{-6}	24.2	75.8	−22.4	4
	$Ni_{0.5}Co_{0.5}S$	377	125	9.4×10^{-6}	23.2	72.7	−17.4	4
	$Ni_{0.4}Co_{0.6}S$	**237**	108	**6.3×10^{-5}**	**9.2**	**45.7**	**26.2**	4
	CoS	**222**	122	**1.4×10^{-4}**	**9.0**	**42.8**	**30.8**	4
Ni-foam platform*	Bare Ni foam	305.71	124.88	3.85×10^{-5}	–	59.0	4.8	2
	Ni/Ni foam 1-1	203.67	160.98	3.73×10^{-4}	–	39.3	36.6	2
	Ni/Ni foam 1-2	217.64	146.97	2.63×10^{-4}	–	42.0	32.2	2
	Ni/MoS_2/Ni foam 1-3	**124.03**	119.55	**8.37×10^{-4}**	–	**23.9**	**61.4**	2
	Ni/MoS_2/Ni foam 1-4	178.67	173.81	7.26×10^{-4}	–	34.5	44.3	2

Notes. "–" indicates that the corresponding parameter was not available or could not be derived reliably from the WP3 dataset. The apparent exchange current density j_0 is obtained by Tafel extrapolation and is consequently more sensitive to the selected fitting interval than directly interpolated characteristic overpotentials. For C-MoFeNiP and the sulfide series, the j_0 values reported in WP3 in mA cm^{-2} were converted here to A cm^{-2}. C-MoFeNiP-1200 is the only material in this comparison supported by a dedicated 22 h alkaline stability experiment together with post-test compositional and morphological characterization; WP3 reports an initial increase in current followed by stabilization and evidence of partial phosphorus loss and surface oxidation. The Ni–Co sulfide parameters originate from the WP3 electrochemical comparison in 1 M KOH; notably, the superior performance of $Ni_{0.4}Co_{0.6}S$ was associated with increased electrochemically accessible area and cooperative dual-phase behavior rather than simply

higher intrinsic site activity. For NiS, the reported kinetic parameters should be regarded as apparent because its polarization response contains a phase-transformation feature.

*The Ni-foam values are WP4-derived calculations from the provided Cycle-7 LSV datasets using the same conversion to RHE, geometric area normalization of 4 cm^2, and Tafel-analysis convention applied previously. WP3 itself documents the consecutive-cycle testing of bare and modified Ni foam in 1 M NaOH at 25 °C.

The quantitative sustainability screening demonstrates that the ranking of the investigated catalysts depends strongly on whether sustainability is considered solely in terms of cathodic energy demand or more broadly in terms of the strength of durability evidence. Among the planar electrodeposited coatings, Ni/MXene Sample 20 showed the lowest η_{10} of 209.52 mV, corresponding to an HER overpotential-related energy penalty of approximately 40.4 kJ mol^{-1} H_2. This represents a 34.7% reduction relative to the C-MoFeNiP-1200 reference. Within the pure Ni series, Sample 19_2 was the strongest candidate, with an estimated energy penalty of approximately 43.0 kJ mol^{-1} H_2, while Ni/MoS_2 Sample 5_3 required approximately 50.0 kJ mol^{-1} H_2.

The three-dimensional Ni-foam electrodes exhibited an even stronger apparent energetic advantage. In particular, Ni/MoS_2/Ni foam 1-3 reached 10 mA cm^{-2} at an overpotential of approximately 124 mV in the Cycle-7 dataset, corresponding to only 23.9 kJ mol^{-1} H_2 of cathodic overpotential-related energy and a theoretical 61.4% reduction relative to C-MoFeNiP-1200. This result supports the use of porous three-dimensional substrates for reducing geometric-current-density overpotential. However, it should not yet be interpreted as evidence that this electrode is the most sustainable catalyst investigated, because the foam results currently have substantially weaker long-term durability and degradation evidence.

Conversely, C-MoFeNiP-1200 does not exhibit the lowest energy penalty, but it currently possesses the strongest durability evidence within WP3. Its R_{ct} decreased to 5.3 Ω with increasing pyrolysis temperature, and the catalyst was subjected to a 22 h alkaline stability experiment. Importantly, post-test analysis revealed chemical reconstruction despite electrochemical stabilization. This observation demonstrates why sustainability assessment cannot be based solely on current retention: stable macroscopic HER performance can coexist with elemental dissolution, oxidation, reconstruction, or progressive catalyst consumption.

The Ni–Co sulfide series provides an additional sustainability trade-off. $Ni_{0.4}Co_{0.6}S$ combines a relatively low η_{10} of 237 mV with R_{ct} = 9.2 Ω, giving an estimated HER kinetic energy penalty of 45.7 kJ mol^{-1} H_2. WP3 further indicates that its high geometric activity originates predominantly from increased electrochemically accessible area and cooperative behavior of the dual-phase structure. The

partial substitution of Co by Ni is also relevant from a resource-sustainability perspective, although a quantitative critical-material or life-cycle benefit cannot be calculated without material inventories.

Overall, the WP3 results therefore identify Ni/MoS_2/Ni foam, Ni/MXene Sample 20, Ni Sample 19_2, $Ni_{0.4}Co_{0.6}S$, and C-MoFeNiP-1200 as complementary candidates for further WP4 investigation rather than establishing a single universally superior catalyst. The first candidates are particularly attractive from an activity and theoretical cathodic-energy perspective, whereas C-MoFeNiP-1200 currently provides the strongest experimental basis for evaluating long-term degradation. This distinction should form the basis of the next WP4 stage, in which identical durability, dissolution, post-test characterization, high-current-density and material-efficiency protocols are applied to the leading candidates.